Scawthorn, C. “Earthquake Engineering”
Structural Engineering Handbook
Ed. Chen Wai-Fah
Boca Raton: CRC Press LLC, 1999

Earthquake Engineering

Charles Scawthorn
EQE International, San Francisco, California and Tokyo, Japan

5.1 Introduction

Earthquakes are naturally occurring broad-banded vibratory ground motions, caused by a number of phenomena including tectonic ground motions, volcanism, landslides, rockbursts, and human-made explosions. Of these various causes, tectonic-related earthquakes are the largest and most important. These are caused by the fracture and sliding of rock along faults within the Earth's crust. A fault is a zone of the earth's crust within which the two sides have moved — faults may be hundreds of miles long, from 1 to over 100 miles deep, and not readily apparent on the ground surface. Earthquakes initiate a number of phenomena or agents, termed seismic hazards, which can cause significant damage to the built environment — these include fault rupture, vibratory ground motion (i.e., shaking), inundation (e.g., tsunami, seiche, dam failure), various kinds of permanent ground failure (e.g., liquefaction), fire or hazardous materials release. For a given earthquake, any particular hazard can dominate, and historically each has caused major damage and great loss of life in specific earthquakes. The expected damage given a specified value of a hazard parameter is termed vulnerability, and the product of the hazard and the vulnerability (i.e., the expected damage) is termed the seismic risk. This is often formulated as

$$E(D) = \int_H E(D \mid H)\, p(H)\, dH \tag{5.1}$$

where

H	=	hazard
$p(\cdot)$	=	refers to probability
D	=	damage

$E(D|H)$ = vulnerability
$E(\cdot)$ = the expected value operator

Note that damage can refer to various parameters of interest, such as casualties, economic loss, or temporal duration of disruption. It is the goal of the earthquake specialist to reduce seismic risk. The probability of having a specific level of damage (i.e., $p(D) = d$) is termed the fragility.

For most earthquakes, shaking is the dominant and most widespread agent of damage. Shaking near the actual earthquake rupture lasts only during the time when the fault ruptures, a process that takes seconds or at most a few minutes. The seismic waves generated by the rupture propagate long after the movement on the fault has stopped, however, spanning the globe in about 20 minutes. Typically earthquake ground motions are powerful enough to cause damage only in the near field (i.e., within a few tens of kilometers from the causative fault). However, in a few instances, long period motions have caused significant damage at great distances to selected lightly damped structures. A prime example of this was the 1985 Mexico City earthquake, where numerous collapses of mid- and high-rise buildings were due to a Magnitude 8.1 earthquake occurring at a distance of approximately 400 km from Mexico City.

Ground motions due to an earthquake will vibrate the base of a structure such as a building. These motions are, in general, three-dimensional, both lateral and vertical. The structure's mass has inertia which tends to remain at rest as the structure's base is vibrated, resulting in deformation of the structure. The structure's load carrying members will try to restore the structure to its initial, undeformed, configuration. As the structure rapidly deforms, energy is absorbed in the process of material deformation. These characteristics can be effectively modeled for a single degree of freedom (SDOF) mass as shown in Figure 5.1 where m represents the mass of the structure, the elastic spring (of stiffness k = force / displacement) represents the restorative force of the structure, and the dashpot damping device (damping coefficient c = force/velocity) represents the force or energy lost in the process of material deformation. From the equilibrium of forces on mass m due to the spring and

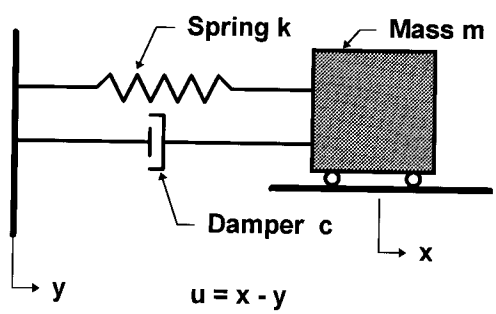

FIGURE 5.1: Single degree of freedom (SDOF) system.

dashpot damper and an applied load $p(t)$, we find:

$$m\ddot{u} + c\dot{u} + ku = p(t) \tag{5.2}$$

the solution of which [32] provides relations between circular frequency of vibration ω, the natural frequency f, and the natural period T:

$$\varpi^2 = \frac{k}{m} \tag{5.3}$$

$$f = \frac{1}{T} = \frac{\varpi}{2\pi} = \frac{1}{2\pi}\sqrt{\frac{k}{m}} \tag{5.4}$$

Damping tends to reduce the amplitude of vibrations. Critical damping refers to the value of damping such that free vibration of a structure will cease after one cycle ($c_{\text{crit}} = 2m\omega$). Damping is conventionally expressed as a percent of critical damping and, for most buildings and engineering structures, ranges from 0.5 to 10 or 20% of critical damping (increasing with displacement amplitude). Note that damping in this range will not appreciably affect the natural period or frequency of vibration, but does affect the amplitude of motion experienced.

5.2 Earthquakes

5.2.1 Causes of Earthquakes and Faulting

In a global sense, tectonic earthquakes result from motion between a number of large plates comprising the earth's crust or lithosphere (about 15 in total), (see Figure 5.2). These plates are driven by the convective motion of the material in the earth's mantle, which in turn is driven by heat generated at the earth's core. Relative plate motion at the fault interface is constrained by friction and/or asperities (areas of interlocking due to protrusions in the fault surfaces). However, strain energy accumulates in the plates, eventually overcomes any resistance, and causes slip between the two sides of the fault. This sudden slip, termed elastic rebound by Reid [101] based on his studies of regional deformation following the 1906 San Francisco earthquake, releases large amounts of energy, which constitutes the earthquake. The location of initial radiation of seismic waves (i.e., the first location of dynamic rupture) is termed the hypocenter, while the projection on the surface of the earth directly above the hypocenter is termed the epicenter. Other terminology includes near-field (within one source dimension of the epicenter, where source dimension refers to the length or width of faulting, whichever is less), far-field (beyond near-field), and meizoseismal (the area of strong shaking and damage). Energy is radiated over a broad spectrum of frequencies through the earth, in body waves and surface waves [16]. Body waves are of two types: P waves (transmitting energy via push-pull motion), and slower S waves (transmitting energy via shear action at right angles to the direction of motion). Surface waves are also of two types: horizontally oscillating Love waves (analogous to S body waves) and vertically oscillating Rayleigh waves.

While the accumulation of strain energy within the plate can cause motion (and consequent release of energy) at faults at any location, earthquakes occur with greatest frequency at the boundaries of the tectonic plates. The boundary of the Pacific plate is the source of nearly half of the world's great earthquakes. Stretching 40,000 km (24,000 miles) around the circumference of the Pacific Ocean, it includes Japan, the west coast of North America, and other highly populated areas, and is aptly termed the Ring of Fire. The interiors of plates, such as ocean basins and continental shields, are areas of low seismicity but are not inactive — the largest earthquakes known to have occurred in North America, for example, occurred in the New Madrid area, far from a plate boundary. Tectonic plates move very slowly and irregularly, with occasional earthquakes. Forces may build up for decades or centuries at plate interfaces until a large movement occurs all at once. These sudden, violent motions produce the shaking that is felt as an earthquake. The shaking can cause direct damage to buildings, roads, bridges, and other human-made structures as well as triggering fires, landslides, tidal waves (tsunamis), and other damaging phenomena.

Faults are the physical expression of the boundaries between adjacent tectonic plates and thus may be hundreds of miles long. In addition, there may be thousands of shorter faults parallel to or branching out from a main fault zone. Generally, the longer a fault the larger the earthquake it can generate. Beyond the main tectonic plates, there are many smaller sub-plates ("platelets") and simple blocks of crust that occasionally move and shift due to the "jostling" of their neighbors and/or the major plates. The existence of these many sub-plates means that smaller but still damaging earthquakes are possible almost anywhere, although often with less likelihood.

FIGURE 5.2: Global seismicity and major tectonic plate boundaries.

Faults are typically classified according to their sense of motion (Figure 5.3). Basic terms include

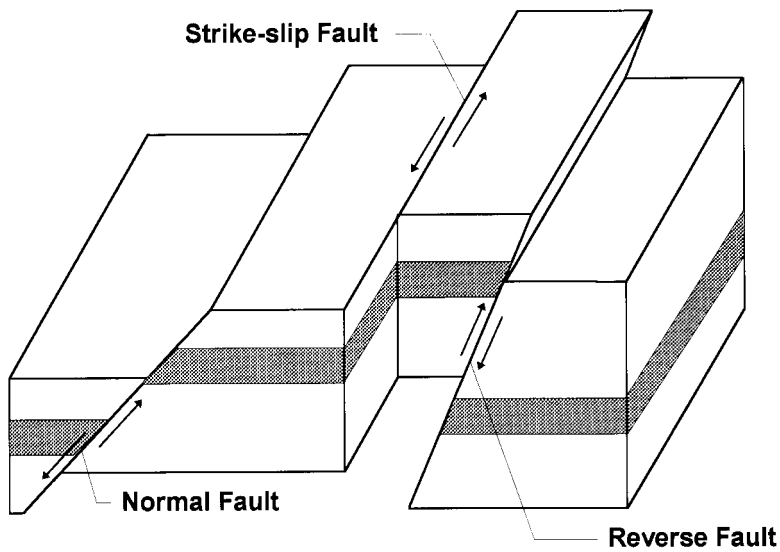

FIGURE 5.3: Fault types.

transform or strike slip (relative fault motion occurs in the horizontal plane, parallel to the strike of the fault), dip-slip (motion at right angles to the strike, up- or down-slip), normal (dip-slip motion, two sides in tension, move away from each other), reverse (dip-slip, two sides in compression, move towards each other), and thrust (low-angle reverse faulting).

Generally, earthquakes will be concentrated in the vicinity of faults. Faults that are moving more rapidly than others will tend to have higher rates of seismicity, and larger faults are more likely than others to produce a large event. Many faults are identified on regional geological maps, and useful information on fault location and displacement history is available from local and national geological surveys in areas of high seismicity. Considering this information, areas of an expected large earthquake in the near future (usually measured in years or decades) can be and have been identified. However, earthquakes continue to occur on "unknown" or "inactive" faults. An important development has been the growing recognition of blind thrust faults, which emerged as a result of several earthquakes in the 1980s, none of which were accompanied by surface faulting [120]. Blind thrust faults are faults at depth occurring under anticlinal folds — since they have only subtle surface expression, their seismogenic potential can be evaluated by indirect means only [46]. Blind thrust faults are particularly worrisome because they are hidden, are associated with folded topography in general, including areas of lower and infrequent seismicity, and therefore result in a situation where the potential for an earthquake exists in any area of anticlinal geology, even if there are few or no earthquakes in the historic record. Recent major earthquakes of this type have included the 1980 M_w 7.3 El- Asnam (Algeria), 1988 M_w 6.8 Spitak (Armenia), and 1994 M_w 6.7 Northridge (California) events.

Probabilistic methods can be usefully employed to quantify the likelihood of an earthquake's occurrence, and typically form the basis for determining the design basis earthquake. However, the earthquake generating process is not understood well enough to reliably predict the times, sizes, and

locations of earthquakes with precision. In general, therefore, communities must be prepared for an earthquake to occur at any time.

5.2.2 Distribution of Seismicity

This section discusses and characterizes the distribution of seismicity for the U.S. and selected areas.

Global

It is evident from Figure 5.2 that some parts of the globe experience more and larger earthquakes than others. The two major regions of seismicity are the circum-Pacific Ring of Fire and the Trans-Alpide belt, extending from the western Mediterranean through the Middle East and the northern India sub-continent to Indonesia. The Pacific plate is created at its South Pacific extensional boundary — its motion is generally northwestward, resulting in relative strike-slip motion in California and New Zealand (with, however, a compressive component), and major compression and subduction in Alaska, the Aleutians, Kuriles, and northern Japan. Subduction refers to the plunging of one plate (i.e., the Pacific) beneath another, into the mantle, due to convergent motion, as shown in Figure 5.4.

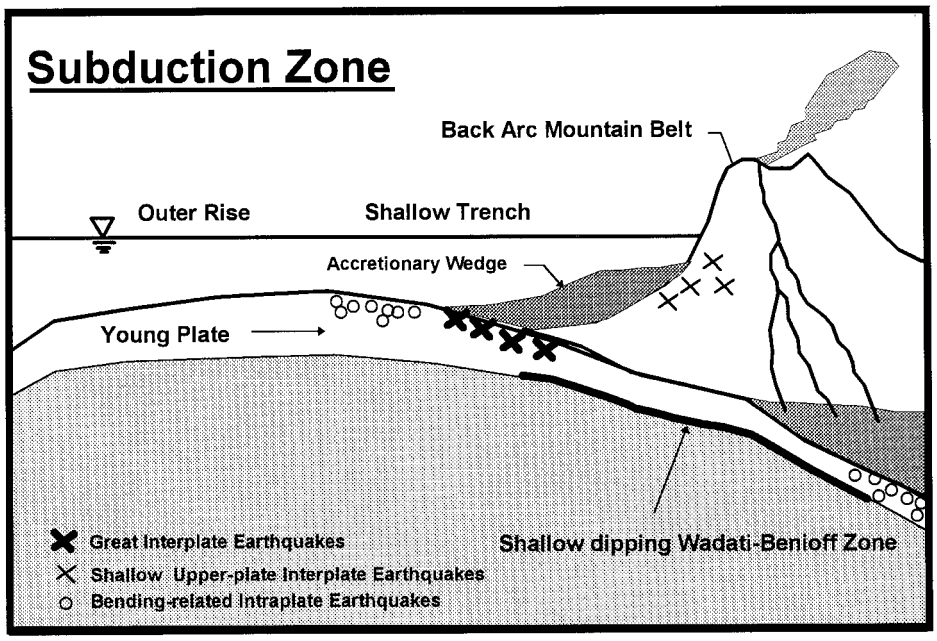

FIGURE 5.4: Schematic diagram of subduction zone, typical of west coast of South America, Pacific Northwest of U.S., or Japan.

Subduction zones are typically characterized by volcanism, as a portion of the plate (melting in the lower mantle) re-emerges as volcanic lava. Subduction also occurs along the west coast of South America at the boundary of the Nazca and South American plate, in Central America (boundary of the Cocos and Caribbean plates), in Taiwan and Japan (boundary of the Philippine and Eurasian plates), and in the North American Pacific Northwest (boundary of the Juan de Fuca and North American

plates). The Trans-Alpide seismic belt is basically due to the relative motions of the African and Australian plates colliding and subducting with the Eurasian plate.

U.S.

Table 5.1 provides a list of selected U.S. earthquakes. The San Andreas fault system in California and the Aleutian Trench off the coast of Alaska are part of the boundary between the North American and Pacific tectonic plates, and are associated with the majority of U.S. seismicity (Figure 5.5 and Table 5.1). There are many other smaller fault zones throughout the western U.S. that are also helping to release the stress that is built up as the tectonic plates move past one another, (Figure 5.6). While California has had numerous destructive earthquakes, there is also clear evidence that the potential exists for great earthquakes in the Pacific Northwest [11].

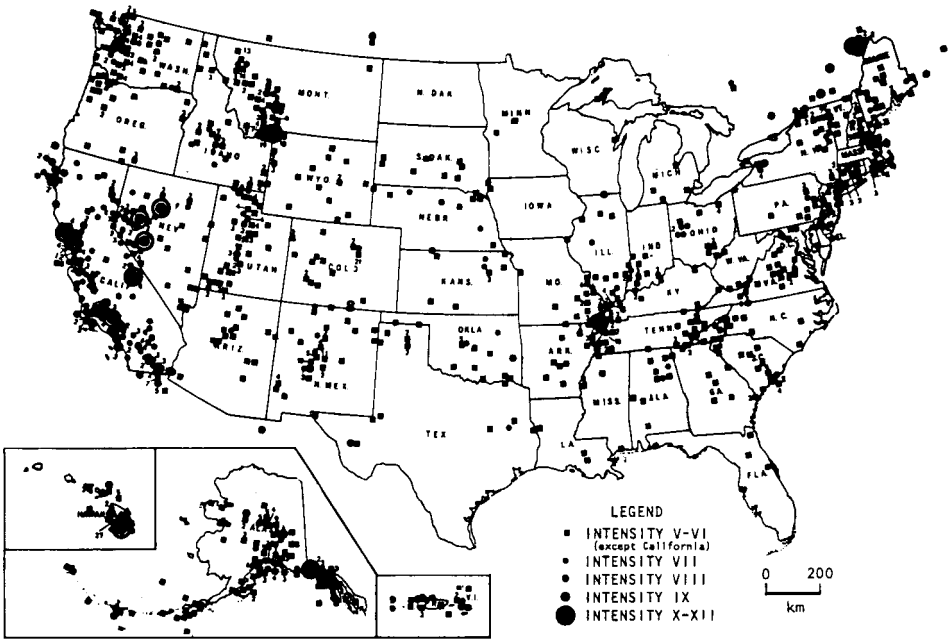

FIGURE 5.5: U.S. seismicity. (From Algermissen, S. T., *An Introduction to the Seismicity of the United States*, Earthquake Engineering Research Institute, Oakland, CA, 1983. With permission. Also after Coffman, J. L., von Hake, C. A., and Stover, C. W., *Earthquake History of the United States*, U.S. Department of Commerce, NOAA, Pub. 41-1, Washington, 1980.)

On the east coast of the U.S., the cause of earthquakes is less well understood. There is no plate boundary and very few locations of active faults are known so that it is more difficult to assess where earthquakes are most likely to occur. Several significant historical earthquakes have occurred, such as in Charleston, South Carolina, in 1886, and New Madrid, Missouri, in 1811 and 1812, indicating that there is potential for very large and destructive earthquakes [56, 131]. However, most earthquakes in the eastern U.S. are smaller magnitude events. Because of regional geologic differences, eastern and central U.S. earthquakes are felt at much greater distances than those in the western U.S., sometimes up to a thousand miles away [58].

TABLE 5.1 Selected U.S. Earthquakes

Yr	M	D	Lat.		Long.		M	MMI	Fat.	USD mills	Locale
1755	11	18						8			Nr Cape Ann, MA (MMI from STA)
1774	2	21						7			Eastern VA (MMI from STA)
1791	5	16						8			E. Haddam, CT (MMI from STA)
1811	12	16	36	N	90	W	8.6	-			New Madrid, MO
1812	1	23	36.6	N	89.6	W	8.4	12			New Madrid, MO
1812	2	7	36.6	N	89.6	W	8.7	12			New Madrid, MO
1817	10	5						8			Woburn, MA (MMI from STA)
1836	6	10	38	N	122	W	-	10	-		California
1838	6	0	37.5	N	123	W	-	10	-		California
1857	1	9	35	N	119	W	8.3	7	-		San Francisco, CA
1865	10	8	37	N	122	W	-	9			San Jose, Santa Cruz, CA
1868	4	3	19	N	156	W	-	10	81		Hawaii
1868	10	21	37.5	N	122	W	6.8	10	3		Hayward, CA
1872	3	26	36.5	N	118	W	8.5	10	50		Owens Valley, CA
1886	9	1	32.9	N	80	W	7.7	9	60	5	Charleston, SC, Ms from STA
1892	2	24	31.5	N	117	W	-	10	-		San Diego County, CA
1892	4	19	38.5	N	123	W	-	9	-		Vacaville, Winters, CA
1892	5	16	14	N	143	E	-	-	-		Agana, Guam
1897	5	31					5.8	8			Giles County, VA (mb from STA)
1899	9	4	60	N	142	W	8.3	-	-		Cape Yakataga, AK
1906	4	18	38	N	123	W	8.3	11	700?	400	San Francisco, CA (deaths more?)
1915	10	3	40.5	N	118	W	7.8	-			Pleasant Valley, NV
1925	6	29	34.3	N	120	W	6.2	-	13	8	Santa Barbara, CA
1927	11	4	34.5	N	121	W	7.5	9			Lompoc, Port San Luis, CA
1933	3	11	33.6	N	118	W	6.3	-	115	40	Long Beach, CA
1934	12	31	31.8	N	116	W	7.1	10			Baja, Imperial Valley, CA
1935	10	19	46.6	N	112	W	6.2	-	2	19	Helena, MT
1940	5	19	32.7	N	116	W	7.1	10	9	6	SE of Elcentro, CA
1944	9	5	44.7	N	74.7	W	5.6	-		2	Massena, NY
1949	4	13	47.1	N	123	W	7	8	8	25	Olympia, WA
1951	8	21	19.7	N	156	W	6.9	-			Hawaii
1952	7	21	35	N	119	W	7.7	11	13	60	Central, Kern County, CA
1954	12	16	39.3	N	118	W	7	10			Dixie Valley, NV
1957	3	9	51.3	N	176	W	8.6	-		3	Alaska
1958	7	10	58.6	N	137	W	7.9	-	5		Lituyabay, AK—Landslide
1959	8	18	44.8	N	111	W	7.7	-			Hebgen Lake, MT
1962	8	30	41.8	N	112	W	5.8	-		2	Utah
1964	3	28	61	N	148	W	8.3	-	131	540	Alaska
1965	4	29	47.4	N	122	W	6.5	7	7	13	Seattle, WA
1971	2	9	34.4	N	118	W	6.7	11	65	553	San Fernando, CA
1975	3	28	42.1	N	113	W	6.2	8	-	1	Pocatello Valley, ID
1975	8	1	39.4	N	122	W	6.1	-	-	6	Oroville Reservoir, CA
1975	11	29	19.3	N	155	W	7.2	9	2	4	Hawaii
1980	1	24	37.8	N	122	W	5.9	7	1	4	Livermore, CA
1980	5	25	37.6	N	119	W	6.4	7	-	2	Mammoth Lakes, CA
1980	7	27	38.2	N	83.9	W	5.2	-	-	1	Maysville, KY
1980	11	8	41.2	N	124	W	7	7	5	3	N Coast, CA
1983	5	2	36.2	N	120	W	6.5	8	-	31	Central, Coalinga, CA
1983	10	28	43.9	N	114	W	7.3	-	2	13	Borah Peak, ID
1983	11	16	19.5	N	155	W	6.6	8	-	7	Kapapala, HI
1984	4	24	37.3	N	122	W	6.2	7	-	8	Central Morgan Hill, CA
1986	7	8	34	N	117	W	6.1	7	-	5	Palm Springs, CA
1987	10	1	34.1	N	118	W	6	8	8	358	Whittier, CA
1987	11	24	33.2	N	116	W	6.3	6	2	-	Superstition Hills, CA
1989	6	26	19.4	N	155	W	6.1	6			Hawaii
1989	10	18	37.1	N	122	W	7.1	9	62	6,000	Loma Prieta, CA
1990	2	28	34.1	N	118	W	5.5	7	-	13	Claremont, Covina, CA
1992	4	23	34	N	116	W	6.3	7			Joshua Tree, CA
1992	4	25	40.4	N	124	W	7.1	8		66	Humboldt, Ferndale, CA
1992	6	28	34.2	N	117	W	6.7	8			Big Bear Lake, Big Bear, CA
1992	6	28	34.2	N	116	W	7.6	9	3	92	Landers, Yucca, CA
1992	6	29	36.7	N	116	W	5.6	-			Border of NV and CA
1993	3	25	45	N	123	W	5.6	7			Washington-Oregon
1993	9	21	42.3	N	122	W	5.9	7	2	-	Klamath Falls, OR
1994	1	16	40.3	N	76	W	4.6	5			PA, Felt, Canada
1994	1	17	34.2	N	119	W	6.8	9	57	30,000	Northridge, CA
1994	2	3	42.8	N	111	W	6	7			Afton, WY
1995	10	6	65.2	N	149	W	6.4	-			AK (Oil pipeline damaged)

Note: STA refers to [3]. From NEIC, Database of Significant Earthquakes Contained in *Seismicity Catalogs,* National Earthquake Information Center, Goldon, CO, 1996. With permission.

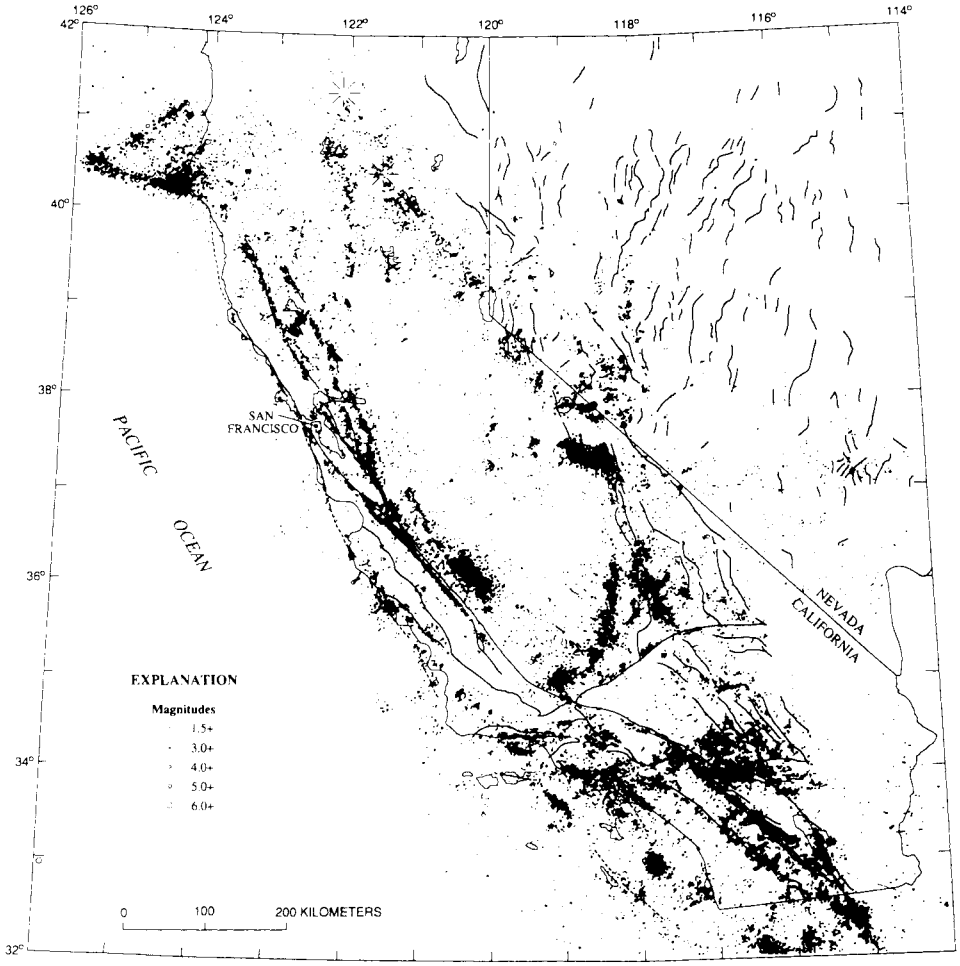

FIGURE 5.6: Seismicity for California and Nevada, 1980 to 1986. $M > 1.5$ (Courtesy of Jennings, C. W., Fault Activity Map of California and Adjacent Areas, Department of Conservation, Division of Mines and Geology, Sacramento, CA, 1994.)

Other Areas

Table 5.2 provides a list of selected 20th-century earthquakes with fatalities of approximately 10,000 or more. All the earthquakes are in the Trans-Alpide belt or the circum-Pacific ring of fire, and the great loss of life is almost invariably due to low-strength masonry buildings and dwellings. Exceptions to this rule are the 1923 Kanto (Japan) earthquake, where most of the approximately 140,000 fatalities were due to fire; the 1970 Peru earthquake, where large landslides destroyed whole towns; and the 1988 Armenian earthquake, where large numbers were killed in Spitak and Leninakan due to poor quality pre-cast concrete construction. The Trans-Alpide belt includes the Mediterranean, which has very significant seismicity in North Africa, Italy, Greece, and Turkey due to the Africa plate's motion relative to the Eurasian plate; the Caucasus (e.g., Armenia) and the Middle East (Iran, Afghanistan), due to the Arabian plate being forced northeastward into the Eurasian plate by the African plate; and the Indian sub-continent (Pakistan, northern India), and the subduction boundary along the southwestern side of Sumatra and Java, which are all part of the Indian-Australian

plate. Seismicity also extends northward through Burma and into western China. The Philippines, Taiwan, and Japan are all on the western boundary of the Philippines sea plate, which is part of the circum-Pacific ring of fire.

Japan is an island archipelago with a long history of damaging earthquakes [128] due to the interaction of four tectonic plates (Pacific, Eurasian, North American, and Philippine) which all converge near Tokyo. Figure 5.7 indicates the pattern of Japanese seismicity, which is seen to be higher in the north of Japan. However, central Japan is still an area of major seismic risk, particularly Tokyo,

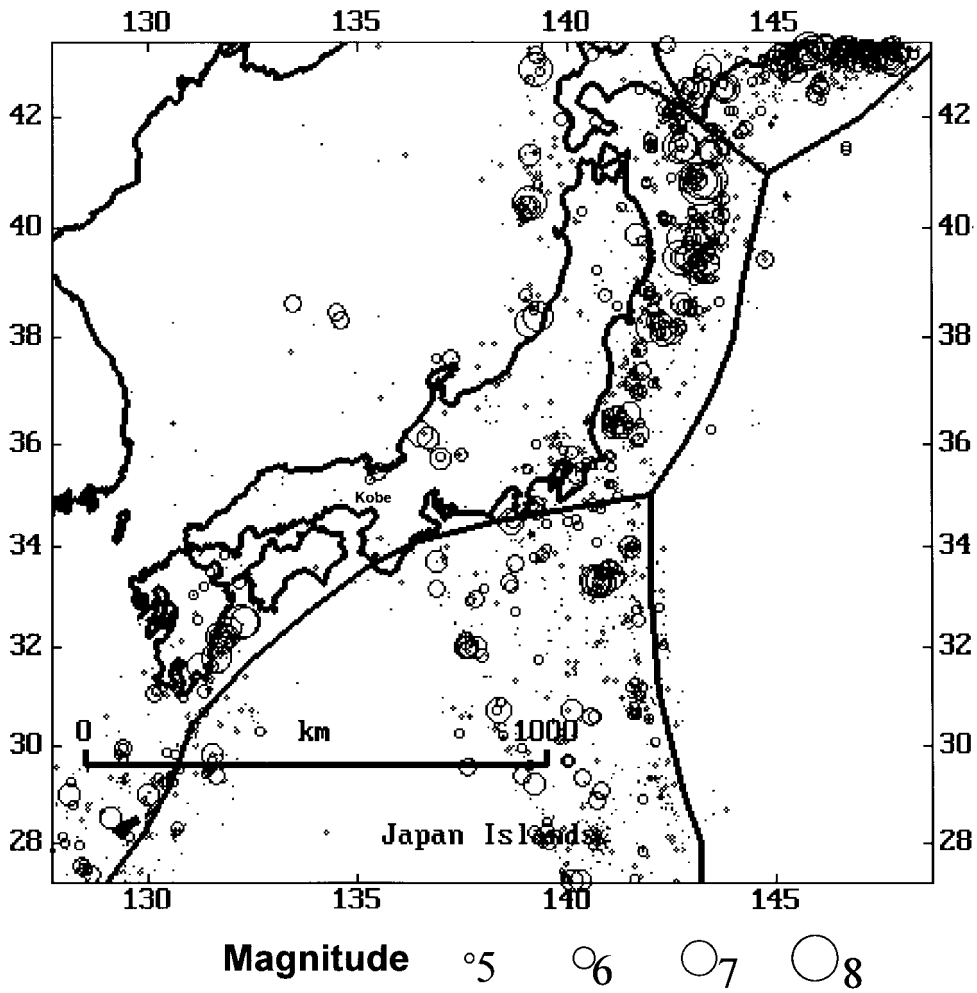

FIGURE 5.7: Japanese seismicity (1960 to 1965).

which has sustained a number of damaging earthquakes in history. The Great Kanto earthquake of 1923 (M7.9, about 140,000 fatalities) was a great subduction earthquake, and the 1855 event (M6.9) had its epicenter in the center of present-day Tokyo. Most recently, the 1995 MW 6.9 Hanshin (Kobe) earthquake caused approximately 6,000 fatalities and severely damaged some modern structures as well as many structures built prior to the last major updating of the Japanese seismic codes (ca. 1981).

The predominant seismicity in the Kuriles, Kamchatka, the Aleutians, and Alaska is due to subduction of the Pacific Plate beneath the North American plate (which includes the Aleutians and extends down through northern Japan to Tokyo). The predominant seismicity along the western boundary of North American is due to transform faults (i.e., strike-slip) as the Pacific Plate displaces northwestward relative to the North American plate, although the smaller Juan de Fuca plate offshore Washington and Oregon, and the still smaller Gorda plate offshore northern California, are driven into subduction beneath North American by the Pacific Plate. Further south, the Cocos plate is similarly subducting beneath Mexico and Central America due to the Pacific Plate, while the Nazca Plate lies offshore South America. Lesser but still significant seismicity occurs in the Caribbean, primarily along a series of trenches north of Puerto Rico and the Windward islands. However, the southern boundary of the Caribbean plate passes through Venezuela, and was the source of a major earthquake in Caracas in 1967. New Zealand's seismicity is due to a major plate boundary (Pacific with Indian-Australian plates), which transitions from thrust to transform from the South to the North Island [108]. Lesser but still significant seismicity exists in Iceland where it is accompanied by volcanism due to a spreading boundary between the North American and Eurasian plates, and through Fenno-Scandia, due to tectonics as well as glacial rebound. This very brief tour of the major seismic belts of the globe is not meant to indicate that damaging earthquakes cannot occur elsewhere — earthquakes can and have occurred far from major plate boundaries (e.g., the 1811-1812 New Madrid intraplate events, with several being greater than magnitude 8), and their potential should always be a consideration in the design of a structure.

TABLE 5.2 Selected 20th Century Earthquakes with Fatalities Greater than 10,000

Yr	M	D	Lat.	Long.	M	MMI	Deaths	Damage USD millions	Locale
1976	7	27	39.5 N	118 E	8	10	655,237	$2,000	China: NE: Tangshan
1920	12	16	36.5 N	106 E	8.5	—	200,000		China: Gansu and Shanxi
1923	9	1	35.3 N	140 E	8.2	—	142,807	$2,800	Japan: Toyko, Yokohama, Tsunami
1908	2	0	38.2 N	15.6 E	7.5	—	75,000		Italy: Sicily
1932	12	25	39.2 N	96.5 E	7.6	—	70,000		China: Gansu Province
1970	5	31	9.1 S	78.8 W	7.8	9	67,000	$500	Peru
1990	6	20	37 N	49.4 E	7.7	7	50,000		Iran: Manjil
1927	5	22	37.6 N	103 E	8	—	40,912		China: Gansu Province
1915	1	13	41.9 N	13.6 E	7	11	35,000		Italy: Abruzzi, Avezzano
1935	5	30	29.5 N	66.8 E	7.5	10	30,000		Pakistan: Quetta
1939	12	26	39.5 N	38.5 E	7.9	12	30,000		Turkey: Erzincan
1939	1	25	36.2 S	72.2 W	8.3	—	28,000	$100	Chile: Chillan
1978	9	16	33.4 N	57.5 E	7.4	—	25,000	$11	Iran: Tabas
1988	12	7	41 N	44.2 E	6.8	10	25,000	$16,200	CIS: Armenia
1976	2	4	15.3 N	89.2 W	7.5	9	22,400	$6,000	Guatemala: Tsunami
1974	5	10	28.2 N	104 E	6.8	—	20,000		China: Yunnan and Sichuan
1948	10	5	37.9 N	58.6 E	7.2	—	19,800		CIS: Turkmenistan: Aschabad
1905	4	4	33 N	76 E	8.6	—	19,000		India: Kangra
1917	1	21	8 S	115 E	—	—	15,000		Indonesia: Bali, Tsunami
1968	8	31	33.9 N	59 E	7.3	—	15,000		Iran
1962	9	1	35.6 N	49.9 E	7.3	—	12,225		Iran: NW
1907	10	21	38.5 N	67.9 E	7.8	9	12,000		CIS: Uzbekistan: SE
1960	2	29	30.4 N	9.6 W	5.9	—	12,000		Morocco: Agadir
1980	10	10	36.1 N	1.4 E	7.7	—	11,000		Algeria: Elasnam
1934	1	15	26.5 N	86.5 E	8.4	—	10,700		Nepal-India
1918	2	13	23.5 N	117 E	7.3	—	10,000		China: Guangdong Province
1933	8	25	32 N	104 E	7.4	—	10,000		China: Sichuan Province
1975	2	4	40.6 N	123 E	7.4	10	10,000		China: NE: Yingtao

From NEIC, Database of Significant Earthquakes Contained in *Seismicity Catalogs*, National Earthquake Information Center, Goldon, CO, 1996.

5.2.3 Measurement of Earthquakes

Earthquakes are complex multi-dimensional phenomena, the scientific analysis of which requires measurement. Prior to the invention of modern scientific instruments, earthquakes were qualitatively measured by their effect or intensity, which differed from point-to-point. With the deployment of seismometers, an instrumental quantification of the entire earthquake event — the unique magnitude of the event — became possible. These are still the two most widely used measures of an earthquake, and a number of different scales for each have been developed, which are sometimes confused.[1] Engineering design, however, requires measurement of earthquake phenomena in units such as force or displacement. This section defines and discusses each of these measures.

Magnitude

An individual earthquake is a unique release of strain energy. Quantification of this energy has formed the basis for measuring the earthquake event. Richter [103] was the first to define earthquake magnitude as

$$M_L = \log A - \log A_o \tag{5.5}$$

where M_L is local magnitude (which Richter only defined for Southern California), A is the maximum trace amplitude in microns recorded on a standard Wood-Anderson short-period torsion seismometer,[2] at a site 100 km from the epicenter, $\log A_o$ is a standard value as a function of distance, for instruments located at distances other than 100 km and less than 600 km. Subsequently, a number of other magnitudes have been defined, the most important of which are surface wave magnitude M_S, body wave magnitude m_b, and moment magnitude M_W. Due to the fact that M_L was only locally defined for California (i.e., for events within about 600 km of the observing stations), surface wave magnitude M_S was defined analogously to M_L using teleseismic observations of surface waves of 20-s period [103]. Magnitude, which is defined on the basis of the amplitude of ground displacements, can be related to the total energy in the expanding wave front generated by an earthquake, and thus to the total energy release. An empirical relation by Richter is

$$\log_{10} E_s = 11.8 + 1.5M_s \tag{5.6}$$

where E_s is the total energy in ergs.[3] Note that $10^{1.5} = 31.6$, so that an increase of one magnitude unit is equivalent to 31.6 times more energy release, two magnitude units increase is equivalent to 1000 times more energy, etc. Subsequently, due to the observation that deep-focus earthquakes commonly do not register measurable surface waves with periods near 20 s, a body wave magnitude m_b was defined [49], which can be related to M_s [38]:

$$m_b = 2.5 + 0.63M_s \tag{5.7}$$

Body wave magnitudes are more commonly used in eastern North America, due to the deeper earthquakes there. A number of other magnitude scales have been developed, most of which tend to *saturate* — that is, asymptote to an upper bound due to larger earthquakes radiating significant amounts of energy at periods longer than used for determining the magnitude (e.g., for M_s, defined by

[1] Earthquake magnitude and intensity are analogous to a lightbulb and the light it emits. A particular lightbulb has only one energy level, or wattage (e.g., 100 watts, analogous to an earthquake's magnitude). Near the lightbulb, the light intensity is very bright (perhaps 100 ft-candles, analogous to MMI IX), while farther away the intensity decreases (e.g., 10 ft-candles, MMI V). A particular earthquake has only one magnitude value, whereas it has many intensity values.

[2] The instrument has a natural period of 0.8 s, critical damping ration 0.8, magnification 2,800.

[3] Richter [104] gives 11.4 for the constant term, rather than 11.8, which is based on subsequent work. The uncertainty in the data make this difference, equivalent to an energy factor = 2.5 or 0.27 magnitude units, inconsequential.

measuring 20 s surface waves, saturation occurs at about $M_s > 7.5$). More recently, seismic moment has been employed to define a moment magnitude M_w([53]; also denoted as bold-face M) which is finding increased and widespread use:

$$\log M_o = 1.5M_w + 16.0 \tag{5.8}$$

where seismic moment M_o (dyne-cm) is defined as [74]

$$M_o = \mu A\bar{u} \tag{5.9}$$

where μ is the material shear modulus, A is the area of fault plane rupture, and $\bar{u}$ is the mean relative displacement between the two sides of the fault (the averaged fault slip). Comparatively, M_w and M_s are numerically almost identical up to magnitude 7.5. Figure 5.8 indicates the relationship between moment magnitude and various magnitude scales.

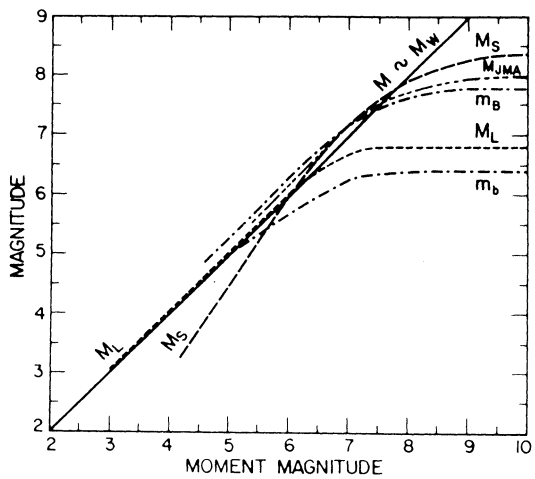

FIGURE 5.8: Relationship between moment magnitude and various magnitude scales. (From Campbell, K. W., Strong Ground Motion Attenuation Relations: A Ten-Year Perspective, *Earthquake Spectra*, 1(4), 759-804, 1985. With permission.)

For lay communications, it is sometimes customary to speak of great earthquakes, large earthquakes, etc. There is no standard definition for these, but the following is an approximate categorization:

Earthquake Magnitude*	Micro Not felt	Small < 5	Moderate $5 \sim 6.5$	Large $6.5 \sim 8$	Great > 8

$*$ Not specifically defined.

From the foregoing discussion, it can be seen that magnitude and energy are related to fault rupture length and slip. Slemmons [114] and Bonilla et al. [17] have determined statistical relations between these parameters, for worldwide and regional data sets, segregated by type of faulting (normal, reverse, strike-slip). The worldwide results of Bonilla et al. for all types of faults are

$$M_s = \quad 6.04 + 0.708 \log_{10} L \quad s = .306 \tag{5.10}$$

$$\log_{10} L = \quad -2.77 + 0.619 M_s \quad s = .286 \tag{5.11}$$

$$M_s = \quad 6.95 + 0.723 \log_{10} d \quad s = .323 \tag{5.12}$$
$$\log_{10} d = \quad -3.58 + 0.550 M_s \quad s = .282 \tag{5.13}$$

which indicates, for example that, for $M_s = 7$, the average fault rupture length is about 36 km (and the average displacement is about 1.86 m). Conversely, a fault of 100 km length is capable of about a $M_s = 7.5$[4]event. More recently, Wells and Coppersmith [130] have performed an extensive analysis of a dataset of 421 earthquakes. Their results are presented in Table 5.3a and b.

Intensity

In general, seismic intensity is a measure of the effect, or the strength, of an earthquake hazard at a specific location. While the term can be applied generically to engineering measures such as peak ground acceleration, it is usually reserved for qualitative measures of location-specific earthquake effects, based on observed human behavior and structural damage. Numerous intensity scales were developed in pre-instrumental times. The most common in use today are the Modified Mercalli Intensity (MMI) [134], Rossi-Forel (R-F), Medvedev-Sponheur-Karnik (MSK) [80], and the Japan Meteorological Agency (JMA) [69] scales.

MMI is a subjective scale defining the level of shaking at specific sites on a scale of I to XII. (MMI is expressed in Roman numerals to connote its approximate nature). For example, moderate shaking that causes few instances of fallen plaster or cracks in chimneys constitutes MMI VI. It is difficult to find a reliable relationship between magnitude, which is a description of the earthquake's total energy level, and intensity, which is a subjective description of the level of shaking of the earthquake at specific sites, because shaking severity can vary with building type, design and construction practices, soil type, and distance from the event.

Note that MMI X is the maximum considered physically possible due to "mere" shaking, and that MMI XI and XII are considered due more to permanent ground deformations and other geologic effects than to shaking.

Other intensity scales are defined analogously (see Table 5.5, which also contains an approximate conversion from MMI to acceleration a [PGA, in cm/s^2, or gals]). The conversion is due to Richter [103] (other conversions are also available [84].

$$\log a = \mathrm{MMI}/3 - 1/2 \tag{5.14}$$

Intensity maps are produced as a result of detailed investigation of the type of effects tabulated in Table 5.4, as shown in Figure 5.9 for the 1994 M_W 6.7 Northridge earthquake. Correlations have been developed between the area of various MMIs and earthquake magnitude, which are of value for seismological and planning purposes.

Figure 10 correlates A_{felt} vs. M_W. For pre-instrumental historical earthquakes, A_{felt} can be estimated from newspapers and other reports, which then can be used to estimate the event magnitude, thus supplementing the seismicity catalog. This technique has been especially useful in regions with a long historical record [4, 133].

Time History

Sensitive strong motion seismometers have been available since the 1930s, and they record actual ground motions specific to their location (Figure 5.11). Typically, the ground motion records, termed *seismographs* or *time histories*, have recorded acceleration (these records are termed *accelerograms*),

[4]Note that $L = g(M_s)$ should not be inverted to solve for $M_s = f(L)$, as a regression for $y = f(x)$ is different than a regression for $x = g(y)$.

Table 5.3a Regressions of Rupture Length, Rupture Width, Rupture Area and Moment Magnitude

Equation[a]	Slip type[b]	Number of events	Coefficients and standard errors a(sa)	b(sb)	Standard deviation s	Correlation coefficient r	Magnitude range	Length/width range (km)
$\mathrm{M} = a + b * \log(SRL)$	SS	43	5.16(0.13)	1.12(0.08)	0.28	0.91	5.6 to 8.1	1.3 to 432
	R	19	5.00(0.22)	1.22(0.16)	0.28	0.88	5.4 to 7.4	3.3 to 85
	N	15	4.86(0.34)	1.32(0.26)	0.34	0.81	5.2 to 7.3	2.5 to 41
	All	77	5.08(0.10)	1.16(0.07)	0.28	0.89	5.2 to 8.1	1.3 to 432
$\log(SRL) = a + b * \mathrm{M}$	SS	43	−3.55(0.37)	0.74(0.05)	0.23	0.91	5.6 to 8.1	1.3 to 432
	R	19	−2.86(0.55)	0.63(0.08)	0.20	0.88	5.4 to 7.4	3.3 to 85
	N	15	−2.01(0.65)	0.50(0.10)	0.21	0.81	5.2 to 7.3	2.5 to 41
	All	77	−3.22(0.27)	0.69(0.04)	0.22	0.89	5.2 to 8.1	1.3 to 432
$\mathrm{M} = a + b * \log(RLD)$	SS	93	4.33(0.06)	1.49(0.05)	0.24	0.96	4.8 to 8.1	1.5 to 350
	R	50	4.49(0.11)	1.49(0.09)	0.26	0.93	4.8 to 7.6	1.1 to 80
	N	24	4.34(0.23)	1.54(0.18)	0.31	0.88	5.2 to 7.3	3.8 to 63
	All	167	4.38(0.06)	1.49(0.04)	0.26	0.94	4.8 to 8.1	1.1 to 350
$\log(RLD) = a + b * \mathrm{M}$	SS	93	−2.57(0.12)	0.62(0.02)	0.15	0.96	4.8 to 8.1	1.5 to 350
	R	50	−2.42(0.21)	0.58(0.03)	0.16	0.93	4.8 to 7.6	1.1 to 80
	N	24	−1.88(0.37)	0.50(0.06)	0.17	0.88	5.2 to 7.3	3.8 to 63
	All	167	−2.44(0.11)	0.59(0.02)	0.16	0.94	4.8 to 8.1	1.1 to 350
$\mathrm{M} = a + b * \log(RW)$	SS	87	3.80(0.17)	2.59(0.18)	0.45	0.84	4.8 to 8.1	1.5 to 350
	R	43	4.37(0.16)	1.95(0.15)	0.32	0.90	4.8 to 7.6	1.1 to 80
	N	23	4.04(0.29)	2.11(0.28)	0.31	0.86	5.2 to 7.3	3.8 to 63
	All	153	4.06(0.11)	2.25(0.12)	0.41	0.84	4.8 to 8.1	1.1 to 350
$\log(RW) = a + b * \mathrm{M}$	SS	87	−0.76(0.12)	0.27(0.02)	0.14	0.84	4.8 to 8.1	1.5 to 350
	R	43	−1.61(0.20)	0.41(0.03)	0.15	0.90	4.8 to 7.6	1.1 to 80
	N	23	−1.14(0.28)	0.35(0.05)	0.12	0.86	5.2 to 7.3	3.8 to 63
	All	153	−1.01(0.10)	0.32(0.02)	0.15	0.84	4.8 to 8.1	1.1 to 350
$\mathrm{M} = a + b * \log(RA)$	SS	83	3.98(0.07)	1.02(0.03)	0.23	0.96	4.8 to 7.9	3 to 5,184
	R	43	4.33(0.12)	0.90(0.05)	0.25	0.94	4.8 to 7.6	2.2 to 2,400
	N	22	3.93(0.23)	1.02(0.10)	0.25	0.92	5.2 to 7.3	19 to 900
	All	148	4.07(0.06)	0.98(0.03)	0.24	0.95	4.8 to 7.9	2.2 to 5,184
$\log(RA) = a + b * \mathrm{M}$	SS	83	−3.42(0.18)	0.90(0.03)	0.22	0.96	4.8 to 7.9	3 to 5,184
	R	43	−3.99(0.36)	0.98(0.06)	0.26	0.94	4.8 to 7.6	2.2 to 2,400
	N	22	−2.87(0.50)	0.82(0.08)	0.22	0.92	5.2 to 7.3	19 to 900
	All	148	−3.49(0.16)	0.91(0.03)	0.24	0.95	4.8 to 7.9	2.2 to 5,184

[a] SRL—surface rupture length (km); RLD—subsurface rupture length (km); RW—downdip rupture width (km); RA—rupture area (km^2).
[b] SS—strike slip; R—reverse; N—normal.
From Wells, D. L. and Coopersmith, K. J., Empirical Relationships Among Magnitude, Rupture Length, Rupture Width, Rupture Area and Surface Displacements, *Bull. Seis. Soc. Am.*, 84(4), 974-1002, 1994. With permission.

Table 5.3b Regressions of Displacement and Moment Magnitude

Equation[a]	Slip type[b]	Number of events	Coefficients and standard errors a(sa)	b(sb)	Standard deviation s	Correlation coefficient r	Magnitude range	Displacement range (km)
$\mathrm{M} = a + b * \log(MD)$	SS	43	6.81(0.05)	0.78(0.06)	0.29	0.90	5.6 to 8.1	0.01 to 14.6
	{ R[c]	*21*	*6.52(0.11)*	*0.44(0.26)*	*0.52*	*0.36*	*5.4 to 7.4*	*0.11 to 6.5* }
	N	16	6.61(0.09)	0.71(0.15)	0.34	0.80	5.2 to 7.3	0.06 to 6.1
	All	80	6.69(0.04)	0.74(0.07)	0.40	0.78	5.2 to 8.1	0.01 to 14.6
$\log(MD) = a + b * \mathrm{M}$	SS	43	−7.03(0.55)	1.03(0.08)	0.34	0.90	5.6 to 8.1	0.01 to 14.6
	{ R	*21*	*− 1.84(1.14)*	*0.29(0.17)*	*0.42*	*0.36*	*5.4 to 7.4*	*0.11 to 6.5* }
	N	16	−5.90(1.18)	0.89(0.18)	0.38	0.80	5.2 to 7.3	0.06 to 6.1
	All	80	−5.46(0.51)	0.82(0.08)	0.42	0.78	5.2 to 8.1	0.01 to 14.6
$\mathrm{M} = a + b * \log(AD)$	SS	29	7.04(0.05)	0.89(0.09)	0.28	0.89	5.6 to 8.1	0.05 to 8.0
	{ R	*15*	*6.64(0.16)*	*0.13(0.36)*	*0.50*	*0.10*	*5.8 to 7.4*	*0.06 to 1.5* }
	N	12	6.78(0.12)	0.65(0.25)	0.33	0.64	6.0 to 7.3	0.08 to 2.1
	All	56	6.93(0.05)	0.82(0.10)	0.39	0.75	5.6 to 8.1	0.05 to 8.0
$\log(AD) = a + b * \mathrm{M}$	SS	29	−6.32(0.61)	0.90(0.09)	0.28	0.89	5.6 to 8.1	0.05 to 8.0
	{ R	*15*	*− 0.74(1.40)*	*0.08(0.21)*	*0.38*	*0.10*	*5.8 to 7.4*	*0.06 to 1.5* }
	N	12	−4.45(1.59)	0.63(0.24)	0.33	0.64	6.0 to 7.3	0.08 to 2.1
	All	56	−4.80(0.57)	0.69(0.08)	0.36	0.75	5.6 to 8.1	0.05 to 8.0

[a] MD—maximum displacement (m); AD—average displacement (M).
[b] SS—strike slip; R—reverse; N—normal.
[c] Regressions for reverse-slip relationships shown in italics and brackets are not significant at a 95% probability level.
From Wells, D. L. and Coopersmith, K. J., Empirical Relationships Among Magnitude, Rupture Length, Rupture Width, Rupture Area and Surface Displacements, *Bull. Seis. Soc. Am.*, 84(4), 974-1002, 1994. With permission.

TABLE 5.4 Modified Mercalli Intensity Scale of 1931

I	Not felt except by a very few under especially favorable circumstances.
II	Felt only by a few persons at rest, especially on upper floors of buildings. Delicately suspended objects may swing.
III	Felt quite noticeably indoors, especially on upper floors of buildings, but many people do not recognize it as an earthquake. Standing motor cars may rock slightly. Vibration like passing truck. Duration estimated.
IV	During the day felt indoors by many, outdoors by few. At night some awakened. Dishes, windows, and doors disturbed; walls make creaking sound. Sensation like heavy truck striking building. Standing motor cars rock noticeably.
V	Felt by nearly everyone; many awakened. Some dishes, windows, etc. broken; a few instances of cracked plaster; unstable objects overturned. Disturbance of trees, poles, and other tall objects sometimes noticed. Pendulum clocks may stop.
VI	Felt by all; many frightened and run outdoors. Some heavy furniture moved; a few instances of fallen plaster or damaged chimneys. Damage slight.
VII	Everybody runs outdoors. Damage negligible in buildings of good design and construction slight to moderate in well built ordinary structures; considerable in poorly built or badly designed structures. Some chimneys broken. Noticed by persons driving motor cars.
VIII	Damage slight in specially designed structures; considerable in ordinary substantial buildings, with partial collapse; great in poorly built structures. Panel walls thrown out of frame structures. Fall of chimneys, factory stacks, columns, monuments, walls. Heavy furniture overturned. Sand and mud ejected in small amounts. Changes in well water. Persons driving motor cars disturbed.
IX	Damage considerable in specially designed structures; well-designed frame structures thrown out of plumb; great in substantial buildings, with partial collapse. Buildings shifted off foundations. Ground cracked conspicuously. Underground pipes broken.
X	Some well-built wooden structures destroyed; most masonry and frame structures destroyed with foundations; ground badly cracked. Rails bent. Landslides considerable from river banks and steep slopes. Shifted sand and mud. Water splashed over banks.
XI	Few, if any (masonry), structures remain standing. Bridges destroyed. Broad fissures in ground. Underground pipelines completely out of service. Earth slumps and land slips in soft ground. Rails bent greatly.
XII	Damage total. Waves seen on ground surfaces. Lines of sight and level distorted. Objects thrown upward into the air.

After Wood, H. O. and Neumann, Fr., Modified Mercalli Intensity Scale of 1931, *Bull. Seis. Soc. Am.*, 21, 277-283, 1931.

TABLE 5.5 Comparison of Modified Mercalli (MMI) and Other Intensity Scales

a[a]	MMI[b]	R-F[c]	MSK[d]	JMA[e]
0.7	I	I	I	0
1.5	II	I to II	II	I
3	III	III	III	II
7	IV	IV to V	IV	II to III
15	V	V to VI	V	III
32	VI	VI to VII	VI	IV
68	VII	VIII-	VII	IV to V
147	VIII	VIII+ to IX−	VIII	V
316	IX	IX+	IX	V to VI
681	X	X	X	VI
(1468)[f]	XI	—	XI	VII
(3162)[f]	XII	—	XII	

[a] gals
[b] Modified Mercalli Intensity
[c] Rossi-Forel
[d] Medvedev-Sponheur-Karnik
[e] Japan Meteorological Agency
[f] a values provided for reference only. MMI > X are due more to geologic effects.

for many years in analog form on photographic film and, more recently, digitally. Analog records required considerable effort for correction due to instrumental drift, before they could be used.

Time histories theoretically contain complete information about the motion at the instrumental location, recording three *traces* or orthogonal records (two horizontal and one vertical). Time histories (i.e., the earthquake motion at the site) can differ dramatically in duration, frequency content, and amplitude. The maximum amplitude of recorded acceleration is termed the peak ground acceleration, PGA (also termed the ZPA, or zero period acceleration). Peak ground velocity (PGV) and peak ground displacement (PGD) are the maximum respective amplitudes of velocity and displacement. Acceleration is normally recorded, with velocity and displacement being determined by numerical integration; however, velocity and displacement meters are also deployed, to a lesser extent. Accel-

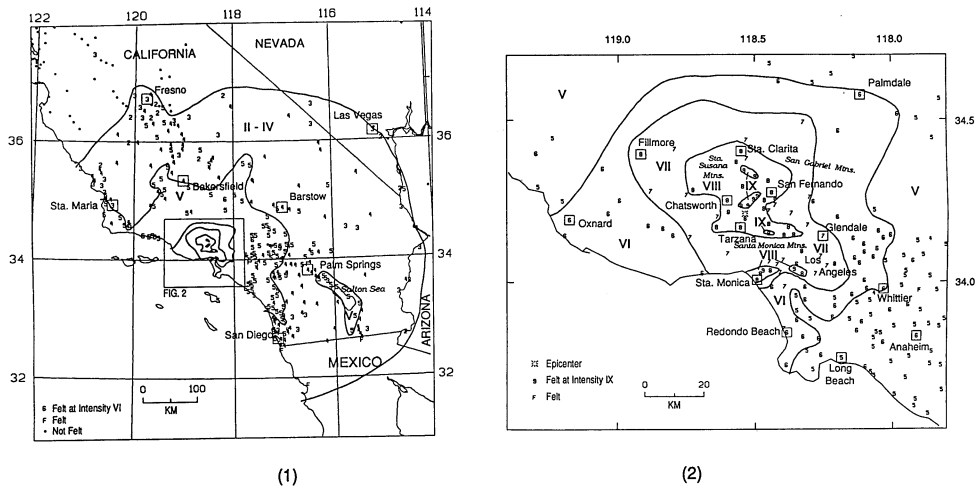

FIGURE 5.9: MMI maps, 1994 M_W 6.7 Northridge Earthquake. (1) Far-field isoseismal map. Roman numerals give average MMI for the regions between isoseismals; arabic numerals represent intensities in individual communities. Squares denote towns labeled in the figure. Box labeled "FIG. 2" identifies boundaries of that figure. (2) Distribution of MMI in the epicentral region. (Courtesy of Dewey, J.W. et al., Spacial Variations of Intensity in the Northridge Earthquake, in Woods, M.C. and Seiple, W.R., Eds., The Northridge California Earthquake of 17 January 1994, California Department of Conservation, Division of Mines and Geology, Special Publication 116, 39-46, 1995.)

eration can be expressed in units of cm/s^2 (termed gals), but is often also expressed in terms of the fraction or percent of the acceleration of gravity (980.66 gals, termed 1g). Velocity is expressed in cm/s (termed kine). Recent earthquakes (1994 Northridge, M_w 6.7 and 1995 Hanshin [Kobe] M_w 6.9) have recorded PGA's of about 0.8g and PGV's of about 100 kine — almost 2g was recorded in the 1992 Cape Mendocino earthquake.

Elastic Response Spectra

If the SDOF mass in Figure 5.1 is subjected to a time history of ground (i.e., base) motion similar to that shown in Figure 5.11, the elastic structural response can be readily calculated as a function of time, generating a structural response time history, as shown in Figure 5.12 for several oscillators with differing natural periods. The response time history can be calculated by direct integration of Equation 5.1 in the time domain, or by solution of the Duhamel integral [32]. However, this is time-consuming, and the elastic response is more typically calculated in the frequency domain

$$v(t) = \frac{1}{2\pi}\int_{\varpi=-\infty}^{\infty} H(\varpi)c(\varpi)\exp(i\varpi t)d\varpi \tag{5.15}$$

where

$v(t)$ = the elastic structural displacement response time history

ϖ = frequency

$H(\varpi)$ = $\frac{1}{-\varpi^2 m + ic + k}$ is the complex frequency response function

$c(\varpi)$ = $\int_{\varpi=-\infty}^{\infty} p(t)\exp(-i\varpi t)dt$ is the Fourier transform of the input motion (i.e., the Fourier transform of the ground motion time history)

which takes advantage of computational efficiency using the Fast Fourier Transform.

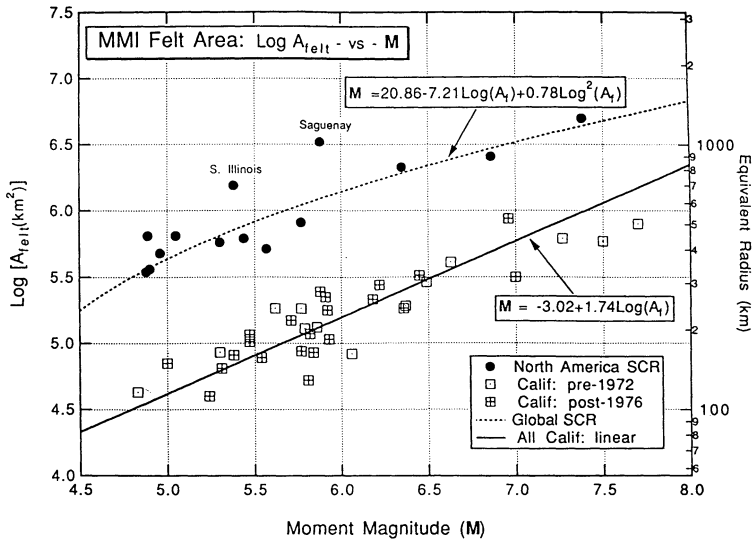

FIGURE 5.10: $\log A_{\text{felt}}$ (km^2) vs. M_W. Solid circles denote ENA events and open squares denote California earthquakes. The dashed curve is the $M_W - A_{\text{felt}}$ relationship of an earlier study, whereas the solid line is the fit determined by Hanks and Johnston, for California data. (Courtesy of Hanks J. W. and Johnston A. C., Common Features of the Excitation and Propagation of Strong Ground Motion for North American Earthquakes, *Bull. Seis. Soc. Am.*, 82(1), 1-23, 1992.)

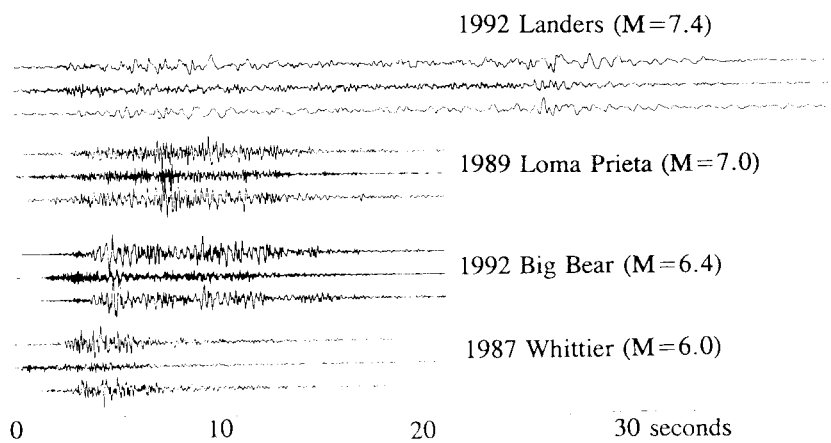

FIGURE 5.11: Typical earthquake accelerograms. (Courtesy of Darragh, R. B., Huang, M. J., and Shakal, A. F., Earthquake Engineering Aspects of Strong Motion Data from Recent California Earthquakes, *Proc. Fifth U.S. Natl. Conf. Earthquake Eng.*, 3, 99-108, 1994, Earthquake Engineering Research Institute. Oakland, CA.)

For design purposes, it is often sufficient to know only the maximum amplitude of the response time history. If the natural period of the SDOF is varied across a spectrum of engineering interest (typically, for natural periods from .03 to 3 or more seconds, or frequencies of 0.3 to 30+ Hz), then the plot of these maximum amplitudes is termed a response spectrum. Figure 5.12 illustrates this process, resulting in S_d, the *displacement response spectrum*, while Figure 5.13 shows (a) the S_d,

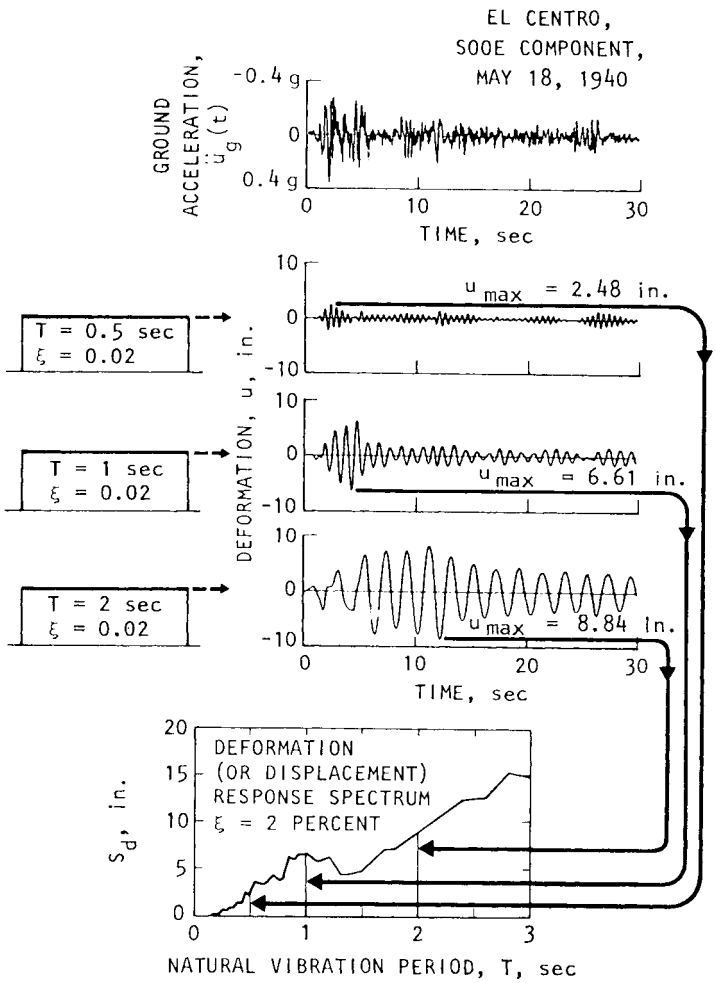

FIGURE 5.12: Computation of deformation (or displacement) response spectrum. (From Chopra, A. K., *Dynamics of Structures, A Primer,* Earthquake Engineering Research Institute, Oakland, CA, 1981. With permission.)

displacement response spectrum, (b) S_v, the *velocity response spectrum* (also denoted PSV, the pseudo spectral velocity, pseudo to emphasize that this spectrum is not exactly the same as the relative velocity response spectrum [63], and (c) S_a, the acceleration *response spectrum*. Note that

$$S_v = \frac{2\pi}{T} S_d = \varpi S_d \tag{5.16}$$

and

$$S_a = \frac{2\pi}{T} S_v = \varpi S_v = \left(\frac{2\pi}{T}\right)^2 S_d = \varpi^2 S_d \tag{5.17}$$

Response spectra form the basis for much modern earthquake engineering structural analysis and design. They are readily calculated *if* the ground motion is known. For design purposes, however, response spectra must be estimated. This process is discussed below. Response spectra may be plotted in any of several ways, as shown in Figure 5.13 with arithmetic axes, and in Figure 5.14 where the

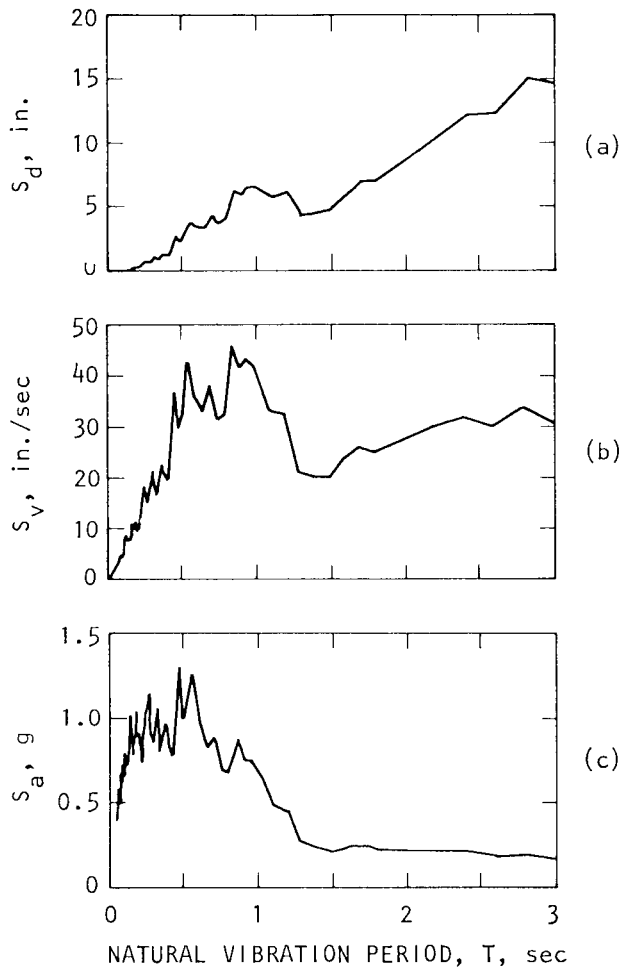

FIGURE 5.13: Response spectra spectrum. (From Chopra, A. K., *Dynamics of Structures, A Primer,* Earthquake Engineering Research Institute, Oakland, CA, 1981. With permission.)

velocity response spectrum is plotted on tripartite logarithmic axes, which equally enables reading of displacement and acceleration response. Response spectra are most normally presented for 5% of critical damping.

While actual response spectra are irregular in shape, they generally have a concave-down arch or trapezoidal shape, when plotted on tripartite log paper. Newmark observed that response spectra tend to be characterized by three regions: (1) a region of constant acceleration, in the high frequency portion of the spectra; (2) constant displacement, at low frequencies; and (3) constant velocity, at intermediate frequencies, as shown in Figure 5.15. If a spectrum amplification factor is defined as the ratio of the spectral parameter to the ground motion parameter (where parameter indicates acceleration, velocity or displacement), then response spectra can be estimated from the data in Table 5.6, provided estimates of the ground motion parameters are available. An example spectra using these data is given in Figure 5.15.

A standardized response spectra is provided in the Uniform Building Code [126] for three soil types. The spectra is a smoothed average of normalized 5% damped spectra obtained from actual ground

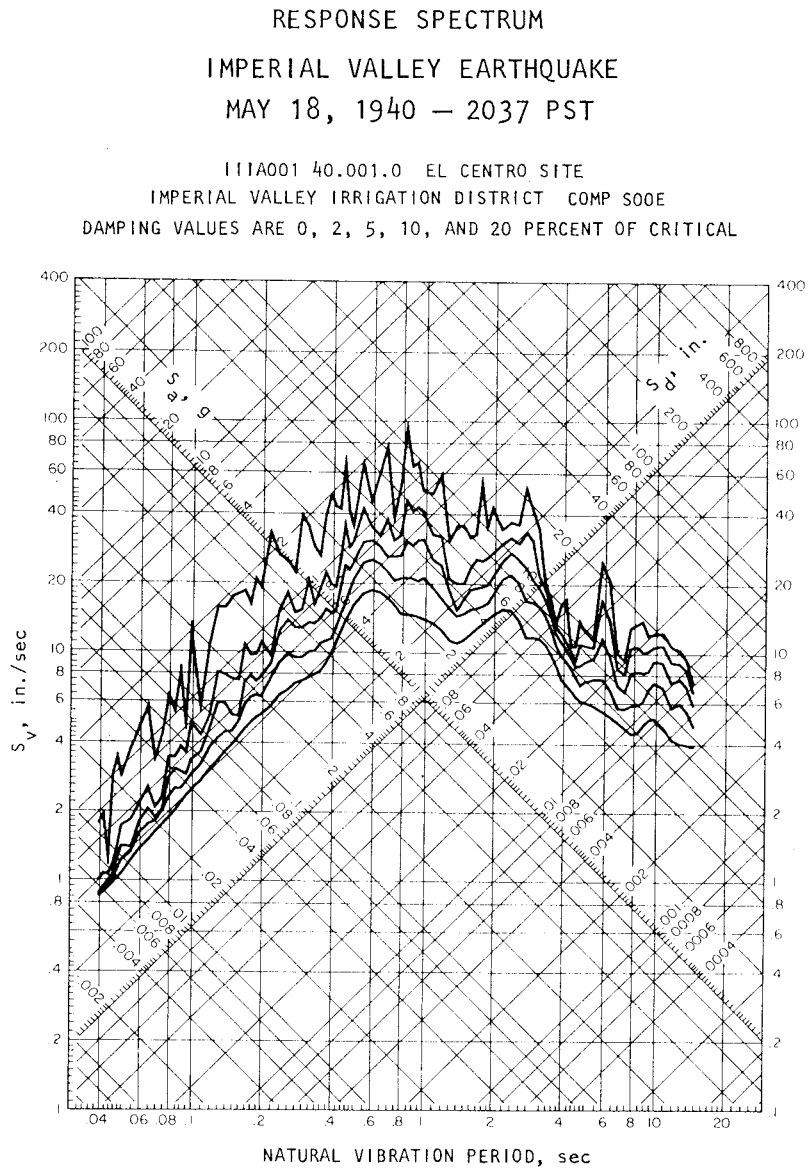

FIGURE 5.14: Response spectra, tri-partite plot (El Centro S 0° E component). (From Chopra, A. K., *Dynamics of Structures, A Primer,* Earthquake Engineering Research Institute, Oakland, CA, 1981. With permission.)

motion records grouped by subsurface soil conditions at the location of the recording instrument, and are applicable for earthquakes characteristic of those that occur in California [111]. If an estimate of ZPA is available, these normalized shapes may be employed to determine a response spectra, appropriate for the soil conditions. Note that the maximum amplification factor is 2.5, over a period range approximately 0.15 s to 0.4 - 0.9 s, depending on the soil conditions. Other methods for estimation of response spectra are discussed below.

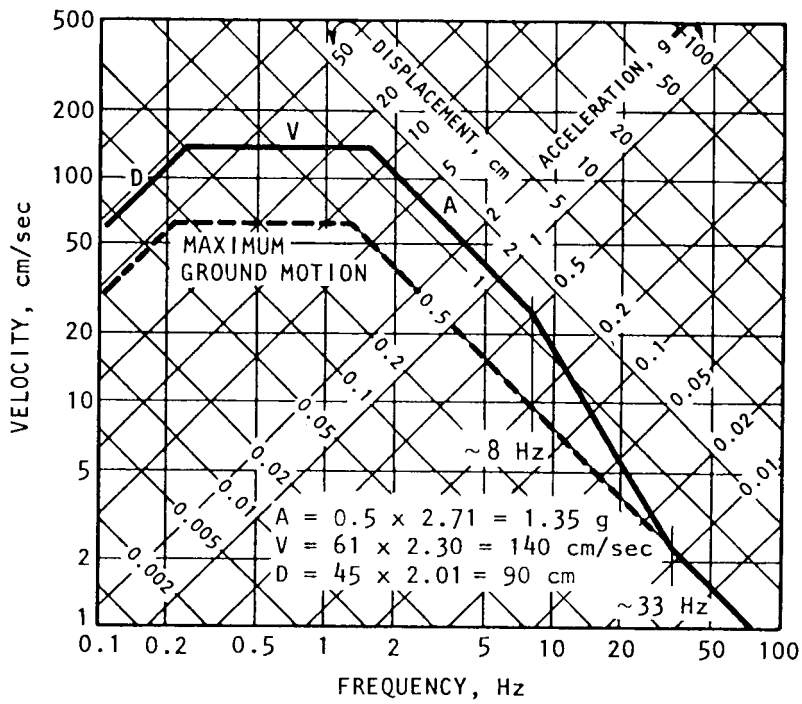

FIGURE 5.15: Idealized elastic design spectrum, horizontal motion (ZPA = 0.5g, 5% damping, one sigma cumulative probability. (From Newmark, N. M. and Hall, W. J., *Earthquake Spectra and Design*, Earthquake Engineering Research Institute, Oakland, CA, 1982. With permission.)

TABLE 5.6 Spectrum Amplification Factors for Horizontal Elastic Response

Damping,	One sigma (84.1%)			Median (50%)		
% Critical	A	V	D	A	V	D
0.5	5.10	3.84	3.04	3.68	2.59	2.01
1	4.38	3.38	2.73	3.21	2.31	1.82
2	3.66	2.92	2.42	2.74	2.03	1.63
3	3.24	2.64	2.24	2.46	1.86	1.52
5	2.71	2.30	2.01	2.12	1.65	1.39
7	2.36	2.08	1.85	1.89	1.51	1.29
10	1.99	1.84	1.69	1.64	1.37	1.20
20	1.26	1.37	1.38	1.17	1.08	1.01

From Newmark, N. M. and Hall, W. J., *Earthquake Spectra and Design*, Earthquake Engineering Research Institute, Oakland, CA, 1982. With permission.

Inelastic Response Spectra

While the foregoing discussion has been for elastic response spectra, most structures are not expected, or even designed, to remain elastic under strong ground motions. Rather, structures are expected to enter the *inelastic* region — the extent to which they behave inelastically can be defined by the ductility factor, μ

$$\mu = \frac{u_m}{u_y} \tag{5.18}$$

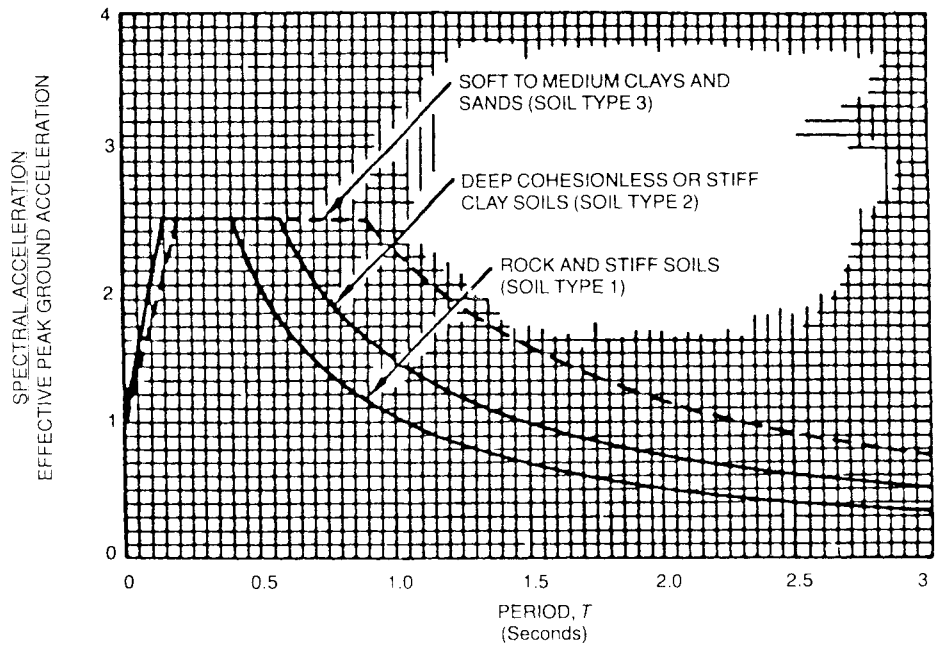

FIGURE 5.16: Normalized response spectra shapes. (From Uniform Building Code, Structural Engineering Design Provisions, vol. 2, Intl. Conf. Building Officials, Whittier, 1994. With permission.)

where u_m is the maximum displacement of the mass under actual ground motions, and u_y is the displacement at yield (i.e., that displacement which defines the extreme of elastic behavior). Inelastic response spectra can be calculated in the time domain by direct integration, analogous to elastic response spectra but with the structural stiffness as a non-linear function of displacement, $k = k(u)$. If elastoplastic behavior is assumed, then elastic response spectra can be readily modified to reflect inelastic behavior [90] on the basis that (a) at low frequencies (0.3 Hz $<$) displacements are the same; (b) at high frequencies ($>$ 33 Hz), accelerations are equal; and (c) at intermediate frequencies, the absorbed energy is preserved. Actual construction of inelastic response spectra on this basis is shown in Figure 5.17, where $DVAA_o$ is the elastic spectrum, which is reduced to D' and V' by the ratio of $1/\mu$ for frequencies less than 2 Hz, and by the ratio of $1/(2\mu - 1)^{1/2}$ between 2 and 8 Hz. Above 33 Hz there is no reduction. The result is the inelastic acceleration spectrum $(D'V'A'A_o)$, while $A''A'_o$ is the inelastic displacement spectrum. A specific example, for ZPA = 0.16g, damping = 5% of critical, and $\mu = 3$ is shown in Figure 5.18.

Response Spectrum Intensity and Other Measures

While the elastic response spectrum cannot directly define damage to a structure (which is essentially inelastic deformation), it captures in one curve the amount of elastic deformation for a wide variety of structural periods, and therefore may be a good overall measure of ground motion intensity. On this basis, Housner defined a response spectrum intensity as the integral of the elastic response spectrum velocity over the period range 0.1 to 2.5 s.

$$SI(h) = \int_{T=0.1}^{2.5} Sv(h, T)dT \tag{5.19}$$

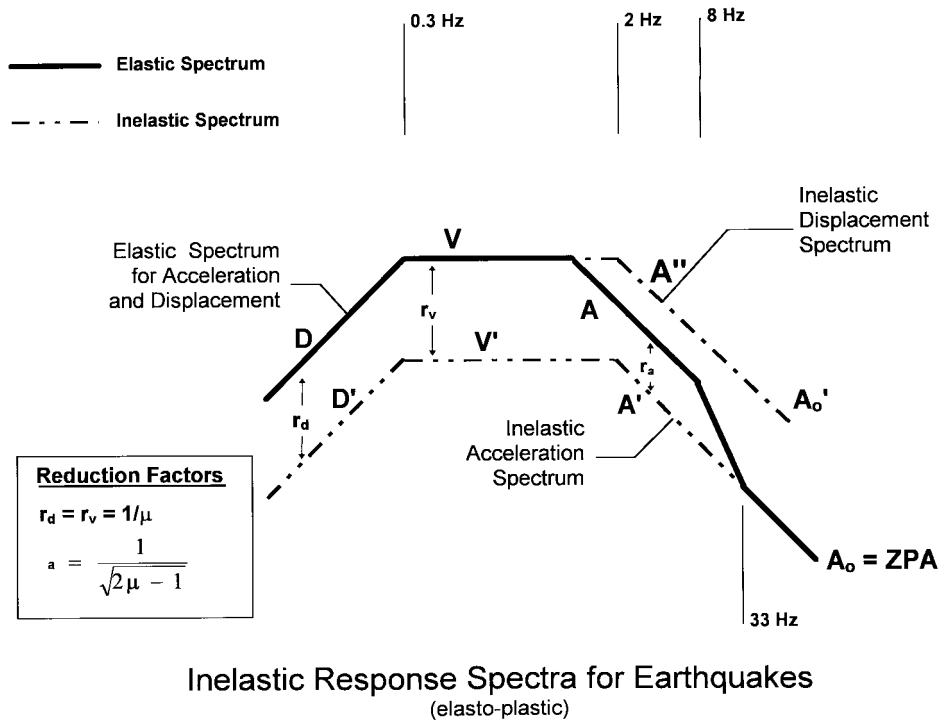

FIGURE 5.17: Inelastic response spectra for earthquakes. (After Newmark, N. M. and Hall, W. J., *Earthquake Spectra and Design*, Earthquake Engineering Research Institute, Oakland, CA, 1982.)

where h = damping (as a percentage of c_{crit}). A number of other measures exist, including Fourier amplitude spectrum [32] and Arias Intensity [8]:

$$I_A = \frac{\pi}{g} \int_0^t a^2(t)dt \tag{5.20}$$

Engineering Intensity Scale

Lastly, Blume [14] defined a measure of earthquake intensity, the Engineering Intensity Scale (EIS), which has been relatively underutilized but is worth noting as it attempts to combine the engineering benefits of response spectra with the simplicity of qualitative intensity scales, such as MMI. The EIS is simply a 10x9 matrix which characterizes a 5% damped elastic response spectra (Figure 5.19). Nine period bands (0.01-.1, -.2, -.4, -.6, -1.0, -2.0, - 4.0, -7.0, -10,0 s), and ten S_v levels (0.01-0.1, -1.0, -4.0, -10.0, -30.0, -60.0, -100., -300., -1000. kine) are defined. As can be seen, since the response spectrum for the example ground motion in period band II (0.1-0.2 s) is predominantly in S_v level 5 (10-30 kine), it is assigned EIS 5 (X is assigned where the response spectra does not cross a period band). In this manner, a nine-digit EIS can be assigned to a ground motion (in the example, it is X56,777,76X), which can be reduced to three digits (5,7,6) by averaging, or even to one digit (6, for this example). Numerically, single digit EIS values tend to be a unit or so lower than the equivalent MMI intensity value.

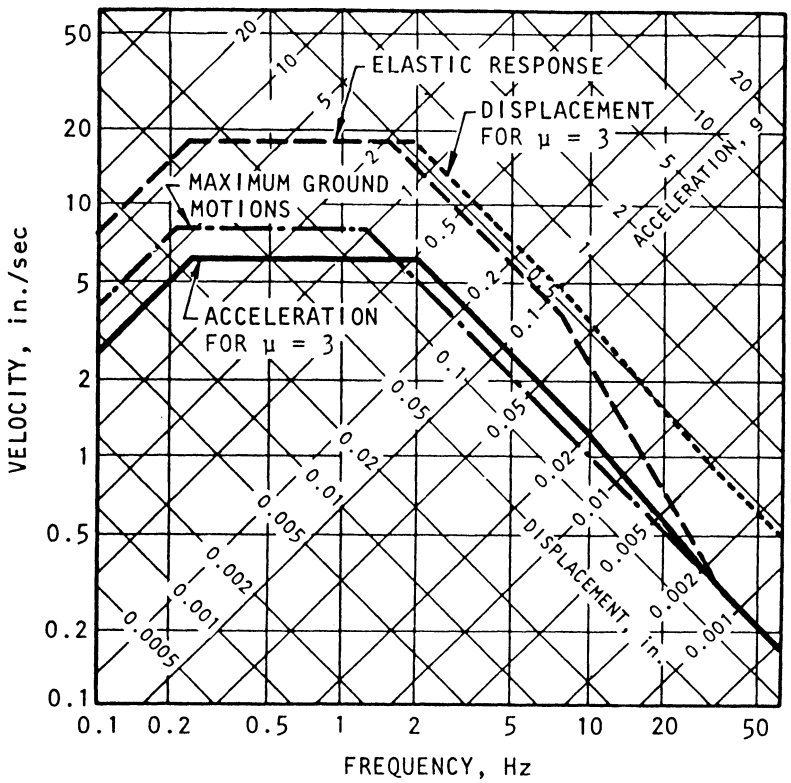

FIGURE 5.18: Example inelastic response spectra. (From Newmark, N. M. and Hall, W. J., *Earthquake Spectra and Design*, Earthquake Engineering Research Institute, Oakland, CA, 1982. With permission.)

5.2.4 Strong Motion Attenuation and Duration

The rate at which earthquake ground motion decreases with distance, termed attenuation, is a function of the regional geology and inherent characteristics of the earthquake and its source. Three major factors affect the severity of ground shaking at a site: (1) source — the size and type of the earthquake, (2) path — the distance from the source of the earthquake to the site and the geologic characteristics of the media earthquake waves pass through, and (3) site-specific effects — type of soil at the site. In the simplest of models, if the seismogenic source is regarded as a point, then from considering the relation of energy and earthquake magnitude and the fact that the volume of a hemisphere is proportion to R^3 (where R represents radius), it can be seen that energy per unit volume is proportional to $C10^{aM}R^{-3}$, where C is a constant or constants dependent on the earth's crustal properties. The constant C will vary regionally — for example, it has long been observed that attenuation in eastern North America (ENA) varies significantly from that in western North America (WNA) — earthquakes in ENA are felt at far greater distances. Therefore, attenuation relations are regionally dependent. Another regional aspect of attenuation is the definition of terms, especially magnitude, where various relations are developed using magnitudes defined by local observatories.

A very important aspect of attenuation is the definition of the distance parameter; because attenuation is the change of ground motion with location, this is clearly important. Many investigators use differing definitions; as study has progressed, several definitions have emerged: (1) hypocentral distance (i.e., straight line distance from point of interest to hypocenter, where hypocentral distance

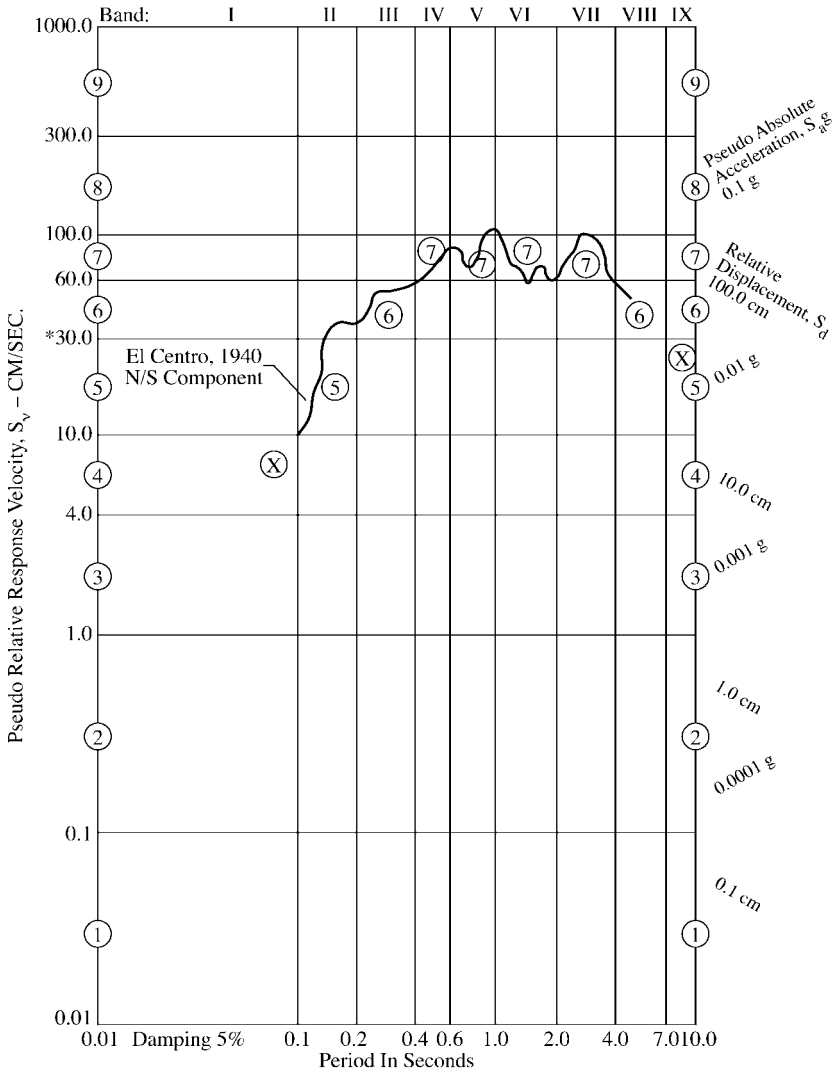

FIGURE 5.19: Engineering intensity scale (EIS) matrix with example. (From Blume, J. A., An Engineering Intensity Scale for Earthquakes and Other Ground Motions, *Bull. Seis. Soc. Am.*, 60(1), 217-229, 1970. With permission.)

may be arbitrary or based on regression rather than observation), (2) epicentral distance, (3) closest distance to the causative fault, and (4) closest horizontal distance from the station to the point on the earth's surface that lies directly above the seismogenic source. In using attenuation relations, it is critical that the correct definition of distance is consistently employed.

Methods for estimating ground motion may be grouped into two major categories: empirical and methods based on seismological models. Empirical methods are more mature than methods based on seismological models, but the latter are advantageous in explicitly accounting for source and path, therefore having explanatory value. They are also flexible, they can be extrapolated with more confidence, and they can be easily modified for additional factors. Most seismological model-based methods are stochastic in nature — Hanks and McGuire's [54] seminal paper has formed the basis

for many of these models, which "assume that ground acceleration is a finite-duration segment of a stationary random process, completely characterized by the assumption that acceleration follows Brune's [23] source spectrum (for California data, typically about 100 bars), and that the duration of strong shaking is equal to reciprocal of the source corner frequency" f_o (the frequency above which earthquake radiation spectra vary with ϖ^{-3} - below f_o, the spectra are proportional to seismic moment [108]). Since there is substantial ground motion data in WNA, seismological model-based relations have had more value in ENA, where few records exist. The Hanks-McGuire method has, therefore, been usefully applied in ENA [123] where Boore and Atkinson [18] found, for hard-rock sites, the relation:

$$\log y = c_0 + c_1 r - \log r \tag{5.21}$$

where

y = a ground motion parameter (PSV, unless c_i coefficients for $a_{\max}$ are used)
r = hypocentral distance (km)
c_i = $\xi_o^i + \sum \xi_n^i (M_W - 6)^n \quad I = 0, 1$ summation for $n = 1, 2, 3$ (see Table 5.7)

TABLE 5.7 Eastern North America Hard-Rock Attenuation Coefficients[a]

Response frequency (Hz)		ξ_0	ξ_1	ξ_2	ξ_3
0.2	c_0:	$1.743E+00$	$1.064E+00$	$-4.293E-02$	$-5.364E-02$
	c_1:	$-3.130E-04$	$1.415E-03$	$-1.028E-03$	
0.5	c_0:	$2.141E+00$	$8.521E-01$	$-1.670E-01$	
	c_1:	$-2.504E-04$		$-2.612E-04$	
1.0	c_0:	$2.300E+00$	$6.655E-01$	$-1.538E-01$	
	c_1:	$-1.024E-03$	$-1.144E-04$	$1.109E-04$	
2.0	c_0:	$2.317E+00$	$5.070E-01$	$-9.317E-02$	
	c_1:	$-1.683E-03$	$1.492E-04$	$1.203E-04$	
5.0	c_0:	$2.239E+00$	$3.976E-01$	$-4.564E-02$	
	c_1:	$-2.537E-03$	$5.468E-04$	$7.091E-05$	
10.0	c_0:	$2.144E+00$	$3.617E-01$	$-3.163E-02$	
	c_1:	$-3.094E-03$	$7.640E-04$		
20.0	c_0:	$2.032E+00$	$3.438E-01$	$-2.559E-02$	
	c_1:	$-3.672E-03$	$8.956E-04$	$-4.219E-05$	
$a_{\max}$	c_0:	$3.763E+00$	$3.354E-01$	$-2.473E-02$	
	c_1:	$-3.885E-03$	$1.042E-03$	$-9.169E-05$	

[a] See Equation 5.21.
From Boore, D.M. and Atkinson, G.M., Stochastic Prediction of Ground Motion and Spectral Response Parameters at Hard-Rock Sites in Eastern North America, *Bull. Seis. Soc. Am.*, 77, 440-487, 1987. With permission.

Similarly, Toro and McGuire [123] furnish the following relation for rock sites in ENA:

$$\ln Y = c_0 + c_1 M + c_2 \ln(R) + c_3 R \tag{5.22}$$

where the c_0 - c_3 coefficients are provided in Table 5.8, M represents m_{Lg}, and R is the closest distance between the site and the causative fault at a minimum depth of 5 km.

These results are valid for hypocentral distances of 10 to 100 km, and m_{Lg} 4 to 7.

More recently, Boore and Joyner [19] have extended their hard-rock relations to deep soil sites in ENA:

$$\log y = a'' + b(m-6) + c(m-6)^2 + d(m-6)^3 - \log r + kr \tag{5.23}$$

where a'' and other coefficients are given in Table 5.9, m is moment magnitude (M_W), and r is hypocentral distance (km) although the authors suggest that, close to long faults, the distance should

TABLE 5.8 ENA Rock Attenuation Coefficients[a]

Y	c_0	c_1	c_2	c_3
PSRV (1 Hz)	−9.283	2.289	−1.000	−.00183
PSRV (5 Hz)	−2.757	1.265	−1.000	−.00310
PSRV (10 Hz)	−1.717	1.069	−1.000	−.00391
PGA (cm/s^2)	2.424	0.982	−1.004	−.00468

[a] See Equation 5.22.
Spectral velocities are given in cm/s; peak acceleration is given in cm/s^2
From Toro, G.R. and McGuire, R.K., An Investigation Into Earthquake Ground Motion Characteristics in Eastern North America, *Bull. Seis. Soc. Am.*, 77, 468-489, 1987. With permission.

be the nearest distance to seismogenic rupture. The coefficients in Table 5.9 should not be used outside the ranges $10 < r < 400$ km, and $5.0 < M_W < 8.5$.

TABLE 5.9 Coefficients for Ground-Motion Estimation at Deep-Soil Sites in Eastern North America in Terms of M_W^a

T (sec)	a'	a''	b	c	d	k	M at max[b]
S_V							
0.05	0.020	1.946	0.431	− 0.028	− 0.018	− 0.00350	8.35
0.10	0.040	2.267	0.429	− 0.026	− 0.018	− 0.00240	8.38
0.15	0.015	2.377	0.437	− 0.031	− 0.017	− 0.00190	8.38
0.20	0.015	2.461	0.447	− 0.037	− 0.016	− 0.00168	8.38
0.30	0.010	2.543	0.472	− 0.051	− 0.012	− 0.00140	8.47
0.40	0.015	2.575	0.499	− 0.066	− 0.009	− 0.00110	8.50
0.50	0.010	2.588	0.526	− 0.080	− 0.007	− 0.00095	8.48
0.75	0.000	2.586	0.592	− 0.111	− 0.001	− 0.00072	8.58
1.00	0.000	2.567	0.655	− 0.135	0.002	− 0.00058	8.57
1.50	0.000	2.511	0.763	− 0.165	0.004	− 0.00050	8.55
2.00	0.000	2.432	0.851	− 0.180	0.002	− 0.00039	8.47
3.00	0.000	2.258	0.973	− 0.176	− 0.008	− 0.00027	8.38
4.00	0.000	2.059	1.039	− 0.145	− 0.022	− 0.00020	8.34
$a_{\max}$	0.030	3.663	0.448	− 0.037	− 0.016	− 0.00220	8.38
$S_{V\,\max}$	0.020	2.596	0.608	− 0.038	− 0.022	− 0.00055	8.51
$S_{A\,\max}$	0.040	4.042	0.433	− 0.029	− 0.017	− 0.00180	8.40

[a] The distance used is generally the hypocentral distance; we suggest that, close to long faults, the distance should be the nearest distance to seismogenic rupture. The response spectra are for random horizontal components and 5% damping. The units of $a_{\max}$ and S_A are cm/s^2; the units of S_V are cm/s. The coefficients in this table should not be used outside the ranges $10 \leq r \leq 400$ km and $5.0 \leq M \leq 8.5$. See also Equation 5.23.
[b] "M at max" is the magnitude at which the cubic equation attains its maximum value; for larger magnitudes, we recommend that the motions be equated to those for "M at max".
From Boore, D.M. and Joyner, W.B., Estimation of Ground Motion at Deep-Soil Sites in Eastern North America, *Bull. Seis. Soc. Am.*, 81(6), 2167-2185, 1991. With permission.

In WNA, due to more data, empirical methods based on regression of the ground motion parameter vs. magnitude and distance have been more widely employed, and Campbell [28] offers an excellent review of North American relations up to 1985. Initial relationships were for PGA, but regression of the amplitudes of response spectra at various periods is now common, including consideration of fault type and effects of soil.

Some current favored relationships are:

Campbell and Bozorgnia [29] (PGA - Worldwide Data)

$$\begin{aligned}\ln(PGA) &= -3.512 + 0.904M - 1.328\ln\sqrt{\{R_s^2 + [0.149\exp(0.647M)]^2\}} \\ &\quad + [1.125 - 0.112\ln(R_s) - 0.0957M]F\end{aligned}$$

$$+ [0.440 - 0.171 \ln(R_s)]S_{sr} + [0.405 - 0.222 \ln(R_s)]S_{hr} + \varepsilon \qquad (5.24)$$

where

PGA	=	the geometric mean of the two horizontal components of peak ground acceleration (g)
M	=	moment magnitude (M_W)
R_s	=	the closest distance to seismogenic rupture on the fault (km)
F	=	0 for strike-slip and normal faulting earthquakes, and 1 for reverse, reverse-oblique, and thrust faulting earthquakes
S_{sr}	=	1 for soft-rock sites
S_{hr}	=	1 for hard-rock sites
$S_{sr} = S_{hr}$	=	0 for alluvium sites
ε	=	a random error term with zero mean and standard deviation equal to $\sigma_{\ln}(PGA)$, the standard error of estimate of $\ln(PGA)$

This relation is intended for meizoseismal applications, and should not be used to estimate PGA at distances greater than about 60 km (the limit of the data employed for the regression). The relation is based on 645 near-source recordings from 47 worldwide earthquakes (33 of the 47 are California records — among the other 14 are the 1985 M_W 8.0 Chile, 1988 M_W 6.8 Armenia, and 1990 M_W 7.4 Manjil Iran events). R_s should not be assigned a value less than the depth of the top of the seismogenic crust, or 3 km. Regarding the uncertainty, ε was estimated as:

$$\sigma_{\ln}(PGA) = \left| \begin{array}{ll} 0.55 & \text{if } PGA < 0.068 \\ 0.173 - 0.140 \ln(PGA) & \text{if } 0.068 \le PGA \le 0.21 \\ 0.39 & \text{if } PGA > 0.21 \end{array} \right.$$

Figure 5.20 indicates, for alluvium, median values of the attenuation of peak horizontal acceleration with magnitude and style of faulting.

Joyner and Boore (PSV - WNA Data) [20, 67]

Similar to the above but using a two-step regression technique in which the ground motion parameter is first regressed against distance and then amplitudes regressed against magnitude, Boore, Joyner, and Fumal [20] have used WNA data to develop relations for PGA and PSV of the form:

$$\log Y = b_1 + b_2(M - 6) + b_3(M - 6)^2 + b_4 r + b_5 \log_{10} r + b_6 G_B + b_7 G_C + \varepsilon_r + \varepsilon_e \qquad (5.25)$$

where

Y	=	the ground motion parameter (in cm/s for PSV, and g for PGA)
M	=	moment magnitude (M_W)
r	=	$(d^2 + h^2)^{(1/2)}$ = distance (km), where h is a fictitious depth determined by regression, and d is the closest horizontal distance from the station to the point on the earth's surface that lies directly above the rupture
G_B, G_C	=	site classification indices ($G_B = 1$ for class B site, $G_C = 1$ for class C site, both zero otherwise), where Site Class A has shear wave velocities (averaged over the upper 30 m) > 750 m/s, Site Class B is 360 to 750 m/s, and Site Class C is 180 to 360 m/s (class D sites, < 180 m/s, were not included). In effect, class A are rock, B are firm soil sites, C are deep alluvium/soft soils, and D would be very soft sites
$\varepsilon_r + \varepsilon_e$	=	independent random variable measures of uncertainty, where ε_r takes on a specific value for each record, and ε_e for each earthquake
b_i, h	=	coefficients (see Table 5.10 and Table 5.11)

The relation is valid for magnitudes between 5 and 7.7, and for distances (d) $\le$ 100 km. The coefficients in Equation 5.25 are for 5% damped response spectra — Boore et al. [20] also provide similar coefficients for 2%, 10%, and 20% damped spectra, as well as for the random horizontal

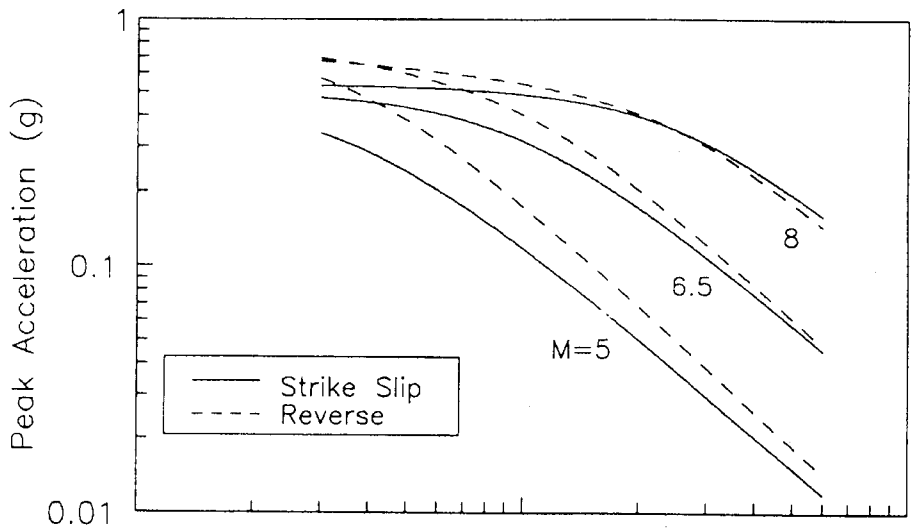

FIGURE 5.20: Campbell and Bozorgnia worldwide attenuation relationship showing (for alluvium) the scaling of peak horizontal acceleration with magnitude and style of faulting. (From Campbell, K.W. and Bozorgnia, Y., Near-Source Attenuation of Peak Horizontal Acceleration from Worldwide Accelerograms Recorded from 1957 to 1993, Proc. Fifth U.S. National Conference on Earthquake Engineering, Earthquake Engineering Research Institute, Oakland, CA, 1994. With permission.)

coefficient (i.e., both horizontal coefficients, not just the larger, are considered). Figure 5.21 presents curves of attenuation of PGA and PSV for Site Class C, using these relations, while Figure 5.22 presents a comparison of this, the Campbell and Bozorgnia [29] and Sadigh et al. [105] attenuation relations, for two magnitude events on alluvium.

The foregoing has presented attenuation relations for PGA (Worldwide) and response spectra (ENA and WNA). While there is some evidence [136] that meizoseismal strong ground motion may not differ as much regionally as previously believed, regional attenuation in the far-field differs significantly (e.g., ENA vs. WNA). One regime that has been treated in a special class has been large subduction zone events, such as those that occur in the North American Pacific Northwest (PNW), in Alaska, off the west coast of Central and South America, off-shore Japan, etc. This is due to the very large earthquakes that are generated in these zones, with long duration and a significantly different path. A number of relations have been developed for these events [10, 37, 81, 115, 138] which should be employed in those regions. A number of other investigators have developed attenuation relations for other regions, such as China, Japan, New Zealand, the Trans-Alpide areas, etc., which should be reviewed when working in those areas (see the References).

In addition to the seismologically based and empirical models, there is another method for attenuation or ground motion modeling, which may be termed semi-empirical methods (Figure 5.23) [129]. The approach discretizes the earthquake fault into a number of subfault elements, finite rupture on each of which is modeled with radiation therefrom modeled via Green's functions. The resulting wave-trains are combined with empirical modeling of scattering and other factors to generate time-histories of ground motions for a specific site. The approach utilizes a rational framework with powerful explanatory features, and offers useful application in the very near-field of large earthquakes, where it is increasingly being employed.

The foregoing has also dealt exclusively with *horizontal* ground motions, yet vertical ground motions can be very significant. The common practice for many years has been to take the ratio (V/H)

TABLE 5.10 Coefficients for 5% Damped PSV, for the Larger Horizontal Component

T(s)	B1	B2	B3	B4	B5	B6	B7	H
.10	1.700	.321	−.104	.00000	−.921	.039	.128	6.18
.11	1.777	.320	−.110	.00000	−.929	.065	.150	6.57
.12	1.837	.320	−.113	.00000	−.934	.087	.169	6.82
.13	1.886	.321	−.116	.00000	−.938	.106	.187	6.99
.14	1.925	.322	−.117	.00000	−.939	.123	.203	7.09
.15	1.956	.323	−.117	.00000	−.939	.137	.217	7.13
.16	1.982	.325	−.117	.00000	−.939	.149	.230	7.13
.17	2.002	.326	−.117	.00000	−.938	.159	.242	7.10
.18	2.019	.328	−.115	.00000	−.936	.169	.254	7.05
.19	2.032	.330	−.114	.00000	−.934	.177	.264	6.98
.20	2.042	.332	−.112	.00000	−.931	.185	.274	6.90
.22	2.056	.336	−.109	.00000	−.926	.198	.291	6.70
.24	2.064	.341	−.105	.00000	−.920	.208	.306	6.48
.26	2.067	.345	−.101	.00000	−.914	.217	.320	6.25
.28	2.066	.349	−.096	.00000	−.908	.224	.333	6.02
.30	2.063	.354	−.092	.00000	−.902	.231	.344	5.79
.32	2.058	.358	−.088	.00000	−.897	.236	.354	5.57
.34	2.052	.362	−.083	.00000	−.891	.241	.363	5.35
.36	2.045	.366	−.079	.00000	−.886	.245	.372	5.14
.38	2.038	.369	−.076	.00000	−.881	.249	.380	4.94
.40	2.029	.373	−.072	.00000	−.876	.252	.388	4.75
.42	2.021	.377	−.068	.00000	−.871	.255	.395	4.58
.44	2.013	.380	−.065	.00000	−.867	.258	.401	4.41
.46	2.004	.383	−.061	.00000	−.863	.261	.407	4.26
.48	1.996	.386	−.058	.00000	−.859	.263	.413	4.16
.50	1.988	.390	−.055	.00000	−.856	.265	.418	3.97
.55	1.968	.397	−.048	.00000	−.848	.270	.430	3.67
.60	1.949	.404	−.042	.00000	−.842	.275	.441	3.43
.65	1.932	.410	−.037	.00000	−.837	.279	.451	3.23
.70	1.917	.416	−.033	.00000	−.833	.283	.459	3.08
.75	1.903	.422	−.029	.00000	−.830	.287	.467	2.97
.80	1.891	.427	−.025	.00000	−.827	.290	.474	2.89
.85	1.881	.432	−.022	.00000	−.826	.294	.481	2.85
.90	1.872	.436	−.020	.00000	−.825	.297	.486	2.83
.95	1.864	.440	−.018	.00000	−.825	.301	.492	2.84
1.00	1.858	.444	−.016	.00000	−.825	.305	.497	2.87
1.10	1.849	.452	−.014	.00000	−.828	.312	.506	3.00
1.20	1.844	.458	−.013	.00000	−.832	.319	.514	3.19
1.30	1.842	.464	−.012	.00000	−.837	.326	.521	3.44
1.40	1.844	.469	−.013	.00000	−.843	.334	.527	3.74
1.50	1.849	.474	−.014	.00000	−.851	.341	.533	4.08
1.60	1.857	.478	−.016	.00000	−.859	.349	.538	4.46
1.70	1.866	.482	−.019	.00000	−.868	.357	.543	4.86
1.80	1.878	.485	−.022	.00000	−.878	.365	.547	5.29
1.90	1.891	.488	−.025	.00000	−.888	.373	.551	5.74
2.00	1.905	.491	−.028	.00000	−.898	.381	.554	6.21

The equations are to be used for $5.0 <= M <= 7.7$ and $d <= 100.0$ km.
From Boore, D. M., Joyner, W. B., and Fumal, T. E., Estimation of Response Spectra and Peak Acceleration from Western North American Earthquakes: An Interim Report, U.S.G.S. Open-File Report 93-509, Menlo Park, CA, 1993. With permission.

TABLE 5.11 Coefficients for the Random and Larger Horizontal Components of Peak Acceleration

Comp.	b_1	b_2	b_3	b_4	b_5	b_6	b_7	h
Random	−.105	.229	0	0	−.778	.162	.251	5.57
Larger	−.038	.216	0	0	−.777	.158	.254	5.48

Courtesy of Boore, D.M., Joyner, W.B., and Fumal, T.E., Estimation of Response Spectra and Peak Acceleration from Western North American Earthquakes: An Interim Report, U.S.G.S. Open-File Report 93-509, Menlo Park, CA, 1993.

as one half or two thirds (practice varies). Recent work [22] has found that response spectra V/H ratio is a function of period, distance to source, and magnitude, with the ratio being larger than 2/3 in the near-field and having a peak at about 0.1 s, and less than 2/3 at long periods.

An important aspect of ground motion is duration — larger earthquakes shake longer, forcing structures through more (typically inelastic) cycles and thus tending to cause more damage. Since

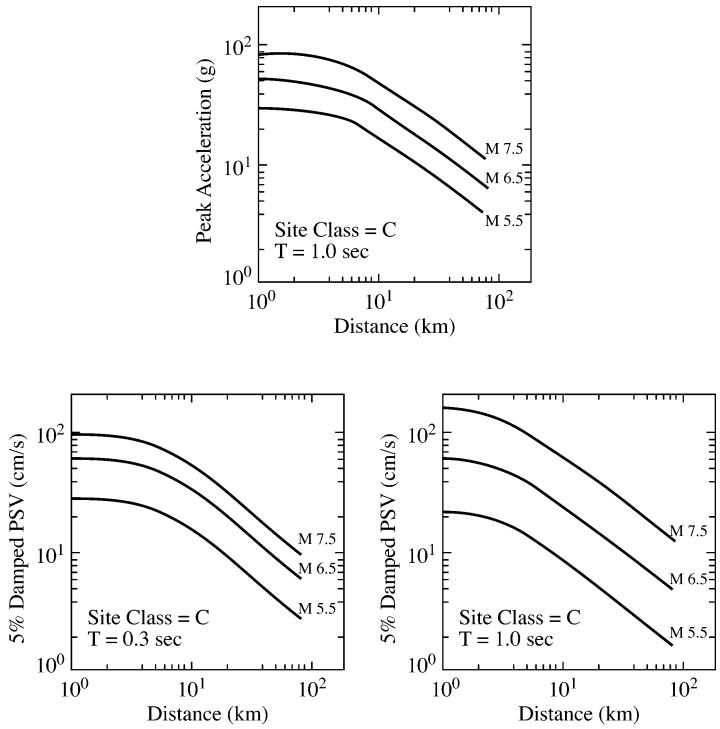

FIGURE 5.21: Attenuation of PGA and PSV for Site Class C. (From Boore, D.M., Joyner, W.B., and Fumal, T.E., Estimation of Response Spectra and Peak Acceleration from Western North American Earthquakes: An Interim Report, U.S.G.S. Open-File Report 93-509, Menlo Park, CA, 1993. With permission.)

a typical fault rupture velocity [16] may be on the order of 2.5 km/s, it can be readily seen from Equation 5.11 that a magnitude 7 event will require about 14 s for fault rupture, and a magnitude 7.5 event about 40 s (and note that the radiated wave train will increase in duration due to scattering). Thus, strong ground motion can be felt for several seconds to significantly longer than a minute. Because the duration of strong ground motion is very significant, there have been a number of attempts at quantifying, and therefore a number of definitions of, strong ground motion. These have included *bracketed duration* D_B (time interval between the first and the last time when the acceleration exceeds some level, usually taken [15] to be 0.05g), *fractional or normalized duration* D_F (elapsed time between the first and the last acceleration excursion greater than α times PGA [70]), and D_{TB} (the time interval during which 90% of the total energy is recorded at the station [124] equal to the time interval between attainment of 5% and 95% of the total Arias intensity of the record). McGuire and Barnhard [78] have used these definitions to examine 50 strong motion records (3 components each), and found:

$$\ln D = c_1 + c_2 M + c_3 S + c_4 V + c_5 \ln R \tag{5.26}$$

where D is D_B, D_F, or D_{TB}, (for D_F, $\alpha = 0.5$ in this case), M is earthquake magnitude, $S = 0{,}1$ for rock or alluvium, $V = 0{,}1$ for horizontal or vertical component, R typically closest distance to the rupture surface (km), and c_i are coefficients in Table 5.12. However, McGuire and Barnhard note that there is large uncertainty in these estimates due to varying source effects, travel paths, etc.

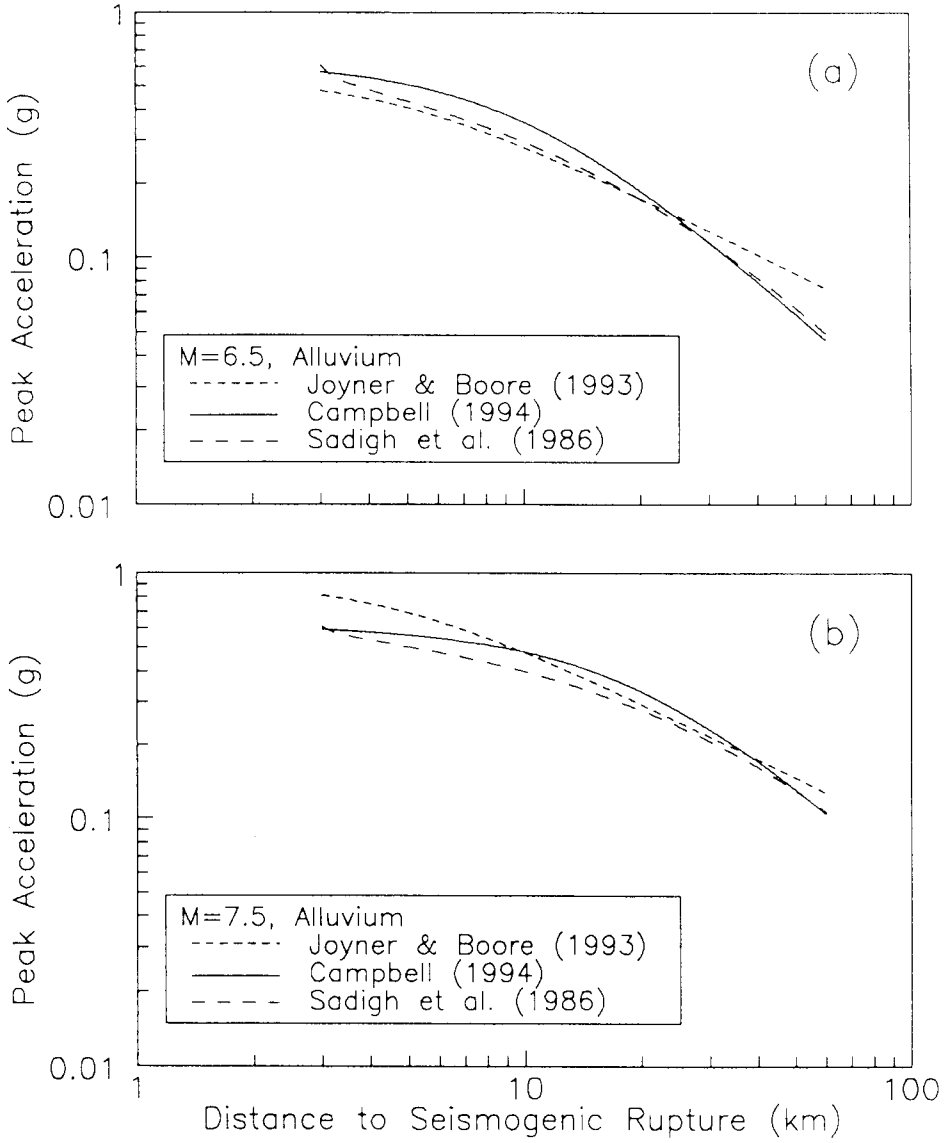

FIGURE 5.22: Comparison of PGA on alluvium, for various relations. (From Campbell, K.W. and Bozorgnia, Y., Near-Source Attenuation of Peak Horizontal Acceleration from Worldwide Accelerograms Recorded from 1957 to 1993, Proc. Fifth U.S. National Conference on Earthquake Engineering, Earthquake Engineering Research Institute, Oakland, CA, 1994. With permission.)

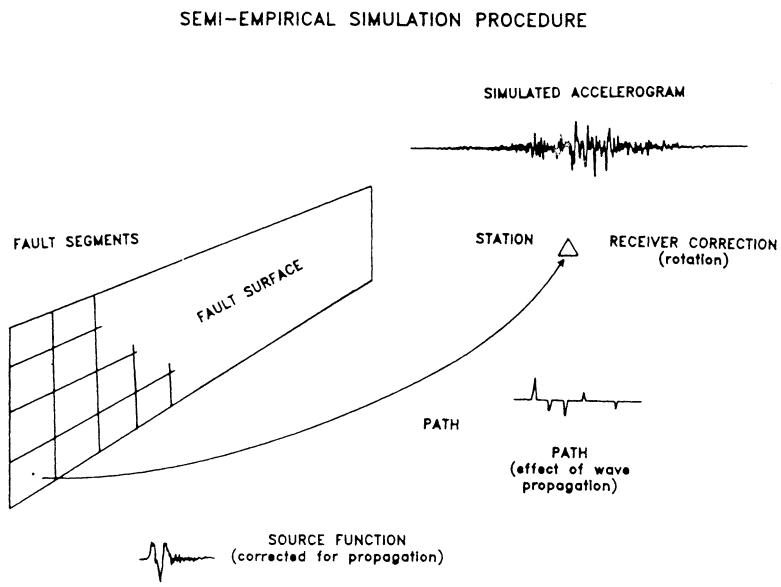

FIGURE 5.23: Semi-empirical ground motion simulation procedure. (From Wald, D.J., Burdick, L.J., and Somerville, P.G., Simulation of Acceleration Time Histories Close to Large Earthquakes, in *Earthquake Engineering and Soil Dynamics II—Recent Advances in Ground-Motion Evaluation*, Thun, J. L. V., Ed., Geotechnical Spec. Publ. No. 20, Am. Soc. Civil Engrs., New York, 1988. With permission.)

TABLE 5.12 Coefficients for Strong Ground Motion Duration Estimation

D	Duration	C_1	C_2	C_3	C_4
D_B	Bracketed	2.3	2.0	0.20	−0.16
D_F	Fractional (normalized)	−4.5	0.74	0.36	0.31
D_{TB}	Trifunac-Brady (time for energy absorption)	0.19	0.15	0.73	0.23

$\ln D = c_1 + c_2 M + c_3 S + c_4 V + c_5 \ln R$
From McGuire, R.K. and Barnhard, T.P., The Usefulness of Ground Motion Duration in Predicting the Severity of Seismic Shaking, *Proc. 2nd U.S. Natl. Conf. on Earthquake Eng.*, Earthquake Engineering Research Institute, Oakland, CA, 1979. With permission.

As Trifunac and Novikova [125] discuss, strong motion duration may be represented by the sum of three terms: $dur = t_0 + t_\Delta + t_{\text{region}}$, where t_0 is the duration of the source fault rupture, t_Δ is the increase in duration due to propagation path effects (scattering), and t_{region} is prolongation effects caused by the geometry of the regional geologic features and of the local soil. This approach will be increasingly useful, but requires additional research. Note that response spectra are not strongly correlated with, or good measures of, duration — that is, an elastic SDOF oscillator will reach its maximum amplitude within several cycles of harmonic motion, and two earthquakes (one of long, the other of short duration, but both with similar PGA) may have similar elastic response spectra.

Lastly, it should be noted that the foregoing has dealt exclusively with attenuation of engineering measures of ground motions — there are also a number of attenuation relations available for MMI, R-F, MSK, and other qualitative measures of ground motion, specific to various regions. However,

the preferred method is to employ attenuation relations for engineering measures, and then convert the results to MMI or other intensity measures, using various conversions [84, 103].

5.2.5 Seismic Hazard and Design Earthquake

The foregoing sections provide an overview of earthquake measures and occurrence. If an earthquake location and magnitude are specified, attenuation relations may be employed to estimate the PGA or response spectra at a site, which can then be employed for design of a structure. However, since earthquake occurrence is a random process, the specification of location and magnitude is not a simple matter. The basic question facing the designer is, *what is the earthquake which the structure should be designed to withstand?* Note that this is termed the design earthquake, although in actuality hazard parameters (e.g., PGA, response spectra) are the specific parameters in question. Basically, three approaches may be employed in determining a design earthquake: they can be characterized as (1) code approach, (2) upper-bound approach, or (3) Probabilistic Seismic Hazard Analysis approach. This section briefly describes these approaches.

Code Approach

The code approach is to simply employ the lateral force coefficients as specified in the applicable design code. Most countries and regions have macro-zoned their jurisdiction [97], and have regional maps available which provide a lateral force coefficient. Figure 5.24 for example is the seismic zonation map of the U.S. which provides a zone factor Z as part of the determination of the lateral force coefficient. This mapping is based on probabilistic methods [3] such that the ground motion parameters are intended to have about a 10% probability of being exceeded during any 50-year period (this is discussed further below). The advantages of this approach are simplicity and ease, and

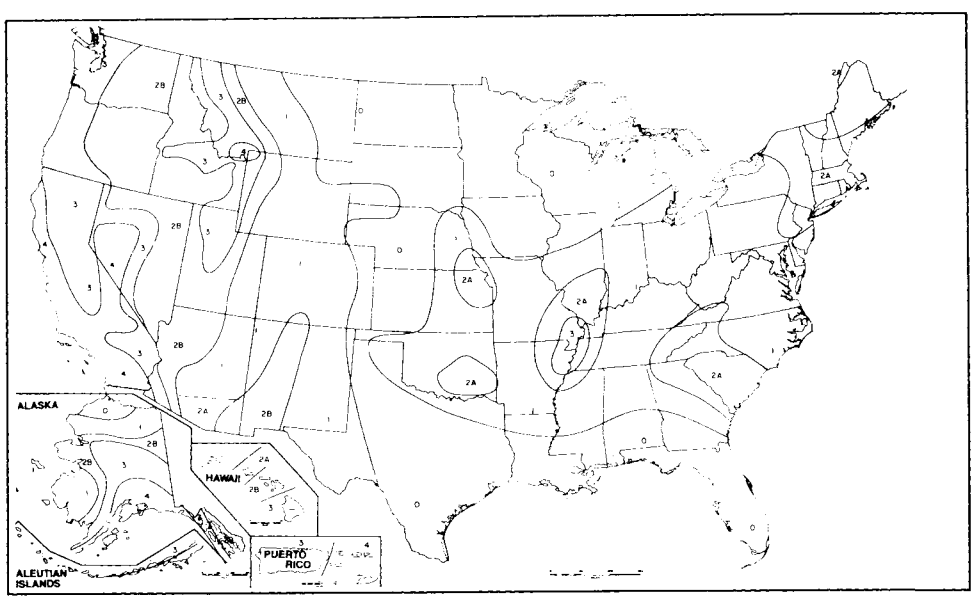

FIGURE 5.24: Seismic zone map of the U.S. (From Uniform Building Code, Vol. 2, Structural Engineering Design Provisions, Intl. Conf. Building Officials, Whittier, 1994. With permission.)

obvious compliance with local requirements. The disadvantages are inappropriateness for unusual structures, and that the methods employed in the mapping have been regional in nature and may have overlooked local geology.

Upper-Bound Approach

The upper-bound approach consists of reviewing the geology and historic seismicity of the region, to determine the largest event that is physically capable of occurring in the vicinity and affecting the site. In high seismicity areas, this approach is feasible because very large faults may be readily identifiable. Using historic data and/or fault length-magnitude relations, a maximum magnitude event can be assigned to the fault and, using attenuation relations, a PGA or other engineering measure can be estimated for the site, based on the distance. This approach has a number of drawbacks including lack of understanding of the degree of conservatism and potentially excessive design requirements, so that it is rarely employed, and then only for critical structures.

Probabilistic Seismic Hazard Analysis

The Probabilistic Seismic Hazard Analysis (PSHA) approach entered general practice with Cornell's [35] seminal paper, and basically employs the theorem of total probability to formulate:

$$P(Y) = \sum_F \sum_M \sum_R p(Y|M, R)p(M) \tag{5.27}$$

where

Y	=	a measure of intensity, such as PGA, response spectral parameters PSV, etc.
$p(Y\|M, R)$	=	the probability of Y given earthquake magnitude M and distance R (i.e., attenuation)
$p(M)$	=	the probability of occurrence of a given earthquake magnitude M
F	=	indicates seismic sources, whether discrete such as faults, or distributed

This process is illustrated in Figure 5.25, where various seismic sources (faults modeled as line sources and dipping planes, and various distributed or area sources, including a background source to account for miscellaneous seismicity) are identified, and their seismicity characterized on the basis of historic seismicity and/or geologic data. The effects at a specific site are quantified on the basis of strong ground motion modeling, also termed attenuation. These elements collectively are the seismotectonic model — their integration results in the seismic hazard.

There is extensive literature on this subject [86, 102], so only key points will be discussed here. Summation is indicated, as integration requires closed form solutions, which are usually precluded by the empirical form of the attenuation relations. The $p(Y|M, R)$ term represents the full probabilistic distribution of the attenuation relation — summation must occur over the full distribution, due to the significant uncertainty in attenuation. The $p(M)$ term is referred to as the magnitude-frequency relation, which was first characterized by Gutenberg and Richter [48] as

$$\log N(m) = a_N - b_N m \tag{5.28}$$

where $N(m)$ = the number of earthquake events equal to or greater than magnitude m occurring on a seismic source per unit time, and a_N and b_N are regional constants (10^{a_N} = the total number of earthquakes with magnitude > 0, and b_N is the rate of seismicity; b_N is typically 1 ± 0.3). Gutenberg and Richter's examination of the seismicity record for many portions of the earth indicated this relation was valid, for selected magnitude ranges. That is, while this relation appears as a straight line when plotted on semi-log paper, the data is only linear for a selected middle range of magnitudes, typically falling below the line for both the smaller and larger magnitudes, as shown in Figure 5.26a for Japan earthquake data for the period 1885 to 1990. The fall-off for smaller magnitudes is usually attributed to lack of instrumental sensitivity. That is, some of the smaller events are not detected.

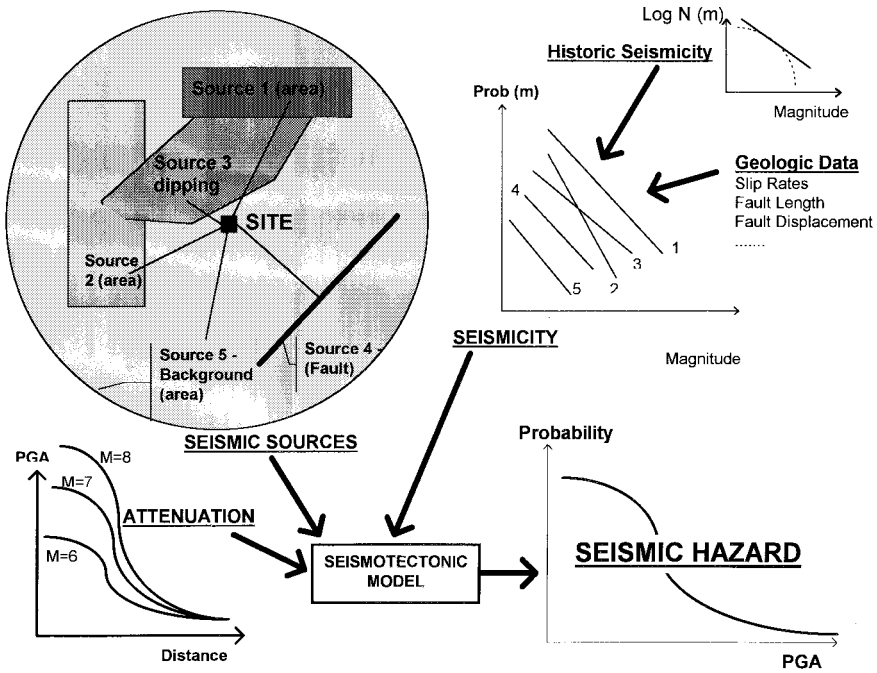

FIGURE 5.25: Elements of seismic hazard analysis — seismotectonic model is composed of seismic sources, whose seismicity is characterized on the basis of historic seismicity and geologic data, and whose effects are quantified at the site via strong motion attenuation models.

Typically, some improved instruments, better able to detect distant small earthquakes, are introduced during any observation period. This can be seen in Figure 5.26(b), where the number of detected earthquakes are relatively few in the early decades of the record. The fall-off for larger magnitudes is usually attributed to two reasons: (1) the observation period is shorter than the return period of the largest earthquakes, and (2) there is some physical limit to the size of earthquakes, so that the Gutenberg-Richter relation cannot be indefinitely extrapolated to larger and larger magnitudes.

The Gutenberg-Richter relation can be normalized to

$$F(m) = 1. - \exp[-B_M(m - M_o)] \tag{5.29}$$

where $F(m)$ is the cumulative distribution function (CDF) of magnitude, B_M is a regional constant, and M_o is a small enough magnitude such that lesser events can be ignored. Combining this with a Poisson distribution to model large earthquake occurrence [44] leads to the CDF of earthquake magnitude per unit time

$$F(m) = \exp[-\exp\{-a_M(m - \mu_M)\}] \tag{5.30}$$

which has the form of a Gumbel [47] extreme value type I (largest values) distribution (denoted $EX_{I,L}$), which is an unbounded distribution (i.e., the variate can assume any value). The parameters a_M and μ_M can be evaluated by a least squares regression on historical seismicity data, although the probability of very large earthquakes tends to be overestimated. Several attempts have been made to account for this (e.g., Cornell and Merz [36]). Yegulalp and Kuo [137] have used Gumbel's Type III (largest value, denoted $EX_{III,L}$) to successfully account for this deficiency. This distribution

$$F(m) = \exp\left[-\left(\frac{w - m}{w - u}\right)^k\right] \tag{5.31}$$

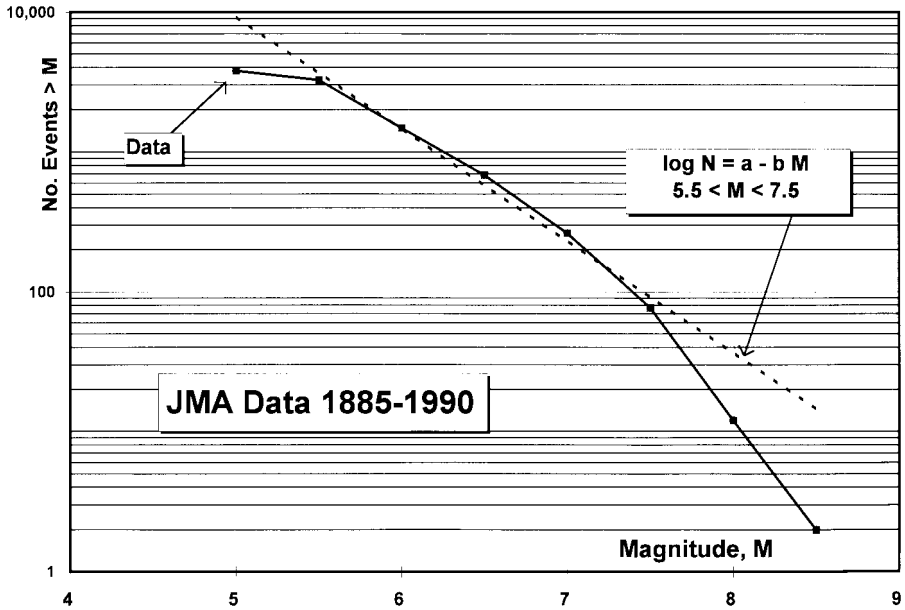

FIGURE 5.26: (a) Plot of seismicity data for Japan, 1885 to 1990, from Japan Meteorological Agency Catalog. Note actual data falls below Gutenberg-Richter relation at smaller and larger magnitudes.

has the advantage that w is the largest possible value of the variate (i.e., earthquake magnitude), thus permitting (when w, u, and k are estimated by regression on historical data) an estimate of the source's largest possible magnitude. It can be shown [137] that estimators of w, u, and k can be obtained by satisfying Kuhn-Tucker conditions although if the data is too incomplete, the $EX_{III,L}$ parameters approach those of the $EX_{I,L}$:

$$u \to \mu_M \qquad\qquad k/(w-u) \to a_M$$

Determination of these parameters requires careful analysis of historical seismicity data (which is highly complex and something of an art [40], and the merging of the resulting statistics with estimates of maximum magnitude and seismicity made on the basis of geological evidence (i.e., as discussed above, maximum magnitude can be estimated from fault length, fault displacement data, time since last event and other evidence, and seismicity can be estimated from fault slippage rates combined with time since last event; see Schwartz [109] for an excellent discussion of these aspects). In a full probabilistic seismic hazard analysis, many of these aspects are treated fully or partially probabilistically, including the attenuation, magnitude-frequency relation, upper- and lower-bound magnitudes for each source zone, geographical bounds of source zones, fault rupture length, and many other aspects. The full treatment requires complex specialized computer codes, which incorporate uncertainty via use of multiple alternative source zonations, attenuation relations, and other parameters [13, 43] often using a logic tree format (Figure 5.27). A number of codes have been developed using the public domain FRISK (Fault Risk) code first developed by McGuire [77].

Several topics are worth briefly noting:

- While analysis of the seismicity of a number of regions indicates that the Gutenberg-Richter relation $\log N(M) = a - bM$ is a good overall model for the magnitude-frequency or probability of occurrence relation, studies of late Quaternary faults during the 1980s

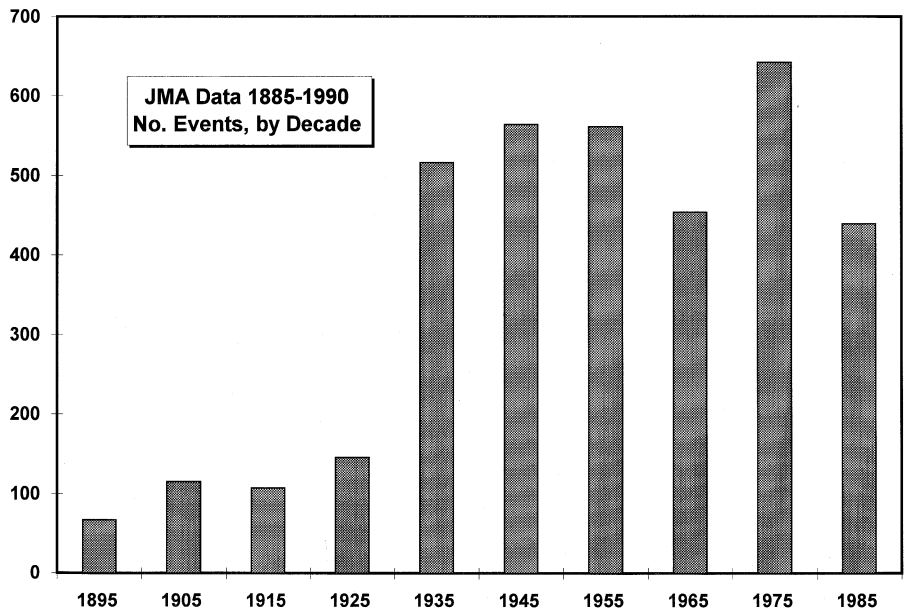

FIGURE 5.26: (b) Number of events by decade, for Japan, 1885 to 1990, from Japan Meteorological Agency Catalog.

indicated that the exponential model is not appropriate for expressing earthquake recurrence on individual faults or fault segments [109]. Rather, it was found that many individual faults tend to generate essentially the same size or characteristic earthquake [109], having a relatively narrow range of magnitudes at or near the maximum that can be produced by the geometry, mechanical properties, and state of stress of the fault. This implies that, relative to the Gutenberg-Richter magnitude-frequency relation, faults exhibiting characteristic earthquake behavior will have relatively less seismicity (i.e., higher b value) at low and moderate magnitudes, and more near the characteristic earthquake magnitude (i.e., lower b value).

- Most probabilistic seismic hazard analysis models assume the Gutenberg-Richter exponential distribution of earthquake magnitude, and that earthquakes follow a Poisson process, occurring on a seismic source zone randomly in time and space. This implies that the time between earthquake occurrences is exponentially distributed, and that the time of occurrence of the next earthquake is independent of the elapsed time since the prior earthquake.[5] The CDF for the exponential distribution is:

$$F(t) = 1 - \exp(-\lambda t) \tag{5.32}$$

Note that this forms the basis for many modern building codes, in that the probabilistic seismic hazard analysis results are selected such that the seismic hazard parameter (e.g., PGA) has a "10% probability of exceedance in 50 years" [126]; that is, if $t = 50$ years and $F(t) = 0.1$ (i.e., only 10% probability that the event has occurred in t years), then $\lambda =$ .0021 per year, or 1 per 475 years. A number of more sophisticated models of earthquake

[5]For this aspect, the Poisson model is often termed a *memoryless* model.

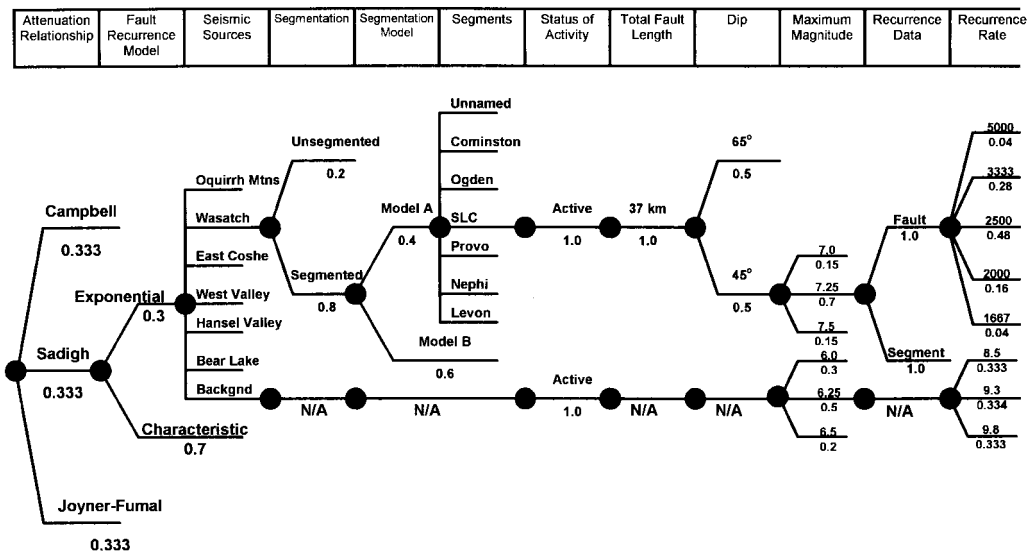

FIGURE 5.27: Hazard model logic tree. Parameter values are shown above the branches and assessed probabilities are shown in parentheses. (From Schwartz, D.P., Geologic Characterization of Seismic Sources: Moving into the 1990s, in *Earthquake Engineering and Soil Dynamics II — Recent Advances in Ground-Motion Evaluation*, Thun, J. L. V., Ed., Geotechnical Spec. Publ. No 20, Am. Soc. Civil Engrs., New York, 1988. With permission. Also after Youngs, R. R. and Coopersmith, K. J., Implication of Fault Slip Rates and Earthquake Recurrence Models to Probabilistic Seismic Hazard Estimates, *Bull. Seis. Soc. Am.*, 75, 939-964, 1987.)

occurrence have been investigated, including time- predictable models [5], and renewal models [68, 91]

- As was seen from the data for Japan in Figure 5.26, historic seismicity observations vary with event size — large magnitude events will have been noted and recorded for perhaps the full length of the historic record, while small magnitude events will only have been recorded with the advent of instruments, with quality of the instrumental record usually improving in more recent times. Thus, in analyzing any historic seismicity record, the issue of completeness is important and should be analyzed. Stepp [121] has developed a method assuming the earthquake sequence can be modeled as a Poisson distribution. If $k_1, k_2, k_3 \ldots k_n$ are the number of events per unit time interval, then $\lambda = \frac{1}{n}\sum_{i=1}^{n} k_i$ and its variance is $\sigma^2 = \lambda/n$ where n equals the number of unit time intervals. Taking the unit time interval to be one year gives $\sigma_\lambda = \sqrt{\lambda}/\sqrt{T}$ as the standard deviation of the estimate of the mean, where T is the sample length (in years). That is, this provides a test for stationarity of the observational quality. If the data for a magnitude interval (say $5.6 < M < 6.5$, to test for quality of observation for events in this magnitude range) is plotted as $\log(\sigma_\lambda)$ vs. $\log(T)$, then the portion of the record with slope $T^{-1/2}$ can be considered homogeneous (Figure 5.28) and used with data for other magnitude ranges (but for different observational periods) similarly tested for homogeneity, to develop estimates of magnitude-frequency parameters. A more recent method is also provided by Habermann [50].
- Equation 5.27 is quite general, and used to develop estimates of MMI, PGA, response spectra, or other measures of seismic hazard. Construction of response spectra is usually

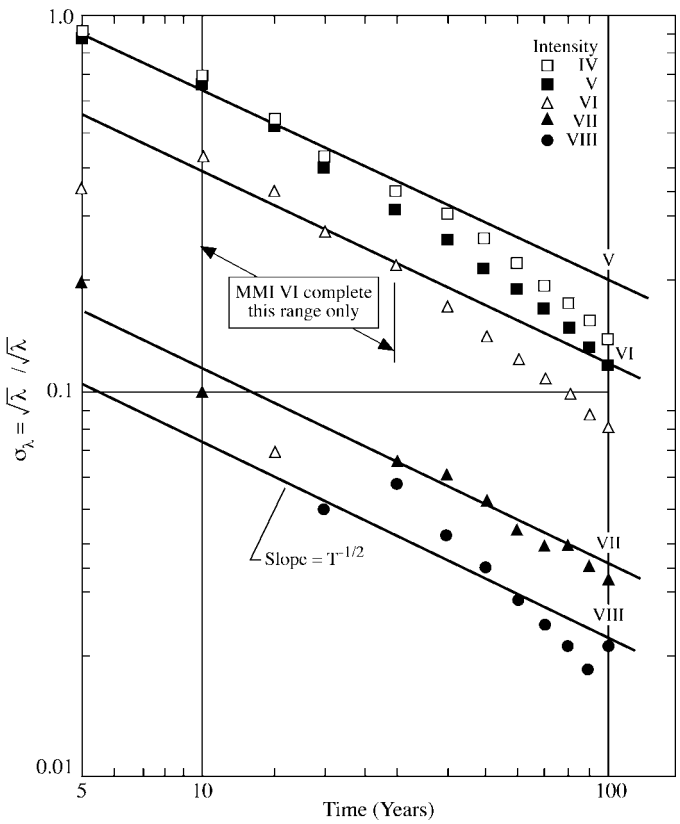

FIGURE 5.28: Standard deviation of the estimate of the man of the annual number of events as a function of sample length and intensity class. (After Stepp, J.C., Analysis of Completeness of the Earthquake Sample in the Puget Sound Area and Its Effect on Statistical Estimates of Earthquake Hazard, Proc. First Conf. Microzonation, Seattle, 1972.)

performed in one of two ways:

1. Using probabilistic seismic hazard analysis to obtain an estimate of the PGA, and using this to scale a normalized response spectral shape. Alternatively, estimating PGA and PSV (also perhaps PSD) and using these to fit a normalized response spectral shape for each portion of the spectra. Since probabilistic response spectra are a composite of the contributions of varying earthquake magnitudes at varying distances, the ground motions of which attenuate differently at different periods, this method has the drawback that the resulting spectra have varying (and unknown) probabilities of exceedance at different periods. Because of this drawback, this method is less favored at present, but still offers the advantage of economy of effort.

2. An alternative method results in the development of uniform hazard spectra [7], and consists of performing the probabilistic seismic hazard analysis for a number of different periods, with attenuation equations appropriate for each period (e.g., those of Boore, Joyner, and Fumal). This method is currently preferred, as the additional effort is not prohibitive and the resulting response spectra has the attribute that the probability of exceedance is independent of frequency. However, the resulting spectra do not represent the response from any one event.

Selection of Design Earthquake

The foregoing discussion has outlined the methods for probabilistic seismic hazard analysis. However, the question still remains, *given the results of a probabilistic seismic hazard analysis, what values of PGA, response spectra, etc. should be employed or equivalently, what is the appropriate probability of exceedance?* This is a complex question; for ordinary building structures, regulated by the local authorities, the default value for the probability of exceedance would be that comparable with the local building code — usually about 10% probability of exceedance in 50 years. The value of probabilistic seismic hazard analysis is that the results are site-specific and utilize the latest and most detailed data on local seismic sources. Those results may indicate, for code-comparable probabilities of exceedance, design parameters either greater or lesser than specified in the code.

Many structures, however, are either (a) atypical, such as large bridges, civil works (e.g., water supply pump stations or treatment plants), data centers, emergency operations centers, etc. or (b) not ordinarily regulated by local authorities, such as industrial structures in large manufacturing or process complexes. For these structures, the choice of the appropriate probability of exceedance is more difficult — their importance may demand design for less frequent events (i.e., smaller probability of exceedance) or, if their failure does not constitute a life-safety hazard, economies in design may be justified.

One approach for addressing this issue involves careful assessment of the total costs of damage associated with varying levels of hazard. This should be undertaken in a cost-benefit framework. The total costs of damage should include not only the value of the structure, but the value of potential losses to equipment and inventory in the structure, and the associated business costs of lost operations while repairs are required. In many cases, design levels exceeding that of the local building code may be found to be warranted, when total costs are considered. It should be noted, however, that assessment of structural damage is not easy, and assessment of damage to equipment and contents, and business costs of lost operations, is even more complex.

It should always be kept in mind that the first goal of the building code and the structural designer is the maintenance of public safety; therefore, designs using parameter values lower than the local building code (i.e., parameters with probabilities of exceedance exceeding those of the local building code) may carry undue risk to safety. Therefore, the parameters of the local building code should normally be taken as indicative of society's criteria for appropriate risk.

5.2.6 Effect of Soils on Ground Motion

The effect of different types of soils on earthquake ground motion and damage has long been noted. By observation of damage and mapping of seismic intensities, such as following the 1906 San Francisco [73] and other earthquakes, it was observed that the greatest damage generally correlated with geologically recent alluvial deposits and non-engineered fills, so that softer soils were generally considered more damaging. However, an S or soil factor to account for site-specific soil effects was only introduced into the base shear formula prevailing in the U.S. in 1976. Prior to that time there had been no variation in the base shear coefficients for different site conditions although it had been pointed out that "the absence of a soil factor... should not be interpreted as meaning that the effect of soil conditions on building response is not important" [111]. The current Uniform Building Code defines four site coefficients, as shown in Table 5.13. Quantification of the effects of soils on ground motion has generally been by either analytical or empirical methods.

Analytical Methods

Analysis of dynamic ground response is usually accomplished using SHAKE [106] or similar programs, which are based on the vertical propagation of shear waves in a layered half-space. The approach involves using equivalent linear properties taking into account non-linear soil behavior —

TABLE 5.13 Site Coefficients[a]

Type	Description	*S* Factor
S_1	A soil profile with either: (a) A rock-like material characterized by a shear-wave velocity greater than 2,500 ft/s (763 m/s) or by other suitable means of classification, or (b) Medium-dense or medium-stiff to stiff soil conditions, where soil depth is less than 200 ft (60 960 mm).	1.0
S_2	A soil profile with predominantly medium-dense to dense or medium-stiff to stiff soil conditions, where the soil depth exceeds 200 ft (60 960 mm).	1.2
S_3	A soil profile containing more than 200 ft (60 960 mm) of soft to medium-stiff clay but not more than 40 ft (12 192 mm) of soft clay.	1.5
S_4	A soil profile containing more than 40 ft (12 192 mm) of soft clay characterized by a shear wave velocity less than 500 ft/s (152.4 m/s).	2.0

[a] The site factor shall be established from properly substantiated geotechnical data. In locations where the soil properties are not known in sufficient detail to determine the soil profile type, soil profile S_3 shall be used. Soil profile S_4 need not be assumed unless the building official determines that soil profile S_4 may be present at the site, or in the event that soil profile S_4 is established by geotechnical data.

After Uniform Building Code, Vol. 2, Structural Engineering Design Provisions, Intl. Conf. Building Officials, Whittier, 1994.

soil properties are unit weight, maximum shear modulus, variation of shear modulus, and damping ratio with shear strain. A one-dimensional vertical shear wave propagation is assumed, and the shear modulus and damping ratio are adjusted iteratively based on strain compatibility. The solution is in the frequency domain to take advantage of the computational efficiency of the Fast Fourier Transform method.

In application, a time history is assumed at a nearby rock or firm soil surface outcrop, and SHAKE or a similar program *deconvolves* the motion, that is, it is used to determine the corresponding time history at some depth (below the layer of interest, usually at the underlying "basement rock"). Using this analytically derived time history at depth then, the same program is used for the profile of interest to determine time histories at the surface or any intervening layer. This procedure is typically employed to determine both (a) the effect of soils on surface ground motions and (b) time histories or equivalent number of cyclic shear stresses for the analysis of liquefaction potential for a layer of interest.

Empirical Methods

Empirical methods generally take the form of a modification factor for the site-specific soil profile to be applied to a "base" ground motion estimate arrived at by attenuation relation or other methods. These modifiers were required previously, when attenuation relations had insufficient data for correlation against varying soil profiles. More recently, with additional data (as seen above), attenuation relations are now available for several different soil types so that this approach is receding, although it is still required at times. Evernden [45] has provided a series of modifiers for MMI, based on a study of a number of U.S. intensity distributions, correlated against surficial geology maps. Seed and Idriss developed a well-known relationship for PGA (Figure 5.29), for four different types of soil deposit:

1. Rock
2. Stiff soil deposits involving cohesionless soils or stiff clays to about 200 ft in depth
3. Deep cohesionless soil deposits with depths greater than about 250 ft
4. Deposits of soft to medium stiff clays and sands

Note that these type-definitions differ from those employed in the model building codes (see Table 5.13).

As Seed and Idriss [113] note, "apart from deposits involving soft to medium stiff clay, values of PGA developed on different types of soil do not differ appreciably, particularly at acceleration levels

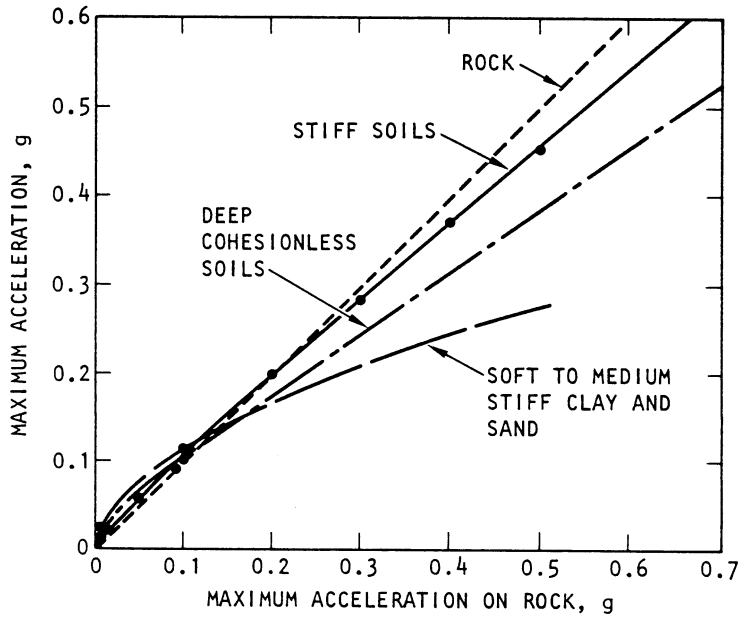

FIGURE 5.29: Approximate relationships between maximum acceleration on rock and other local site conditions. (From Seed, H.B. and Idriss, I.M., Ground Motions and Soil Liquefaction During Earthquakes, Earthquake Engineering Research Institute, Oakland, CA, 1982. With permission.)

less than about 0.3 to 0.4g". However, PGV do differ significantly with a general pattern as indicated in Table 5.14, the significance of which was first noted by Newmark [89].

TABLE 5.14 Typical PGV/PGA Ratios

Geologic condition	PGV / PGA
Rock	55 cm/s/g
Stiff soils (< 200 ft)	110 cm/s/g
Deep stiff soils (> 200 ft)	135 cm/s/g

From Seed, H.B. and Idriss, I.M., Ground Motions and Soil Liquefaction during Earthquakes, Earthquake Engineering Research Institute, Oakland, CA, 1982. With permission.

Similar but more detailed ratios form the basis for development of response spectra [83, 98] and future lateral force provisions are tending to be based on the velocity portion of the spectrum as well as PGA [21, 24].

5.2.7 Liquefaction and Liquefaction-Related Permanent Ground Displacement

Liquefaction refers to a process resulting in a soil's loss of shear strength, due to a transient excess of pore water pressure. The process is shown in Figure 5.30 and typically consists of loose granular

soil with a high water table being strongly shaken during an earthquake; that is, cyclically sheared. The soil particles initially have large voids between them. Due to shaking, the particles are displaced

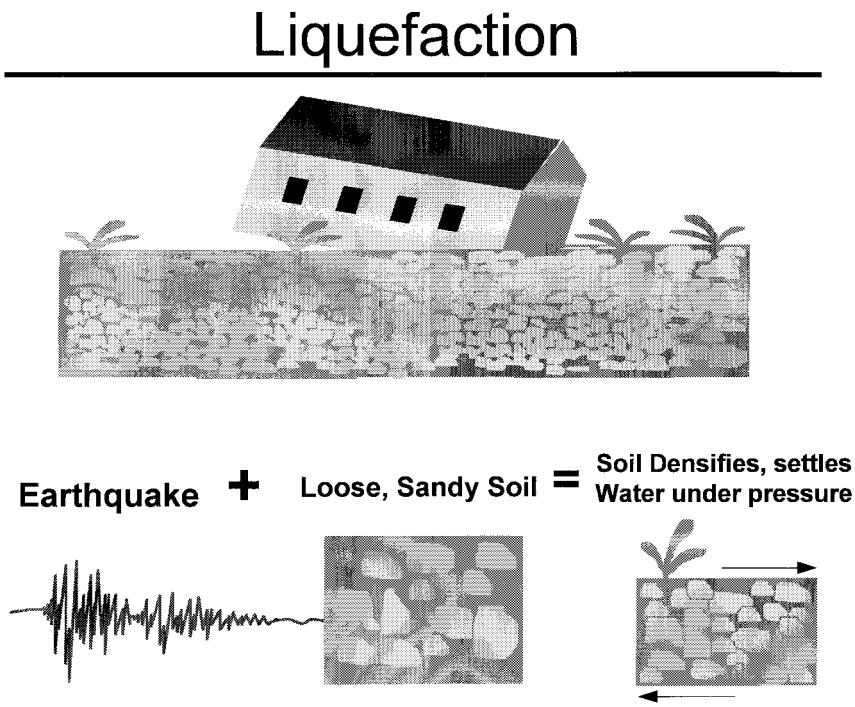

FIGURE 5.30: Soil Liquefaction — loose granular soil density under shaking, settling, and putting ground water under pressure. The pressure is relieved when the water migrates to the surface, where it produces sand boils.

relative to each other, and tend to more tightly pack,[6] decreasing the void volume. The water, which had occupied the voids (and being incompressible), comes under increased pressure and migrates upward towards or to the surface, where the pressure is relieved. The water usually carries soil with it, and the resulting ejecta are variously termed sand boils or mud volcanoes (Figure 5.31).

Seismic liquefaction of soils was noted in numerous earthquakes but the phenomenon was first well understood following the 1964 Alaska and, particularly, 1964 Niigata (Japan) earthquakes, where dramatic effects were observed [51, 93, 95, 111]. Liquefaction is a major source of damage in earthquakes, since (a) the soil's loss of shear strength results in partial or total loss of bearing capacity, resulting in foundation failure unless the structure is founded below the liquefying layer; (b) liquefaction may result in large lateral spreads and permanent ground displacements, often measured in meters and occasionally resulting in catastrophic slides, such as occurred at Turnagain Heights in the 1964 Alaska earthquake [112]; and (c) for both of these reasons, various lifelines, particularly buried water, wastewater, and gas pipes, typically sustain numerous breaks which can result in system failure and lead to major secondary damage, such as fire following earthquake.

[6] Analogous to a can of coffee grounds, which "tamps" down when struck against the tabletop.

FIGURE 5.31: Photograph of sand boils.

FIGURE 5.31: *(Continued)* Photograph of sand boils.

Recent earthquakes where these effects occurred and liquefaction was a significant agent of damage have included:

- 1989 M 7.1 Loma Prieta (San Francisco) — major liquefaction and resulting disruption at Port of Oakland; significant liquefaction in Marina and other districts of San Francisco, causing building damage and numerous underground pipe failures [93].
- 1990 M 7.7 Philippines — major liquefaction in Dagupan City with many low-and mid-rise buildings collapsed or left tilting; many bridge failures due to lateral spreading of embankments causing piers to fail.
- 1991 M 7.4 Valle de la Estrella (Costa Rica) — numerous bridge failures due to lateral spreading of embankments causing piers to fail.
- 1994 M 6.9 Hanshin (Kobe, Japan) — major liquefaction in port areas, resulting in widespread ground failure, port disruption, and a portion of approximately 2,000 underground pipe breaks.

Evaluating liquefaction potential requires consideration of a number of factors, including grain-size distribution — generally, poorly graded sands (i.e., most particles about the same size) are much more susceptible to liquefaction than well- graded (i.e., particles of many differing sizes), since good grading results in better natural packing and better grain-grain contact. Silts and clays are generally much less susceptible to liquefaction, although the potential should not be ignored, and

large-grained sands and gravels have such high permeability that pore water pressures usually dissipate before liquefaction can occur. Relative density is basically a measure of the packing — higher relative density means better packing and more grain-grain contact, while lower relative density, or looseness, indicates a higher potential for liquefaction. Water table depth is critical, as only submerged deposits are susceptible to liquefaction. A loose sandy soil above the water table is not liquefiable by itself, although upward-flowing water from a lower liquefying layer can initiate liquefaction even above the pre-event water table. Note also that water table depths can fluctuate significantly, seasonally, or over longer periods and for natural reasons or due to human intervention. Earthquake acceleration and duration are also critical, as these are the active causative agents for liquefaction. Acceleration must be high enough and duration long enough to cause sufficient shear strains to mobilize grain redistribution.

The basic evaluation procedure for liquefaction involves a comparison of the deposit's cyclic shear *capacity* with the *demand* imposed by an earthquake (Figure 5.32), where capacity and demand refer to the number of cycles of shear stress of a given amplitude, under similar confining pressures (comparable to the deposit's *in situ* conditions).

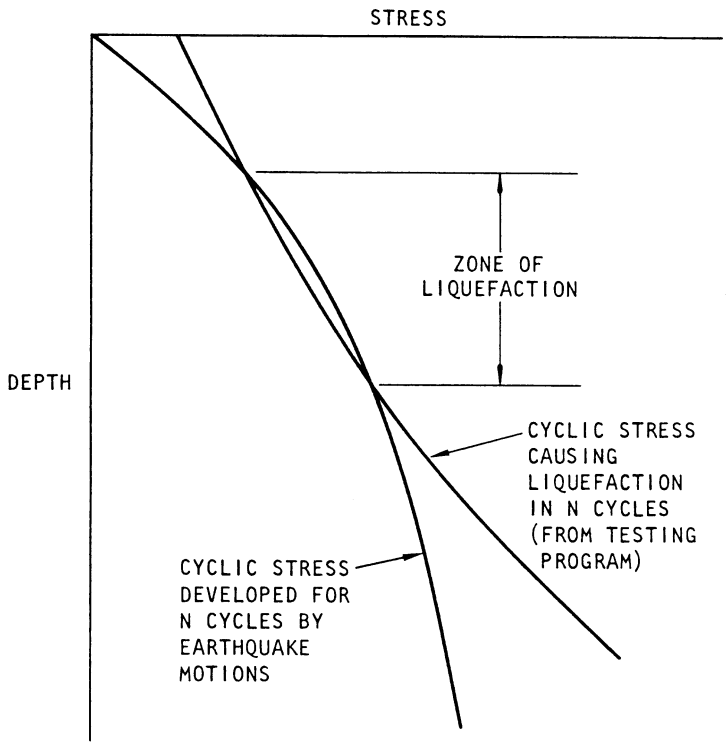

FIGURE 5.32: Method of evaluating liquefaction potential. (From Seed, H.B. and Idriss, I.M., Ground Motions and Soil Liquefaction During Earthquakes, Earthquake Engineering Research Institute, Oakland, CA, 1982. With permission.)

Determination of a soil's capacity against liquefaction can be determined by laboratory tests of undisturbed soil samples, in dynamic triaxial or cyclic simple shear tests for the appropriate confining pressures, or by correlation of these properties with some measurable *in situ* characteristic, such as

blow count (N value) from a Standard Penetration Test (SPT). Demand can be determined via analysis of dynamic ground response using SHAKE or a similar program (see previous discussion), or by Seed's simplified procedure [113].

Simplified Procedure for Evaluation of Liquefaction Potential

The procedure developed by Seed is based on the assumption of the shear stresses induced at any point in a soil deposit during an earthquake being

a) the mass of the soil column above the point (equal to $\gamma h/g$, where γ is the unit weight of soil, h is the depth of the point, and g is gravity)

b) times the maximum ground acceleration, $a_{\max}$

c) then being corrected by a factor r_d to account for the soil column's deformable behavior, so that the maximum shear stress is $\tau_{\max} = \gamma h/g \cdot a_{\max} \cdot r_d$. The factor r_d is indicated in Figure 5.33. Note that while a range is indicated, most liquefiable soils are in the top 40 ft or so of a profile, where the range is relatively narrow. If the average value is used, the error is on the order of 5%.

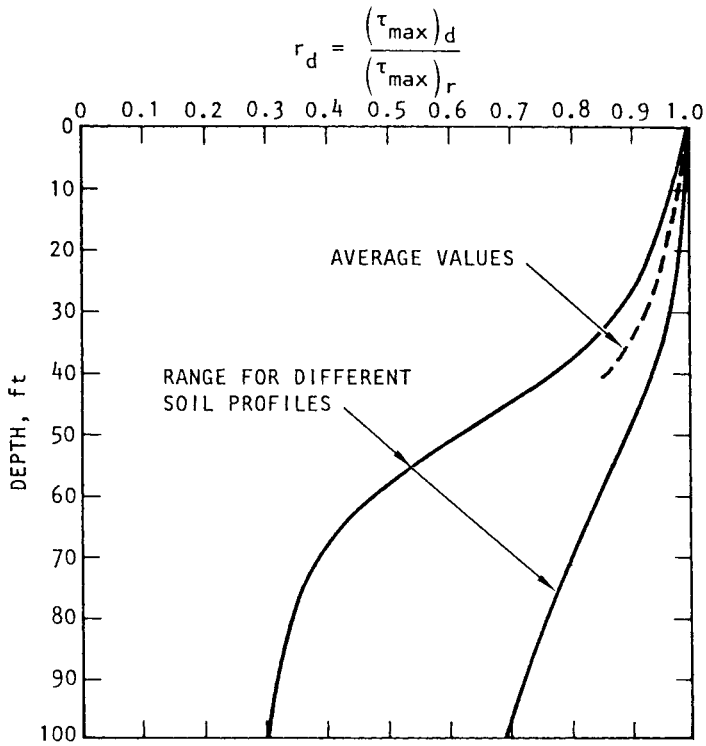

FIGURE 5.33: Range of values of r_d for different soil profiles. (From Seed, H.B. and Idriss, I.M., Ground Motions and Soil Liquefaction During Earthquakes, Earthquake Engineering Research Institute, Oakland, CA, 1982. With permission.)

Finally, Seed reduces the maximum shear stress by a factor of 0.65, to an "equivalent uniform average shear stress", so that τ_{av}, the average cyclic shear stress, is:

$$\tau_{av} = 0.65 \cdot \gamma h/g \cdot a_{\max} \cdot r_d \tag{5.33}$$

τ_{av} and the above values provide a simple procedure for evaluation of the average cyclic shear stresses induced at different depths by a given earthquake for which the maximum ground surface acceleration is known [113]. In order to determine a soil's capacity against liquefaction, Seed studied SPT data from a number of sites where liquefaction had and had not occurred. He found that if the SPT data were

a) normalized to an effective overburden pressure of 1 ton per square foot by a factor C_N (Figure 5.34, C_N is a function of the effective overburden pressure at the depth where the penetration test was conducted) to obtain N_1 (measured penetration of the soil under an effective overburden pressure of 1 ton per square foot, so that $N_1 = C_N \cdot N$)

b) plotted against the cyclic stress ratio, τ_{av}/σ'_v, where σ'_v is the effective overburden pressure (effective meaning buoyant weight is used for soils below the water table)

then a reasonable boundary could be drawn between sites where liquefaction had and had not occurred, and could also be extended to various magnitudes (Figure 5.35). The extension to various magnitudes was based on the number of cycles of τ_{av} caused by an earthquake, termed significant stress cycles N_c, which depends on the duration of ground shaking, and thus on the magnitude of the event. Representative numbers are indicated in the following table:

Magnitude	5-1/4	6	6-3/4	7-1/2	8-1/2
N_c (number of significant stress cycles)	$2 \sim 3$	5	10	15	26

In Figure 5.35, the region to the left of the curve (for the appropriate magnitude) is the region of liquefaction. Figure 5.35 is appropriate for sandy soils ($D_{50} > 0.25$ mm) and can be used for silty sands provided N_1 for the silty sand is increased by 7.5 before entering the chart [113].

As an example of Seed's simplified procedure for evaluation of liquefaction potential, consider a site located such that 0.3g maximum ground surface is expected, due to a magnitude 8 earthquake. If the water table is at 5 ft below the ground surface, then the induced cyclic stress ratio is found to be:

$$\begin{aligned} \tau_{av}/\sigma'_v &= \left[0.65 \cdot \gamma h/g \cdot a_{\max} \cdot r_d\right]/\sigma'_v \\ &= (0.65)(15 \times 110)(0.3)(0.95)/(5 \times 110 + 10 \times 47.5) = 0.3 \end{aligned}$$

If the SPT blow count at 15 ft depth is $N = 13$, then $N_1 = 16$. From Figure 5.35 we see that for a magnitude 8 earthquake and $N_1 = 16$, liquefaction is expected if the induced cyclic stress ratio is 0.16 or greater. Given its value of 0.3, liquefaction is to be expected.

Normally, results of an evaluation of liquefaction potential are expressed in terms of a factor of safety against liquefaction, or:

$$\text{Factor of Safety} \quad = \tau_l/\tau_d \tag{5.34}$$

where

τ_l = average cyclic stress required to cause liquefaction in N cycles (i.e., the soil's *capacity*)

τ_d = average cyclic stress induced by an earthquake for N cycles (i.e., the earthquake's *demand*)

In the example above, the factor of safety is 0.53 (= 0.16 / 0.30).

The foregoing has outlined the estimation of the occurrence of liquefaction. An important aspect (particularly for lifelines) is, given liquefaction, "What are the permanent ground displacements (PGD)?". Liquefaction-related PGD can be vertical, lateral, or a combination. Only lateral PGD are discussed here. Lateral PGD may be of three general types [92] (Figure 5.36):

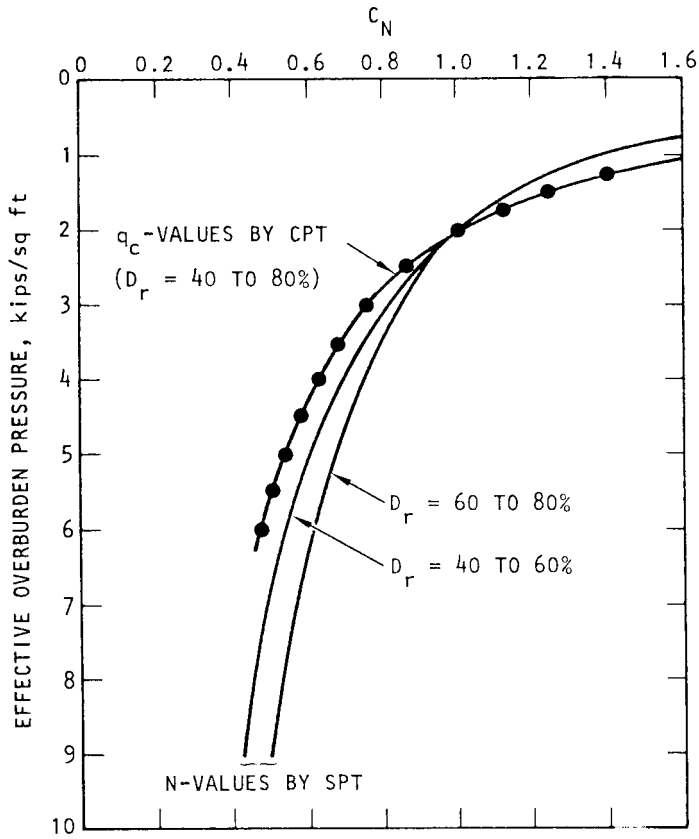

FIGURE 5.34: Chart for values of C_N. (From Seed, H.B. and Idriss, I.M., Ground Motions and Soil Liquefaction During Earthquakes, Earthquake Engineering Research Institute, Oakland, CA, 1982. With permission.)

- Flow failure on steep slopes, characterized by large displacements.
- Ground oscillation, *n* flat ground with liquefaction at depth decoupling surface soil layers from the underlying unliquefied ground. This decoupling allows large transient ground oscillations, although the residual PGD are usually small and chaotic.
- Lateral spread lies between flow failure and ground oscillation, occurring on horizontal ground or flat slopes, but resulting in large PGD, typically on the order of meters.

There are several methods available for quantification of PGD, including finite element analysis [100], sliding block analysis [27, 88], and empirical procedures [12]. Empirical procedures offer significant advantages when high confidence or precision is not required, and are the only feasible methods for estimation of lateral PGD in certain situations, such as extensive lifelines (e.g., buried pipelines).

Regarding empirical relations, Bartlett and Youd [12] analyzed nearly 500 horizontal displacement vectors from U.S. and Japanese earthquakes, ranging in magnitude from 6.4 to 9.2. In consideration of the influence of free-face (i.e., near steep banks), two empirical relations were developed:

For free-face conditions:

$$\log D_H = -16.3658 + 1.1782M - 0.9275 \log R - 0.0133R$$

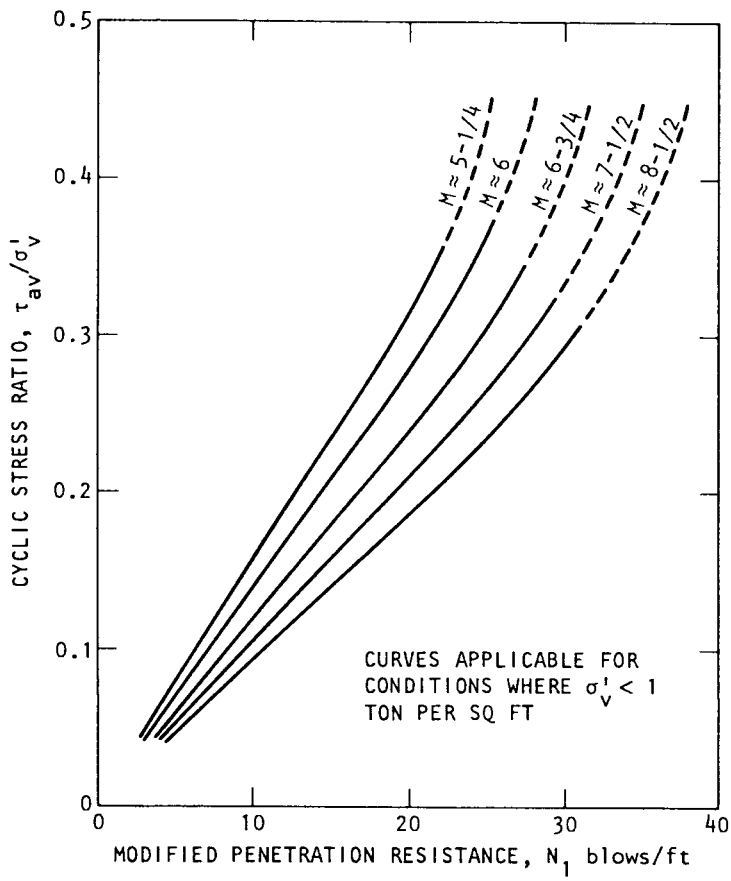

FIGURE 5.35: Chart for evaluation of liquefaction potential for sands for different magnitude earthquakes. (From Seed, H.B. and Idriss, I.M., Ground Motions and Soil Liquefaction During Earthquakes, Earthquake Engineering Research Institute, Oakland, CA, 1982. With permission.)

$$+ 0.6572 \log W + 0.3483 \log T_{15} + 4.527 \log(100 - F_{15}) - 0.9224 D50_{15} \tag{5.35}$$

For ground slope conditions:

$$\log D_H = -15.7870 + 1.1782M - 0.9275 \log R - 0.0133R + 0.4293 \log S + 0.3483 \log T_{15} + 4.527 \log(100 - F_{15}) - 0.9224 D50_{15} \tag{5.36}$$

where

D_H = estimated lateral ground displacement in meters

$D50_{15}$ = average mean grain size in granular layers included in T_{15}, in millimeters

F_{15} = average fines content (fraction of sediment sample passing a No. 200 sieve) for granular layers included in T_{15}, in percent

M = earthquake magnitude (moment magnitude)

R = horizontal distance from the site to the nearest point on a surface project of the seismic source zone, in kilometers

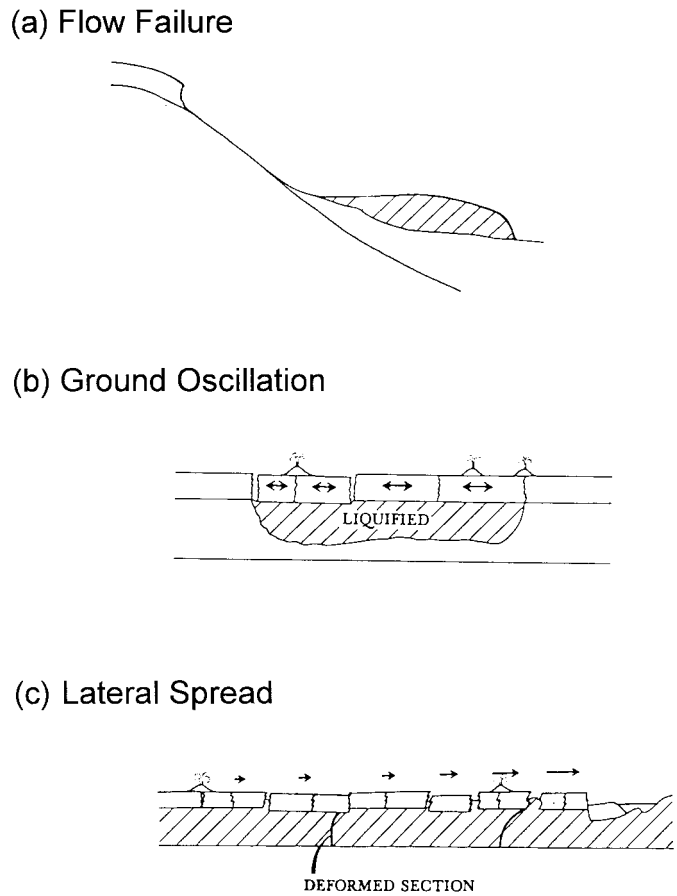

FIGURE 5.36: Modes of lateral permanent ground displacement due to liquefaction. (After NRC, *Liquefaction of Soils During Earthquakes,* National Research Council, National Academy Press, Washington, 1985.)

S	=	ground slope, in percent
T_{15}	=	cumulative thickness of saturated granular layers with corrected blow counts (N_1) less than 15, in meters
W	=	ratio of the height (H) of the free-face to the distance (L) from the base of the free-face to the point in question, in percent

Allowable ranges for these parameters are indicated in Table 5.15. Displacements estimated using these relations are considered generally valid within a factor of 2 (note that doubling the estimated displacement would provide an estimate with a high likelihood of not being exceeded).

Mitigation of liquefaction is accomplished by a number of methods, including:

- Excavation and replacement, that is, if the structure is sufficiently large or important, and the liquefiable layer sufficiently shallow, it may be cost- effective to place the foundation of the structure below the liquefiable layer. Note, however, that liquefaction may still occur around the structure, with possible disruption of adjacent streets, entrances, and utilities.

TABLE 5.15 Ranges of Input Values for Independent Variables for Which Predicted Results are Verified by Case-History Observations

Variable	Range of values in case history database
Magnitude	$6.0 < M < 8.0$
Free-face ratio	$1\% < W < 20\%$
Ground slope	$0.1\% < S < 6\%$
Thickness of loose layer	$0.3\text{ m} < T_{15} < 12\text{ m}$
Fines content	$0\% < F_{15} < 50\%$
Mean grain size	$0.1\text{ mm} < d50_{15} < 1\text{ mm}$
Depth to bottom of section	Depth to bottom of liquefied zone < 15 m

After Bartlett, S.F. and Youd, T.L., Empirical Analysis of Horizontal Ground Displacement Generated by Liquefaction-Induced Lateral Spread, Tech Rept. NCEER-92-0021, National Center of Earthquake Engineering Research, Buffalo, NY, 1992.

- Compaction can be accomplished by a number of methods, more complete details being given in Mitchell [82] and Hausmann [57]. Methods include:
  - { Vibrostabilization:

    Vibro-compaction, in which a vibrating pile or head accompanied by water jetting is dynamically injected into the ground and then withdrawn. Vibration of the head as it is withdrawn compacts an annulus of soil, and this is repeated on a closely spaced grid. Sand may be backfilled to compensate for volume reduction. This technique achieves good results in clean granular soils with less than about 20% fines.

    Vibro-replacement (stone columns) is used in soils with higher fines content ($> 20\%$) or even in clayey soils which cannot be satisfactorily vibrated. The stone columns act as vertical drains (see below).
  - { Dynamic compaction via the use of heavy dropped weights or small explosive charges. Weights up to 40 tons are dropped from heights up to 120 ft on a grid pattern, attaining significant compaction to depths of a maximum of 40 ft. Best used in large open areas due to vibrations, noise, and flying debris.
  - { Compaction piles
- *Grouting*, where grout is injected at high pressure, filling voids in the soil. This technique offers the advantage of being able to be used in small, difficult to access areas (e.g., in basements of buildings, under bridges). Grouting can be used in several ways:
  - { Compaction — a very stiff soil-cement-water mixture is injected and compacts an annulus around the borehole, this being repeated on a closely spaced grid.
  - { Chemical — low-viscosity chemical gels are injected, forming a strong sandstone-like material. Long-term stability of the grout should be taken into account.
  - { Jet-grouting — very high pressure water jets are used to cut a cylindrical hole to the desired depth, and the material is replaced or mixed with admixtures to form a stabilized column.
- *Soil-mixing* [65] — large rotary augers are used to churn up and mix the soil with admixtures and form stabilized columns or walls.
- *Permeability* can be enhanced by a number of methods, including:
  - { Placement of stone columns — rather than by vibro-replacement, a hole is augured or clamshell-excavated, and filled with gravel or cobbles, on a closely spaced grid.

If liquefaction occurs, any increase in pore water pressure is dissipated via the high permeability of the stone columns.

{ Soil wicks — similar to stone columns, but *wicks* consisting of geotextiles are inserted into the ground on a very closely spaced grid. Their high permeability similarly dissipates any increase in pore water pressure.

- *Grouting* — many materials are available to cement or otherwise create adhesion between soil grains, thus decreasing their cyclic mobility and any packing due to shaking.

Figure 5.37 illustrates the general soil particle size ranges for applicability of various stabilization techniques.

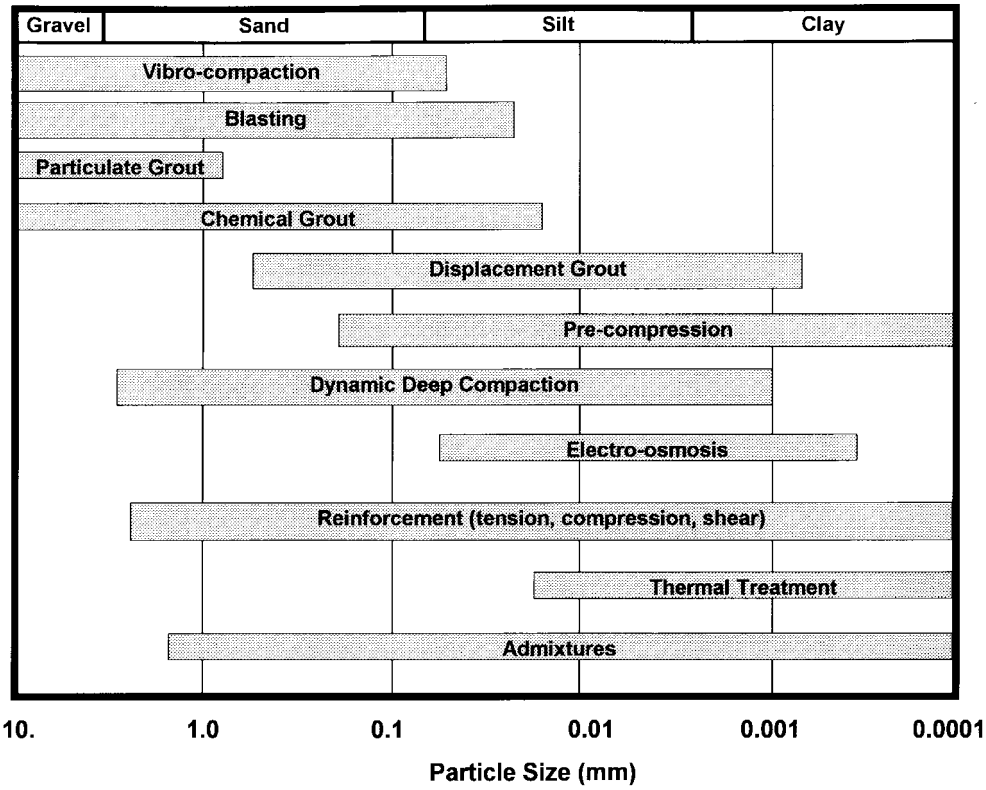

FIGURE 5.37: Applicable grain size ranges for different stabilization methods. (From Mitchell, J.K., Soil Improvement: State-of-the-Art, *Proc. 10th Intl. Conf. Soil Mech. Found. Eng.*, 4, 509-565, 1981. With permission.)

5.3 Seismic Design Codes

5.3.1 Purpose of Codes

The purpose of design codes in general is to develop a better built environment and improve public safety. The Uniform Building Code (UBC) is typical of many design codes, and states as its purpose:

> The purpose of this code is to provide minimum standards to safeguard life or limb, health, property and public welfare by regulating .....

In this and many other codes, it needs to be emphasized that these are minimums standards; that is, codes define design requirements, procedures, and other aspects that are the minimum considered necessary to achieve the code's purposes. Seismic design codes are a subset, and are generally a section or portion of many building and other design codes. The UBC sections on earthquake design are based on the SEAOC "Blue Book" (i.e., the *Recommended Lateral Force Requirements* of the Structural Engineers Association of California, SEAOC [111]), which states:

> The primary purpose of these recommendations is to provide minimum standards for use in building design regulation to maintain public safety in the extreme earthquakes likely to occur at the building's site. The SEAOC recommendations primarily are intended to safeguard against major failures and loss of life, not to limit damage, maintain functions or provide for easy repair....Structures designed in conformance with these recommendations should, in general, be able to:
>
> 1. Resist minor levels of earthquake ground motion without damage;
> 2. Resist moderate levels of earthquake ground motion without structural damage, but possibly experience some nonstructural damage;
> 3. Resist major levels of earthquake ground motion having an intensity equal to the strongest either experienced or forecast for the building site, without collapse, but possibly with some structural as well as nonstructural damage.
>
> It is expected that structural damage, even in a major earthquake, will be limited to a repairable level for structures that meet these requirements.

The general public, and many decision-makers (i.e., building owners, public officials, investors, etc.), are often not aware that substantial damage can be incurred by a structure in an earthquake, even though the structure is in conformance with the latest design codes (and has been approved as such by local building officials).

Designers should make it a practice to inform owners and other decision-makers of this aspect of earthquake design, and that exceeding minimum requirements may be cost-effective, when costs of damage and disruption are considered.

5.3.2 Historical Development of Seismic Codes

While there is some evidence that efforts were made to codify apparently successful building aspects following earthquakes in earlier times, the first codifications of the concept of equivalent lateral force (ELF) in earthquake resistant building design occurred in the early 20th century. San Francisco was rebuilt after the earthquake and fire of 1906 under provisions that a 30 psf wind force, to affect both wind and earthquake resistance, would be adequate for a building designed with a proper system of bracing [111]. Following the 1908 M7.5 Messina (Italy) earthquake, which killed over 80,000:

> The government of Italy responded to the Messina earthquake by appointing a special committee composed of nine practicing engineers and five professors of engineering... The report of this committee appears to be the first engineering recommendation that earthquake resistant structures be designed by means of the equivalent static method (the percent g method)...M. Panetti, Professor of Applied Mechanics in Turin...recommended that the first story be designed for a horizontal force equal to 1/12 the weight above and the second and third stories to be designed for 1/8 of the building weight above [59].

The ELF concept was proposed in Japan in 1914 by Prof. Riki [96] but not required. It was also used by leading structural engineers in the U.S., but without clear codification.

Following the 1923 Tokyo earthquake, the Japanese Urban Building Law Enforcement Regulations were revised in 1924 to introduce a 0.10 seismic coefficient. Following the 1925 Santa Barbara earthquake in California, the International Conference of Building Officials in 1927 adopted the UBC which "suggested" an ELF ranging from 0.075 to 0.10g for cities located in an area "subject to earthquake shocks" [111]. In 1933, as a result of the Long Beach earthquake, the Field Act in California required all public school buildings to be designed per an ELF (0.10g for masonry, 0.02∼0.05 for other types), and the Riley Act required all buildings be designed per an ELF of 0.02g. The 1935 UBC required 0.08g. Concepts of dynamic response of structures were perhaps first adopted by Los Angeles and, in 1952, the ASCE *Lateral Forces of Earthquake and Wind* report [6] appeared, which related lateral force coefficients to the fundamental period of the structure and provided a framework for codification of dynamic analysis of structures. In Japan, the Building Standard Law was proclaimed in 1950, and required an ELF of 0.20g.

In 1959 the first edition of the SEAOC "Blue Book" appeared. Since that time, the Blue Book (written entirely on a volunteer basis by members of SEAOC) has traditionally been adopted for the seismic provisions of the UBC and other model codes in the U.S., and in many other countries, with modifications appropriate to local conditions. Following a series of earthquakes in the 1960s and 1970s,[7] the UBC was significantly revised in 1976 to generally increase the ELF and, perhaps more importantly, change a number of other requirements, such as concrete detailing. Also introduced was the "R_W" factor, intended to account for and take advantage of overstrength and ductility of LFRS. However, the R_W values are based on professional judgement and experience and their qualification, on a rational basis, has proven challenging. Similarly, the Japanese Building Standard Law was revised in 1971 and 1981 to significantly decrease spacing of hoops or other transverse concrete reinforcement and other respects.

In 1978 the Applied Technology Council's ATC3-06 [9] was issued, marking a major step forward in seismic hazard and dynamic response analysis. That effort has since been continued by the Building Seismic Safety Council (BSSC) founded in 1979 as a result of the passage in 1977 by the U.S. Congress of the Earthquake Hazards Reduction Act (PL 95-124) and creation of the National Earthquake Hazards Reduction Program (NEHRP). BSSC's NEHRP Recommended Provisions for Seismic Regulations for New Buildings were last updated in 1994 [25].

This brief history has only discussed, in very abbreviated form, the development of building seismic design codes, primarily for the U.S. and, to a lesser extent, for Japan. It is summarized, to some extent, in Figure 5.38 which shows a number of earthquakes that have been significant for code development, as well as showing selected other developments, and the general range in the increase in the ELF seismic coefficient. Note also the growth in the number of strong motion records, from the first in the 1933 Long Beach earthquake, to 1971 where the approximately 100 records obtained in that event effectively doubled the number of available records worldwide, to the thousands available today.

5.3.3 Selected Seismic Codes

In the U.S., building code enforcement derives from the police power of the state, which is typically administered either at the state or local level (which grants this power to cities and other jurisdictions), unless pre-emptied by state or federal regulation. Each jurisdiction can thus choose to write its own building ordinances and codes but, practically, many jurisdictions choose to adopt a so-called model

[7] For example, 1964 Alaska, 1964 Niigata, 1967 Santa Rosa, 1968 Tokachi-Oki, 1971 San Fernando, and 1978 Miyagiken-oki.

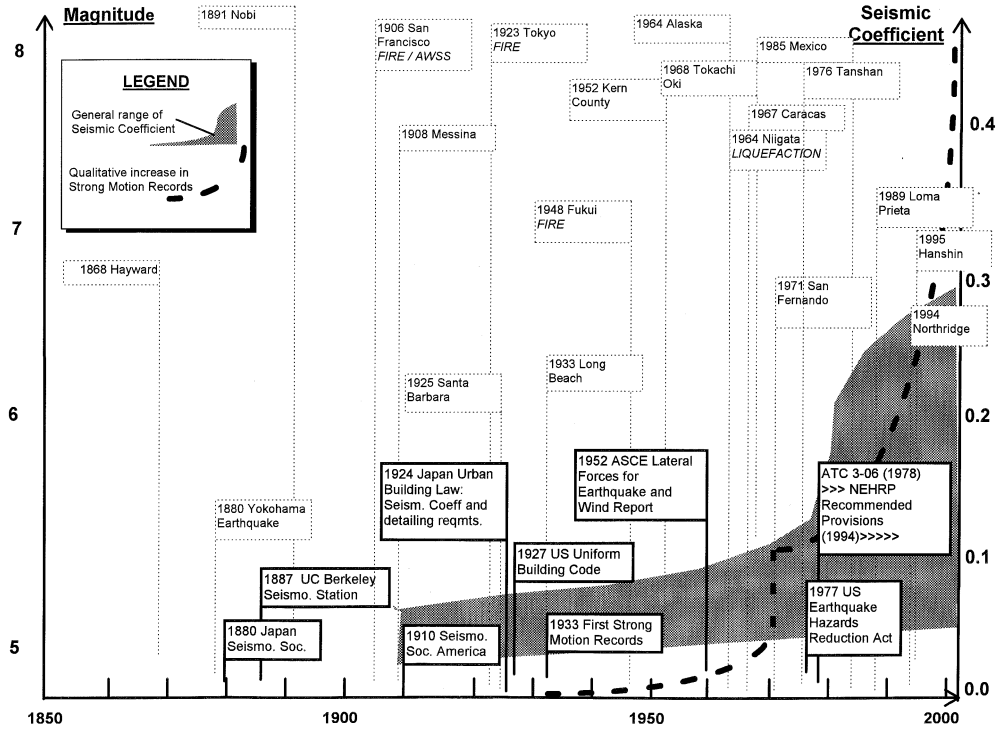

FIGURE 5.38: Schematic development of seismic design codes.

code, of which three exist in the U.S. — the UBC written by the International Conference of Building Officials (ICBO, founded about 1921), the BOCA National Code, written by the Building Officials & Code Administrators International (BOCA, founded in 1915), and the Standard Building Code (SBC) written by the Southern Building Code Congress International (SBCCI, founded more than 50 years ago). The UBC serves as the model code primarily for jurisdictions in the western U.S., BOCA in the central and northeast, and the SBC in the southeast portion of the U.S. (see Figure 5.39). Seismic provisions in these three model codes follow similar formats, derived from the SEAOC Blue Book as discussed above, but adoption of specific provisions varies. In 1994 these three organizations adopted a common format, and will join to write a single International Building Code (IBC) by the year 2000, under the umbrella of the Council of American Building Officials (CABO). The seismic provisions of the IBC will draw on the NEHRP Recommended Provisions [25] as well as a new performance-based *Vision 2000* code format currently under development by SEAOC.

Seismic design of monolithic reinforced concrete structures in the U.S. is guided by the provisions of ACI-318 [1] of the American Concrete Institute (ACI) — the commentary to ACI-318 is a valuable guide to understanding seismic effects on reinforced concrete.

Seismic design codes for other countries and for non-building structures cannot be covered in detail here. A few selected resources include Earthquake Resistant Regulations [64], which is a compilation of earthquake building design codes and regulations used in seismically active regions of the world (seismic regulations for 37 countries are included); the International Handbook of Earthquake Engineering [97], which presents a good explanation of seismic codes and some design practices for 34 countries, as well as a summary of the main developments in seismic code activity for each country; and the so-called Tri-services Manual [127], which provides criteria and guidance for the design of structures to resist the effects of earthquakes, including architectural components,

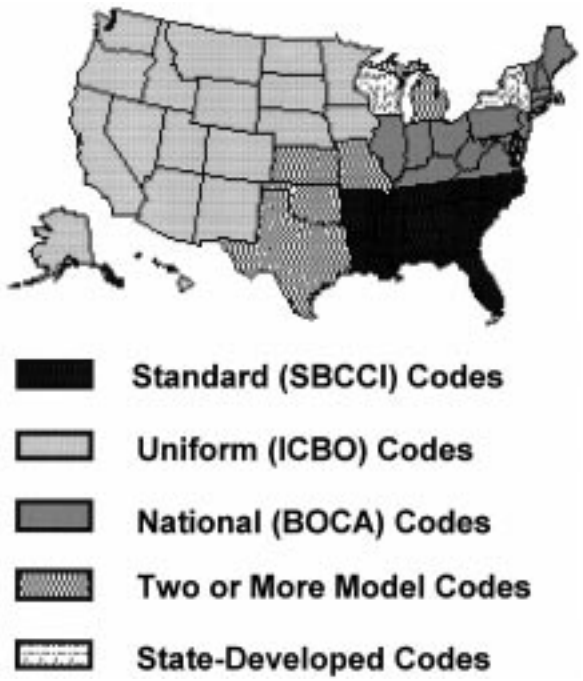

FIGURE 5.39: Geographic influence of model codes. (After CABO www.cabo.org.)

mechanical and electrical equipment supports, some structures other than buildings, and utility systems. Another useful resource is the Practice of Earthquake Hazard Assessment [79], which summarizes probabilistic seismic hazard assessment as it is practiced in 88 seismically active countries throughout the world. Table 5.16 summarizes the countries that are treated by each of these resources.

5.4 Earthquake Effects and Design of Structures

Many different types of earthquake damage occur in structures. This section discusses general earthquake performance of buildings and selected transportation and industrial structures, with the emphasis more towards buildings, especially those typically built in the western U.S. Specific aspects of structural analysis and design of buildings, other structures, steel, concrete, wood, masonry, and other topics are discussed in other chapters.

5.4.1 Buildings

In buildings, earthquake damage can be divided into two categories: structural damage and non-structural damage, both of which can be hazardous to building occupants. Structural damage means degradation of the building's structural support systems (i.e., vertical and lateral force resisting systems), such as the building frames and walls. Non-structural damage refers to any damage that does not affect the integrity of the structural support system. Examples of non-structural damage are a chimney collapsing, windows breaking or ceilings falling, piping damage, disruption of pumps, control panels, telecommunications equipment, etc. Non-structural damage can still be life-threatening and costly. The type of damage to be expected is a complex issue that depends on the structural type and age of the building, its configuration, construction materials, the site conditions, the proximity of

TABLE 5.16 Table of Countries and Related Seismic Design Code Information

Country	E	I	P	S	U	Country	E	I	P	S	U
Afghanistan			X	X		Ecuador			X	X	
Albania			X	X		Egypt	X	X	X	X	
Algeria	X	X		X		El Salvador	X	X	X		
Angola				X		Equatorial Guinea				X	
Argentina	X	X	X	X		Ethiopia	X	X	X		
Australia	X	X	X	X		Fiji			X	X	
Austria	X		X	X		Finland			X	X	
Azores				X	X	France	X	X	X	X	
Bahama Islands				X	X	French West Indies				X	
Bahrain				X		Gabon				X	
Bangladesh			X	X		Gambia				X	
Belgium			X	X		Germany	X		X	X	
Belize				X		Ghana				X	
Benin				X		Greece	X	X	X	X	
Bermuda				X	X	Greenland				X	X
Bolivia			X	X		Grenada				X	
Botswana				X		Guatemala				X	
Brazil			X	X		Guinea				X	
Brunei				X		Haiti				X	
Bulgaria	X	X	X	X		Honduras				X	
Burma				X		Hong Kong				X	
Burundi				X		Hungary		X	X	X	
Cameroon				X		Iceland				X	X
Canada	X	X	X	X		India	X	X	X	X	
Canal Zone				X	X	Indonesia	X	X		X	
Cape Verde				X		Iran	X	X	X	X	
Caroline Islands				X	X	Iraq				X	
Central African Rep.				X		Ireland			X	X	
Chad				X		Israel	X	X	X	X	
Chile	X	X	X	X		Italy	X	X	X	X	
China	X	X	X	X		Ivory Coast			X	X	
Colombia	X	X	X	X		Jamaica			X	X	
Congo				X		Japan	X	X	X	X	X
Costa Rica	X	X	X	X		Johnston Island				X	X
Cuba	X	X	X			Jordan			X	X	
Cyprus			X	X		Kenya				X	
Czech Republic			X	X		Korea				X	
Denmark				X		Kuwait				X	
Djibouti				X		Kwajalein				X	
Dominican Rep.				X		Laos				X	
Eastern Caribbean			X	X		Lebanon				X	
						Leeward Islands				X	X
						Lesotho				X	

TABLE 5.16 Table of Countries and Related Seismic Design Code Information *(continued)*

Country	E	I	P	S	U	Country	E	I	P	S	U
Liberia				X		South Yemen				X	
Libya				X		Spain	X	X	X	X	
Luxembourg				X		Sri Lanka				X	
Malagasy Rep.				X		Swaziland				X	
Malawi				X		Sweden				X	
Malaysia			X	X		Switzerland	X		X	X	
Mali				X		Syria				X	
Malta				X		Taiwan		X	X	X	
Marcus Island					X	Tanzania				X	
Mariana				X	X	Thailand		X	X	X	
Islands				X		Togo				X	
Marshall				X		Trinidad &			X	X	X
Islands						Tobago					
Mauritania				X		Tunisia			X	X	
Mauritius				X		Turkey	X	X	X	X	X
Mexico	X	X		X		Uganda				X	
Morocco				X		United Arab				X	
Mozambique				X		Emir's					
Nepal			X	X		United			X	X	
Netherlands			X	X		Kingdom					
New Zealand	X	X	X	X		Upper Volta				X	
Nicaragua	X			X		Uruguay				X	
Niger				X		USA	X	X	X	X	X
Nigeria			X	X		USSR, Former	X	X	X	X	
Norway			X	X		Venezuela	X	X		X	
Oman				X		Vietnam			X	X	
Pakistan				X		Wake Island				X	X
Panama				X		Yemen Arab				X	
Papua New			X	X		Rep.					
Guinea						Yugoslavia	X	X	X	X	
Paraguay				X		Fmr					
Peru	X	X		X		Zaire			X	X	
Philippines	X			X	X	Zambia				X	
Poland			X	X		Zimbabwe				X	
Portugal	X	X			X						
Puerto Rico		X		X	X	E: Earthquake Resistant Regulations: A World List-1992					
Quatar				X							
Rep. of				X							
Rwanda											
Romania	X	X	X	X		P: Practice of Earthquake Hazard Assessment					
Samoa				X	X						
Saudi Arabia				X							
Senegal				X		I: International Handbook of Earthquake Engineering					
Seychelles				X							
Sierra Leone				X							
Singapore				X							
Slovakia			X			S: Seismic Design for Buildings					
Somalia				X							
South Africa			X	X		U: Uniform Building Code					

After NCEER http://nceer.eng.buffalo.edu/bibs/intcodes.html

the building to neighboring buildings, and the type of non-structural elements.

How Earthquake Forces are Resisted

Buildings experience horizontal distortion when subjected to earthquake motion (Figure 5.40). When these distortions become large, the damage can be catastrophic. Therefore, most buildings are designed with lateral force resisting systems (LFRS) to resist the effects of earthquake forces and

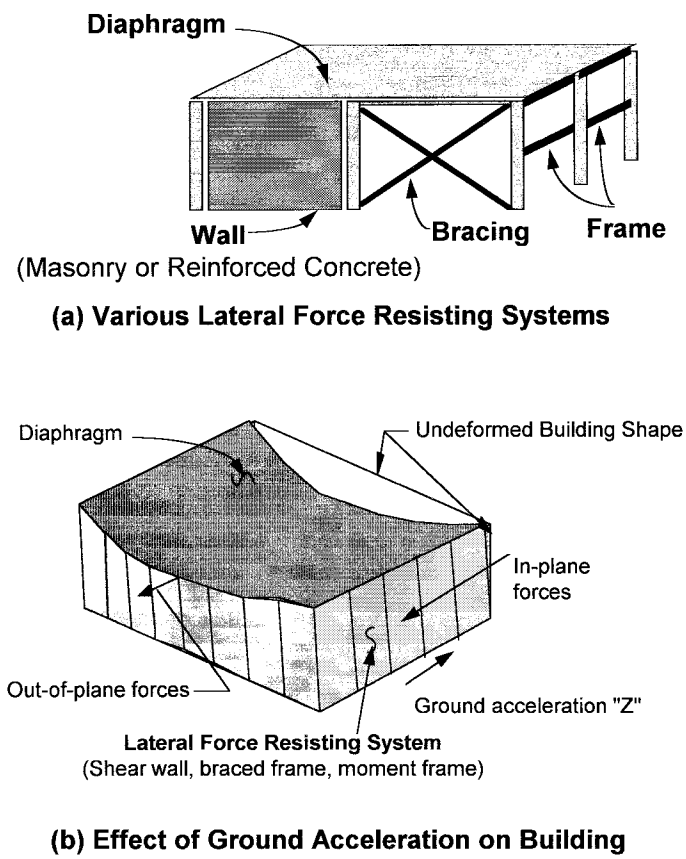

FIGURE 5.40: Resistance of earthquake forces: (a) variety of LFRS and (b) effect of ground acceleration on building.

maintain displacements within specified limits. LFRS are usually capable of resisting only forces that result from ground motions parallel to them. However, the combined action of LFRS along the width and length of a building can typically resist earthquake motion from any direction. LFRS differ from building to building because the type of system is controlled to some extent by the basic layout and structural elements of the building. Basically, LFRS consist of axial- (tension and/or compression), shear- and/or bending-resistant elements.

In wood frame stud-wall buildings, the resistance to lateral loads is typically provided by (a) for older buildings, especially houses, wood diagonal “let-in” bracing, and (b) for newer (primarily post-WW2) buildings, plywood siding “shear walls”. Without the extra strength provided by the bracing or

plywood, walls would distort excessively or "rack", resulting in broken windows, stuck doors, cracked plaster, and, in extreme cases, collapse.

The earthquake resisting systems in modern steel buildings take many forms. Many types of bracing configurations have been used (diagonal, "X", "V", "K", etc). Moment-resisting steel frames are also capable of resisting lateral loads. In this type of construction, the connections between the beams and the columns are designed to resist the rotation of the column relative to the beam. Thus, the beam and the column work together and resist lateral movement by bending. This is contrary to the braced frame, where loads are resisted through tension and compression forces in the braces. Steel buildings are sometimes constructed with moment resistant frames in one direction and braced frames in the other, or with integral concrete or masonry shear walls.

In concrete structures, shear walls[8] are sometimes used to provide lateral resistance, in addition to moment-resisting frames. Ideally, these shear walls are continuous reinforced-concrete walls extending from the foundation to the roof of the building, and can be exterior or interior walls. They are interconnected with the rest of the concrete frame, and thus resist the motion of one floor relative to another. Shear walls can also be constructed of reinforced brick, or reinforced concrete masonry units.

Certain problems in earthquake resistiveness are independent of building type and include the following:

- Configuration, or the general vertical and/or horizontal shape of buildings, is an important factor in earthquake performance and damage. Buildings that have simple, regular, symmetric configurations generally display the best performance in earthquakes. The reasons for this are (1) non-symmetric buildings tend to have twist (i.e., have significant torsional modes) in addition to shaking laterally, and (2) the various "wings" of a building tend to act independently, resulting in differential movements, cracking, and other damage. Rotational motion introduces additional damage, especially at re-entrant or "internal" corners of the building. The term "configuration" also refers to the geometry of lateral load resisting systems as well as the geometry of the building. Asymmetry can exist in the placement of bracing systems, shear walls, or moment-resisting frames that are used to provide earthquake resistance in a building. This type of asymmetry of the LFRS can result in twisting or differential motion, with the same consequences as asymmetry in the building plan. An important aspect of configuration is soft story, which is a story of a building significantly less stiff than adjacent stories (that is, a story in which the lateral stiffness is 70% or less than that in the story above, or less than 80% of the average stiffness of the three stories above [25]). Soft stories often (but not always) occur on the ground floor, where commercial or other reasons require a greater story height, and large windows or openings for ingress or commercial display (e.g., the building might have masonry curtain walls for the full height, except at the ground floor, where these are replaced with large windows, for a store's display). Due to inadequate stiffness, a disproportionate amount of the entire building's drift is concentrated at the soft story, resulting in non-structural and potential structural damage. Many older buildings with soft stories, built prior to recognition of this aspect, collapse due to excessive ductility demands at the soft story.
- Pounding is the collision of adjacent buildings during an earthquake due to insufficient lateral clearance. Such collision can induce very high and unforeseen accelerations and

[8] Termed shear walls because the depth-to-length ratio is so large that, deformation is primarily due to shear rather than bending.

story shears in the overall structure. Additionally, if adjacent buildings have varying story heights, a relatively rigid floor or roof diaphragm may impact an adjacent building at or near mid-column height, causing bending or shear failure in the columns, and subsequent story collapse. Under earthquake lateral loading, buildings deflect significantly. These deflections or drift are limited by code, and adjacent buildings must be separated by a seismic gap equal to the sum of their actual calculated drifts (i.e., ideally, each building set back from its property line by the drift). Pounding has been the cause of a number of building collapses, most notably in the 1985 Mexico City earthquake.

Estimation of Earthquake Forces

As discussed above, estimation of the forces an earthquake may impose on a building may be accomplished by use of an Equivalent Lateral Force (ELF) procedure, or by development of a design basis earthquake using probabilistic methods involving seismicity magnitude-frequency relations, attenuation, etc. For many years, the UBC and other codes determined the ELF according to varients on the equation $V = ZICKSW$ (parameters defined below with the exception of K, varied by type of structure). The current UBC [126] at present determined the minimum ELF, as follows:

$$V = \frac{ZIC}{R_W} W \tag{5.37}$$

where

V = total design lateral force or shear at the base

Z = a seismic zone factor given in Table 16-I of the UBC, and varying between 0.075 (Zone 1, low seismicity areas) and 0.40 (Zone 4, high seismicity areas)

I = importance factor given in Table 16-K of the UBC, varying between $1.0 \sim 1.25$

C = $\frac{1.25S}{T^{2/3}} \leq 2.75$ (and C/R_W shall be ≥ 0.075)

R_W = a numerical coefficient defined in UBC Tables 16-N and 16-P, and varying between $4 \sim 12$ for buildings, and $3 \sim 5$ for selected nonbuilding structures

S = site coefficient for soil characteristics given in UBC Table 16-J (see Table 5.13 of this section)

T = fundamental period of vibration, in seconds, of the structure in the direction under consideration

W = total seismic dead load

In 1997, the UBC revised the determination of total design base shear to be determined according to:

$$V = \frac{C_v I}{RT} W$$

except that the total design base shear need not exceed the following:

$$V = \frac{2.5 C_a I}{R} W$$

nor be less than $V = 0.11 C_a I W$. In this, note that R is not the same as the previous R_W. The new term, R, still accounts for inherent overstrength and global ductility of LFRS, but is somewhat less (R varies from a minimum of 2.8 to a maximum of 8.5) such that base shear levels are increased by about 40% on average. C_a and C_v are seismic coefficients depending on soil type and seismic zone, effectively replacing the previous S factor. In Seismic Zone 4 (the highest), total design base shear is further limited to not be less than $V = 0.8 Z N_v (I/R) W$, where N_v is a near-source factor used in the determination of C_v, related to the proximity of the structure to known faults (and depending on slip rate and maximum magnitude, for the fault; note that there is an analogous N_a). Another important addiction is a Reliability/Redundancy Factor $1.0 \leq \rho \leq 1.5$, which can significantly increase the total design base shear for non-redundant structures.

A number of other requirements and conditions are detailed in the UBC and other seismic codes, and the reader is referred to them for details.

Types of Buildings and Typical Earthquake Performance

The typical earthquake performances of different types of common construction systems are described in this section, to provide insights into the type of damage that may be expected and the strengthening that may be necessary.

Wood Frame Wood frame structures tend to be mostly low rise (one to three stories, occasionally four stories). Vertical framing may be of several types: stud wall, braced post and beam, or timber pole:

- Stud walls are typically constructed of 2 in. by 4 in. wood members set vertically about 16 in. apart — multiple story buildings may have 2x6 or larger studs. These walls are braced by plywood sheathing or by diagonals made of wood or steel. Most detached single and low-rise multiple family residences in the U.S. are of stud wall wood frame construction.
- Post and beam construction is not very common in the U.S., although it is the basis of the traditional housing in other countries (e.g., Europe, Japan), and in the U.S. is found mostly in older housing and larger buildings (i.e., warehouses, mills, churches, and theaters). This type of construction consists of larger rectangular (6 in. by 6 in. and larger) or sometimes round wood columns framed together with large wood beams or trusses.
- Timber pole buildings are a less common form of construction found mostly in suburban/rural areas. Generally adequate seismically when first built, they are more often subject to wood deterioration due to the exposure of the columns, particularly near the ground surface. Together with an often found "soft story" in this building type, this deterioration may contribute to unsatisfactory seismic performance.

Stud wall buildings have performed very well in past U.S. earthquakes for ground motions of about 0.5g or less, due to inherent qualities of the structural system and because they are lightweight and low rise. Cracking in plaster and stucco may occur, and these act to degrade the strength of the building to some extent (i.e., the plaster and stucco may in fact form part of the LFRS, sometimes by design). This is usually classified as non-structural damage but, in fact, dissipates a lot of the earthquake induced energy. However, the most common type of structural damage in older wood frame buildings results from a lack of connection between the superstructure and the foundation — so-called "cripple wall" construction. This kind of construction is common in the milder climes of the western U.S., where full basements are not required, and consists of an air space (typically 2 $\sim$ 3 ft) left under the house. The short stud walls under the first floor (termed by carpenters a cripple wall because of their less than full height) were usually built without bracing, so that there is no adequate LFRS for this short height. Plywood sheathing nailed to the cripple studs may be used to strengthen the cripple walls. Additionally, the mud sill in these older (typically pre-WW2) housings may not be bolted to the foundation. As a result, houses can slide off their foundations when not properly bolted to the foundation, resulting in major damage to the building as well as to plumbing and electrical connections. Overturning of the entire structure is usually not a problem because of the low-rise geometry. In many municipalities, modern codes require wood structures to be bolted to their foundations. However, the year that this practice was adopted will differ from community to community and should be checked.

Garages often have a very large door opening in one wall with little or no bracing. This wall has almost no resistance to lateral forces, which is a problem if a heavy load such as a second story sits on top of the garage (so-called house over garage, or HOGs). Homes built over garages have sustained significant amounts of damage in past earthquakes, with many collapses. Therefore, the house-over-garage configuration, which is found commonly in low-rise apartment complexes and some newer suburban detached dwellings, should be examined more carefully and perhaps strengthened.

Unreinforced masonry chimneys also present a life-safety problem. They are often inadequately tied to the building and therefore fall when strongly shaken. On the other hand, chimneys of reinforced masonry generally perform well.

Some wood frame structures, especially older buildings in the eastern U.S., have masonry veneers that may represent another hazard. The veneer usually consists of one wythe of brick (a wythe is a term denoting the width of one brick) attached to the stud wall. In older buildings, the veneer is either insufficiently attached or has poor quality mortar, which often results in peeling off of the veneer during moderate and large earthquakes.

Post and beam buildings tend to perform well in earthquakes, if adequately braced. However, walls often do not have sufficient bracing to resist horizontal motion and thus they may deform excessively.

The 1994 M_W 6.7 Northridge earthquake was the largest earthquake to occur directly within an urbanized area since the 1971 San Fernando earthquake; ground motions were as high as 0.9g, and substantial numbers of modern wood-frame dwellings sustained significant damage, including major cracking of veneers, gypsum board walls, and splitting of wood wall studs. It may be inferred from this, as well as the performance observed in the more sparsely populated epicentral regions of the 1989 M_W 7.1 Loma Prieta earthquake, that the U.S. single family dwelling design begins to sustain substantial non-structural and structural damage for PGA in excess of about 0.5g.

Steel Frame Buildings Steel frame buildings generally may be classified as either moment resisting frames (MRF) or braced frames, based on their lateral force resisting systems. In concentric braced frames, the lateral forces or loads are resisted by the tension only, or tensile and compressive strength of the bracing, which can assume a number of different configurations including diagonal, 'V', inverted "V" (also termed chevron), "K", etc. A recent development in seismic bracing is the eccentric brace frame (EBF). Here the bracing is slightly offset from the main beam to column connection, and a short section of beam is expected to deform significantly under major seismic forces and thereby dissipate a considerable portion of the energy. Moment resisting frames resist lateral loads and deformations by the bending stiffness of the beams and columns (there is no bracing).

Steel frame buildings have tended to perform satisfactorily in earthquakes with ground motions less than about 0.5g because of their strength, flexibility, and lightness. Collapse in earthquakes has been very rare, although steel frame buildings did collapse, for example, in the 1985 Mexico City earthquake. More recently, following the 1994 M_W 6.7 Northridge earthquake, a number of MRF were found to have sustained serious cracking in the beam column connection (see Figure 5.41, which shows one of a number of different types of cracking that were found following the Northridge earthquake). The cracking typically initiated at the lower beam flange location and propagated upward into the shear panel. Similar cracking was also observed following the 1995 M_W 6.9 Hanshin (Kobe) earthquake, which experienced similar levels of ground motion as Northridge. More worrisome is that, as of this writing, some steel buildings in the San Francisco Bay Area have been found to have similar cracking, presumably as a result of the 1989 M_W 7.1 Loma Prieta earthquake. As a result, there is an on-going effort by a consortium of research organizations, termed SAC (funded by the Federal Emergency Management Agency) to better understand and develop solutions for this problem.

Light gage steel buildings are used for agricultural structures, industrial factories, and warehouses. They are typically one story in height, sometimes without interior columns, and often enclose a large floor area. Construction is typically of steel frames spanning the short dimension of the building and resisting lateral forces as moment frames. Forces in the long direction are usually resisted by diagonal steel rod bracing. These buildings are usually clad with lightweight metal or reinforced concrete siding, often corrugated. Because these buildings are low-rise, lightweight, and constructed of steel members, they usually perform relatively well in earthquakes. Collapses do not usually occur. Some typical problems are (a) insufficient capacity of tension braces can lead to their elongation and, in turn, building damage, and (b) inadequate connection to the foundation can allow the building columns to slide.

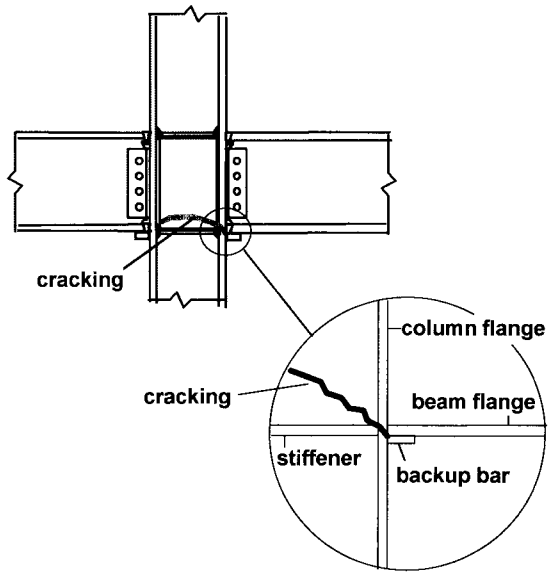

FIGURE 5.41: Example steel moment-frame connection cracking.

Concrete Buildings Several construction subtypes fall under this category: (a) moment resisting frames (nonductile or ductile), (b) shear wall structures, and (c) pre-cast, including tilt-up structures. The most prevalent of these is nonductile reinforced concrete frame structures with or without infill walls built in the U.S. between about 1920 and (in the western U.S.) about 1972. In many others portions of the U.S. this type of construction continues to the present. This group includes large multistory commercial, institutional, and residential buildings constructed using flat slab frames, waffle slab frames, and the standard girder-column type frames. These structures generally are more massive than steel frame buildings, are under-reinforced (i.e., have insufficient reinforcing steel embedded in the concrete) and display low ductility. Some typical problems are: (a) large tie spacings in columns can lead to a lack of concrete confinement and/or shear failure; (b) placement of inadequate rebar splices at the same location can lead to column failure; (c) insufficient shear strength in columns can lead to shear failure prior to the development of moment hinge capacity; (d) insufficient shear tie anchorage can prevent the column from developing its full shear capacity; (e) lack of continuous beam reinforcement can result in hinge formation during load reversal ; (f) inadequate reinforcing of beam-column joints or location of beam bar splices at columns can lead to failures; and (g) the relatively low stiffness of the frame can lead to substantial non-structural damage.

Ductile RC frames where special reinforcing details are required in order to furnish satisfactory load-carrying performance under large deflections (termed ductility) have usually only been required in the highly seismic portions of the U.S. since the late 1960s (first provisions appeared in the 1967 UBC). ACI-318 [1] provides comprehensive treatment for the ductile detailing, which involves a number of special requirements including close spacing of lateral reinforcement in order to attain confinement of a concrete core, appropriate relative dimensioning of beams and columns, 135° hooks on lateral reinforcement, hooks on main beam reinforcement within the column, etc.

Concrete shear wall buildings consist of a concrete box or frame structural system with walls constituting the main LFRS. The entire structure, along with the usual concrete diaphragm, is typically cast in place. Shear walls in buildings can be located along the perimeter, as interior walls, or around the service or elevator core. This building type generally tends to perform better than concrete frame

buildings. They are heavier than steel frame buildings but they are also rigid due to the shear walls. Some types of damage commonly observed in taller buildings are caused by vertical discontinuities, pounding, and/or irregular configuration. Other damages specific to this building type are (a) shear cracking and distress occurring around openings in concrete shear walls during large seismic events; (b) shear failure occurring at wall construction joints usually at a load level below the expected capacity; and (c) bending failures resulting from insufficient chord steel lap lengths.

Tilt-up buildings are a common type of construction in the western U.S., and consist of concrete wall panels cast on the ground and then tilted upward into their final positions. More recently, wall panels are fabricated off-site and trucked in. The wall panels are welded together at embedments, or held in place by cast-in-place columns or steel columns, depending on the region. The floor and roof beams are often glue-laminated wood or steel open webbed joists that are attached to the tilt-up wall panels; these panels may be load bearing or non-load bearing, depending on the region. These buildings tend to be low-rise industrial or office buildings. Before 1973 in the western U.S., many tilt-up buildings did not have sufficiently strong connections or anchors between the walls and the roof and floor diaphragms. During an earthquake, weak anchors pulled out of the walls, causing the floors or roofs to collapse. The connections between concrete panels are also vulnerable to failure. Without these, the building loses much of its lateral force-resisting capacity. For these reasons, many tilt-up buildings were damaged in the 1971 San Fernando earthquake. Since 1973, tilt-up construction practices have changed in California and other high seismicity regions, requiring positive wall-diaphragm connection and prohibiting cross-grain bending in wall ledgers. (Such requirements may not have yet been made in other regions of the country.) However, a large number of these older, pre-1970s vintage tilt-up buildings still exist and have not been retrofitted to correct this wall-anchor defect. These buildings are a prime source of seismic risk. In areas of low or moderate seismicity, inadequate wall anchor details continue to be employed. Damage to tilt-up buildings was observed again in the 1994 M_W 6.7 Northridge earthquake, where the primary problems were poor wall anchorage into the concrete, and excessive forces due to flexible roof diaphragms amplifying ground motion to a greater extent than anticipated in the code.

Precast concrete frame construction, first developed in the 1930s, was not widely used until the 1960s. The precast frame is essentially a post and beam system in concrete where columns, beams, and slabs are prefabricated and assembled on site. Various types of members are used: vertical load carrying elements may be T's, cross shapes, or arches and are often more than one story in height. Beams are often T's and double T's, or rectangular sections. Prestressing of the members, including pre-tensioning and post-tensioning, is often employed. The LFRS is often concrete CIP shear walls. The earthquake performance of this structural type varies greatly and is sometimes poor. This type of building can perform well if the details used to connect the structural elements have sufficient strength and ductility (toughness). Because structures of this type often employ cast-in-place concrete shear walls for lateral load resistance, they experience the same types of damage as other shear wall building types. Some of the problem areas specific to precast frames are (a) failure of poorly designed connections between prefabricated elements; (b) accumulated stresses due to shrinkage and creep and due to stresses incurred in transportation; (c) loss of vertical support due to inadequate bearing area and/or insufficient connection between floor elements and columns; and (d) corrosion of metal connectors between prefabricated elements. A number of pre-cast parking garages failed in the 1994 M_W 6.7 Northridge earthquake, including a large structure at the Cal State Northridge campus which sustained a progressive failure. This structure had a perimeter pre-cast MRF and interior non-ductile columns — the MRF sustained large but tolerable deflections; however, interior non-ductile columns failed under these deflections, resulting in an interior collapse, which then pulled the exterior MRF's over.

Masonry Reinforced masonry buildings are mostly low-rise perimeter bearing wall structures, often with wood diaphragms although precast or cast-in-place concrete is sometimes used.

Floor and roof assemblies usually consist of timber joists and beams, glue-laminated beams, or light steel joists. The bearing walls consist of grouted and reinforced hollow or solid masonry units. Interior supports, if any, are often wood or steel columns, wood stud frames, or masonry walls. Generally, they are less than five stories in height although many mid-rise masonry buildings exist. Reinforced masonry buildings can perform well in moderate earthquakes if they are adequately reinforced and grouted and if sufficient diaphragm anchorage exists.

Most unreinforced masonry (URM) bearing wall structures in the western U.S. were built before 1934, although this construction type was permitted in some jurisdictions having moderate or high seismicity until the late 1940s or early 1950s (in low-seismicity jurisdictions, URM may still be a common type of construction even today). These buildings usually range from one to six stories in height and construction typically varies according to the type of use, although wood floor and roof diaphragms are common. Smaller commercial and residential buildings usually have light wood floor/roof joists supported on the typical perimeter URM wall and interior wood load bearing partitions. Larger buildings, such as industrial ware- houses, have heavier floors and interior columns, usually of wood. The bearing walls of these industrial buildings tend to be thick, often as much as 24 in. or more at the base. Wall thicknesses of residential buildings range from 9 in. at upper floors to 17 in. at lower floors. Unreinforced masonry structures are recognized as perhaps the most hazardous structural type. They have been observed to fail in many modes during past earthquakes. Typical problems are

1. Insufficient anchorage—Because the walls, parapets, and cornices were not positively anchored to the floors, they tend to fall out. The collapse of bearing walls can lead to major building collapses. Some of these buildings have anchors as a part of the original construction or as a retrofit. These older anchors exhibit questionable performance.
2. Excessive diaphragm deflection—Because most of the floor diaphragms are constructed of wood sheathing, they are very flexible and permit large out-of-plane deflection at the wall transverse to the direction of the force. The large drift, occurring at the roof line, can cause the masonry wall to collapse under its own weight.
3. Low shear resistance—The mortar used in these older buildings is often made of lime and sand, with little or no cement, and has very little shear strength. The bearing walls will be heavily damaged and collapse under large loads.
4. Wall slenderness—Some of these buildings have tall story heights and thin walls. This condition, especially in non-load bearing walls, will result in out-of-plane failure, under severe lateral load. Failure of a non-load-bearing wall represents a falling hazard, whereas the collapse of a load- bearing wall will lead to partial or total collapse of the structure.

Innovative techniques can be divided into two broad categories: passive control (base isolation, energy dissipation) and active control, which increasingly are being applied to the design of new structures or to the retrofit of existing structures against wind, earthquakes, and other external loads [117]. The distinction between passive and active control is that passive systems require no active intervention or energy source, while active systems typically monitor the structure and incoming ground motion, and seek to actively control masses or forces in the structure (via moving weights, variable tension tendons, etc.) so as to develop a structural response (ideally) equal and opposite to the structural response due to the incoming ground motion. Recently developed semi-active control systems appear to combine the best features of both approaches, offering the reliability of passive devices, yet maintaining the versatility and adaptability of fully active systems. Magnetorheological (MR) dampers, for example, are new semi-active control devices that use MR fluids to create controllable damper. Initial results indicate that these devices are quite promising for civil engineering applications [30, 41, 42, 118].

Passive Control

Base isolation consists of softening of the shear capacity of a structure's connection with the ground, while maintaining vertical load carrying capacity, so as to reduce the earthquake ground motion input to the structure [71]. This has mostly been accomplished to date via the use of various types of rubber, lead-rubber, rubber-steel composite, or other types of bearings, beneath columns. Key aspects of most of the base isolation systems developed to date are: (1) they are economically limited to selected classes of structures (not too tall or short); (2) they require additional foundation expense, including special treatment of incoming utility lines; and (3) they require a certain amount of "rattlespace" around the structure, to accomodate the additional displacements that the bearings will undergo. For new structures, these requirements are not especially onerous, and a number of new structures in Japan, and a few in other countries, have been designed for base isolation. Most applications of this technology in the U.S., however, have been for the retrofit of existing (usually historic [26, 72]) structures, where the technology permitted increased seismic capacity without major modification to the architectural features. The technique has been applied to a number of highway bridges in the U.S., as well as some industrial structures.

Supplemental Damping — If damping can be significantly increased, then structural response (and therefore forces and displacements) are greatly reduced [34, 55]. Supplemental damping systems include *friction* systems (e.g., Sumitomo, Pall, and Friction-Slip) based on Coulomb friction, *self-centering* friction resistance that is proportional to displacement (e.g., Fluor-Daniel Energy Dissipating Restraint), or various *energy dissipation* mechanisms: ADAS (added damping and stiffness) elements, which utilize the yielding of mild-steel X-plates; viscoelastic shear dampers using a 3M acrylic copolymer as the dissipative element; or Nickel-Titanium alloy shape-memory devices that take advantage of reversible, stress-induced phase changes in the alloy to dissipate energy [2]. These systems are generally still in the developmental stage, although there are no special obstacles for implementation of the ADAS system [85, 132, 135], which has seen one application to date in the U.S. [99, 107] and more in other countries.

Active Control

Active control depends on actively modifying a structure's mass, stiffness, or geometric properties during its dynamic response, in such a manner as to counteract and reduce excessive displacements [76]. Tuned mass dampers, reliance on liquid sloshing [75], and active tensioning of tendons are methods currently under investigation [61, 62, 116]. Most methods of active control are real-time, relying on measurement of structural response, rapid structural computation, and fast-acting energy sources. A number of issues of reliability remain to be resolved [119].

5.4.2 Non-Building Structures

Bridges

The most vulnerable components of conventional bridges have been support bearings, abutments, piers, footings, and foundations. A common deficiency is that unrestrained expansion joints are not equipped to handle large relative displacements (inadequate support length), and simple bridge spans fall. Skewed bridges, in particular, have performed poorly in past earthquakes because they respond partly in rotation, resulting in an unequal distribution of forces to bearings and supports. Rocker bearings have proven most vulnerable. Roller bearings generally remain stable in earthquakes, except they may become misaligned and horizontally displaced. Elastomeric bearing pads are relatively stable although they have been known to "walk out" under severe shaking. Failure of backfill near abutments is common and can lead to tilting, horizontal movement or settlement of abutments, spreading and settlement of fills, and failure of foundation members. Abutment damage rarely leads to bridge collapse. Liquefaction of saturated soils in river channels and floodplains and

subsequent loss of support have caused many bridge failures in past earthquakes, notably in the 1990 M_W 7.7 Philippines and 1991 M_W 7.1 Costa Rica earthquakes. Pounding of adjacent, simply supported spans can cause bearing damage and cracking of the girders and deck slab. Piers have failed in a number of earthquakes including most recently the 1994 M_W 6.7 Northridge and 1995 MW 6.9 Hanshin (Kobe) earthquakes, primarily because of insufficient transverse confining steel, and inadequate longitudinal steel splices and embedment into the foundation. Bridge superstructures have not exhibited any particular weaknesses other than being dislodged from their bearings.

Regarding aseismic design, bridge behavior during an earthquake can be very complex. Unlike buildings, which generally are connected to a single foundation through the diaphragm action of the base slab, bridges have multiple supports with varying foundation and stiffness characteristics. In addition, longitudinal forces are resisted by the abutments through a combination of passive backwall pressures and foundation embedment when the bridge moves toward an abutment, but by the abutment foundation only as the bridge moves away from an abutment. Significant movement must occur at bearings before girders impact abutments and bear against them, further complicating the response. To accurately assess the dynamic response of all but the simplest bridges, a three-dimensional dynamic analysis should be performed. Special care is required for design of hinges for continuous bridges. Restraint for spans or adequate bearing lengths to accommodate motions are the most effective ways to mitigate damage. In order to prevent damage to piers, proper confinement, splices, and embedment into the foundation should be provided. Similarly, sufficient steel should be provided in footings. Loads resisted by bridges may be reduced through use of energy absorption features including ductile columns, lead-filled elastomeric bearings, and restrainers. Foundation failure can be prevented by ensuring sufficient bearing capacity, proper foundation embedment, and sufficient consolidation of soil behind retaining structures.

In general, railway bridges may be steel, concrete, wood, or masonry construction, and their spans may be any length. Included are open and ballasted trestles, drawbridges, and fixed bridges. Bridge components include a bridge deck, stringers and girder, ballast, rails and ties, truss members, piers, abutments, piles, and caissons. Railroads sometimes share major bridges with highways (suspension bridges), but most railway bridges are older and simpler in configuration than highway bridges. Bridges that cross streams or narrow drainage passages typically have simple-span deck plate girders or beams. Longer spans use simple trusses supported on piers. Only a few of the more recently constructed bridges have continuous structural members.

The major cause of damage to trestles is displacement of unconsolidated sediments on which the substructures are supported, resulting in movement of pile-supported piers and abutments. Resulting superstructure damage has consisted of compressed decks and stringers, as well as collapsed spans. Shifting of the piers and abutments may shear anchor bolts. Girders can also shift on their piers. Failures of approaches or fill material behind abutments can result in bridge closure. Movable bridges are more vulnerable than fixed bridges; slight movement of piers supporting drawbridges can result in binding so that they cannot be opened without repairs.

Industrial Structures

Most large water, oil, and other storage tanks are unanchored, cylindrical tanks supported directly on the ground. Smaller tanks may be anchored, and tanks can also be elevated or buried. Older oil tanks are either fixed or floating roof, while more modern larger tanks are almost exclusively floating-roofed. Potable water tanks are invariably fixed roof. Diameters range from approximately 40 ft to more than 250 ft. Tank height on larger tanks is nearly always less than the diameter. Construction materials include welded, bolted, or riveted steel (for water), concrete and sometimes (for water or chemicals, and in smaller sizes) fiberglass. Tank foundations may consist of sand or gravel, or a concrete ring wall supporting the shell, supported on piles in poor soils. On-ground storage tanks are subject to a variety of earthquake damage mechanisms, generally due to sliding or

rocking. Rocking is typically due to fluid sloshing, which must be considered for most tanks [60]. Specific failure modes include:

1. failure of weld between baseplate and wall
2. buckling of tank wall (termed elephant foot buckling)
3. rupture of attached rigid piping due to sliding or rocking of the tank
4. implosion of tank resulting from rapid loss of contents and negative internal pressure
5. differential settlement
6. anchorage failure or tearing of tank wall
7. failure of roof-to-shell connection or damage to roof seals for floating roofs (and loss of contents)
8. failure of shell at bolts or rivets because of tensile hoop stresses
9. total collapse

Torsional rotations of floating roofs may damage attachments such as guides, ladders, etc. Aseismic design practices for ground storage tanks include the use of flexible piping, pressure relief valves, and well-compacted foundations and concrete ring walls that prevent differential settlement. Adequate freeboard to prevent sloshing against the roof should be maintained. Positive attachment between the roof and shell should be provided for fix-roofed tanks. The bottom plate and its connection to the shell should be stiffened to resist uplift forces, and the baseplate should be protected against corrosion. Abrupt changes in thickness between adjacent courses should be avoided. Properly detailed ductile anchor bolts may be feasible on smaller steel tanks. Maintaining a height-to-diameter ratio of between 0.3 and 0.7 for tanks supported on the ground controls seismic loading.

In general, ports/cargo handling equipment comprise buildings (predominantly warehouses), waterfront structures, cargo handling equipment, paved aprons, conveyors, scales, tanks, silos, pipelines, railroad terminals, and support services. Building type varies, with steel frame being a common construction type. Waterfront structures include quay walls, sheet-pile bulkheads, and pile-supported piers. Quay walls are essentially waterfront masonry or caisson walls with earth fills behind them. Piers are commonly wood or concrete construction and often include batter piles to resist lateral transverse loads. Cargo handling equipment for loading and unloading ships includes cranes for containers, bulk loaders for bulk goods, and pumps for liquid fuels. Additional handling equipment is used for transporting goods throughout port areas. By far the most significant source of earthquake-induced damage to port and harbor facilities has been porewater pressure buildup in the saturated cohesionless soils that prevail at these facilities. This pressure buildup can lead to application of excessive lateral pressures to quay walls by backfill materials, liquefaction, and massive submarine sliding. This has occurred in a number of earthquakes including the 1985 M_W 7.8 Chile and 1989 M_W 7.1 Loma Prieta earthquakes but most notably and on a massive scale in the 1995 M_W 6.9 Hanshin (Kobe) earthquake, where several kilometers of deep-water caisson rotated outward, rendering dozens of ship berths unusable.

Electric transmission substations generally receive power at high voltages (often 220 kV or more) and step it down to lower voltages for distribution. The substations generally consist of one or more control buildings, steel towers, conductors, ground wires, underground cables, and extensive electrical equipment including banks of circuit breakers, switches, wave traps, buses, capacitors, voltage regulators, and massive transformers. Circuit breakers (oil or gas) protect transformers against power surges due to short circuits. Buses provide transmission linkage of the many and varied components within the substation. Transformers and voltage regulators serve to maintain the predetermined voltage or to step down or step up from one voltage to another. Porcelain lightning arresters are used to protect the system from voltage spikes caused by lightning. Long, cantilevered porcelain components (e.g., bushings and lightning arresters) are common on many electrical equipment items.

In earthquakes, unanchored or improperly anchored equipment may slide or topple, experiencing damage or causing attached piping and conduit to fail. In the yard, steel towers are typically damaged only by soil failures. Porcelain bushings, insulators, and lightning arresters are brittle and vulnerable to shaking and are frequently damaged, especially at the highest voltages. Transformers are large, heavy pieces of equipment that are frequently unanchored or inadequately anchored, so that they may shift, tear the attached conduit, break bushings, damage radiators, and spill insulating oil. Transformers in older substations that are mounted on rails frequently have fallen off their rails unless anchored. Frequently, inadequate slack in conductors or rigid bus bars result in porcelain damage due to differential motion of supports. Aseismic design practice includes the use of damping devices for porcelain; proper anchorage for equipment (avoid the use of friction clips); provision of conductor slack between equipment in the substation; use of breakaway connectors to reduce loads on porcelain bushings and insulators; and replacement of single cantilever-type insulator supports with those having multiple supports. Transformer radiators that cantilever from the body of a transformer can be braced. Adequate spacing between equipment can reduce the likelihood of secondary damage resulting from adjacent equipment falling.

5.5 Defining Terms

Attenuation: the rate at which earthquake ground motion decreases with distance.

Body waves: vibrational waves transmitted through the body of the earth, which are of two types: P waves (transmitting energy via dilatational or push-pull motion), and slower S waves (transmitting energy via shear action at right angles to the direction of motion).

Characteristic earthquake: a relatively narrow range of magnitudes at or near the maximum that can be produced by the geometry, mechanical properties, and state of stress of a fault [110].

Completeness: homogeneity of the seismicity record.

Corner frequency, f_o : the frequency above which earthquake radiation spectra vary with ϖ^{-3} - below f_o, the spectra are proportional to seismic moment.

Cripple wall: a carpenters term indicating a wood frame wall of less than full height, usually built without bracing.

Critical damping: the value of damping such that free vibration of a structure will cease after one cycle ($c_{crit} = 2m\omega$).

Damping: represents the force or energy lost in the process of material deformation (damping coefficient $c =$ force per velocity).

Design (basis) earthquake: the earthquake (as defined by various parameters, such as PGA, response spectra, etc.) for which the structure will be, or was, designed.

Dip-slip: motion at right angles to the strike, up- or down-slip.

Dip: the angle between a plane, such as a fault, and the earth's surface.

Ductile detailing: special requirements such as for reinforced concrete and masonry, close spacing of lateral reinforcement to attain confinement of a concrete core, appropriate relative dimensioning of beams and columns, 135° hooks on lateral reinforcement, hooks on main beam reinforcement within the column, etc.

Ductile frames: frames required to furnish satisfactory load-carrying performance under large deflections (i.e., ductility). In reinforced concrete and masonry this is achieved by ductile detailing.

Ductility factor: the ratio of the total displacement (elastic plus inelastic) to the elastic (i.e., yield) displacement.

Epicenter: the projection on the surface of the earth directly above the hypocenter.

Far-field: beyond near-field, also termed teleseismic.

Fault: a zone of the earths crust within which the two sides have moved — faults may be hundreds of miles long, from 1 to over 100 miles deep, and not readily apparent on the ground surface.

Fragility: the probability of having a specific level of damage given a specified level of hazard.

Hypocenter: the location of initial radiation of seismic waves (i.e., the first location of dynamic rupture).

Intensity: a metric of the effect, or the strength, of an earthquake hazard at a specific location, commonly measured on qualitative scales such as MMI, MSK, and JMA.

Lateral force resisting system: a structural system for resisting horizontal forces due, for example, to earthquake or wind (as opposed to the vertical force resisting system, which provides support against gravity).

Liquefaction: a process resulting in a soil's loss of shear strength, due to a transient excess of pore water pressure.

Magnitude-frequency relation: the probability of occurrence of a selected magnitude — the most common is $\log_{10} n(m) = a - bm$ [48].

Magnitude: a unique measure of an individual earthquake's release of strain energy, measured on a variety of scales, of which the moment magnitude M_W (derived from seismic moment) is preferred.

Meizoseismal: the area of strong shaking and damage.

MMI (modified mercalli intensity) scale: see Table 5.4.

MSK: see table 5.5.

Near-field: within one source dimension of the epicenter, where source dimension refers to the length or width of faulting, whichever is less. (Alternatively termed near-source, this region is also defined as limited to about 10 km from the fault rupture surface, where the large velocity pulse dominated spectra are common.)

Non-ductile frames: frames lacking ductility or energy absorption capacity due to lack of ductile detailing — ultimate load is sustained over a smaller deflection (relative to ductile frames) and for fewer cycles.

Normal fault: a fault that exhibits dip-slip motion, where the two sides are in tension and move away from each other.

Peak ground acceleration (PGA): the maximum amplitude of recorded acceleration (also termed the ZPA, or zero period acceleration).

Pounding: the collision of adjacent buildings during an earthquake due to insufficient lateral clearance.

Response spectrum: a plot of maximum amplitudes (acceleration, velocity, or displacement) of a single degree of freedom oscillator (SDOF), as the natural period of the SDOF is varied across a spectrum of engineering interest (typically, for natural periods from .03 to 3 or more seconds, or frequencies of 0.3 to 30+ hz).

Reverse fault: a fault that exhibits dip-slip motion, where the two sides are in compression and move away towards each other.

Sand boils or mud volcanoes: ejecta of solids (i.e., sand, silt) carried to the surface by water, due to liquefaction.

Seismic hazard: a generic term for the expected seismic intensity at a site, more commonly measured using engineering measures, such as PGA, response spectra, etc.

Seismic hazards: the phenomena and/or expectation of an earthquake-related agent of damage, such as fault rupture, vibratory ground motion (i.e., shaking), inundation (e.g., tsunami, seiche, dam failure), various kinds of permanent ground failure (e.g., liquefaction), fire, or hazardous materials release.

Seismic moment: the moment generated by the forces generated on an earthquake fault during slip.

Seismic risk: the product of the hazard and the vulnerability (i.e., the expected damage or loss, or associated full probability distribution).

Seismotectonic model: a mathematical model representing the seismicity, attenuation, and related environment.

Soft story: a story of a building significantly less stiff than adjacent stories (that is, the lateral stiffness is 70% or less than that in the story above, or less than 80% of the average stiffness of the three stories above [25]).

Spectrum amplification factor: the ratio of a response spectral parameter to the ground motion parameter (where parameter indicates acceleration, velocity, or displacement).

Strike: the intersection of a fault and the surface of the earth, usually measured from north (e.g., the fault strike is N 60° W).

Subduction: refers to the plunging of a tectonic plate (e.g., the Pacific) beneath another plate (e.g., the North American) down into the mantle, due to convergent motion.

Surface waves: vibrational waves transmitted within the surficial layer of the earth, which are of two types: horizontally oscillating Love waves (analogous to *s* body waves) and vertically oscillating Rayleigh waves.

Thrust fault: low-angle reverse faulting (blind thrust faults are faults at depth occurring under anticlinal folds — they have only subtle surface expression).

Transform or strike slip fault: a fault where relative fault motion occurs in the horizontal plane, parallel to the strike of the fault.

Uniform hazard spectra: response spectra with the attribute that the probability of exceedance is independent of frequency.

Vulnerability: the expected damage given a specified value of a hazard parameter.

References

[1] ACI. 1995. *Building Code Requirements for Structural Concrete (ACI 318-95) and Commentary (ACI 318R-95)*, American Concrete Institute, Farmington Hills, MI.

[2] Aiken, I.D., Nims, D.K., Whittaker, A.S., and, Kelly, J.M. 1993. Testing of Passive Energy Dissipation Systems. *Earthquake Spectra*, 9(3), 336-370.

[3] Algermissen, S.T. 1983. *An Introduction to the Seismicity of the United States*, Earthquake Engineering Research Institute, Oakland, CA.

[4] Ambrayses, N.N. and Melville, C.P. 1982. *A History of Persian Earthquakes*, Cambridge University Press, Massachusetts.

[5] Anagnos, T. and Kiremidjian, A. S. 1984. Temporal Dependence in Earthquake Occurrence, in *Proc. Eighth World Conf. Earthquake Eng.*, 1, 255-262, Earthquake Engineering Research Institute, Oakland, CA.

[6] Anderson, Blume, Degenkolb et al. 1952. Lateral Forces of Earthquake and Wind, *Trans. Am. Soc. Civil Engrs.*, 117, *Am. Soc. Civil Engrs.*, New York.

[7] Anderson, J. G. and Trifunac, M D. 1977. Uniform Risk Absolute Acceleration Spectra, *Advances In Civil Engineering Through Engineering Mechanics: Proceedings Of The Second Annual Engineering Mechanics Division Specialty Conference*, Raleigh, NC, May 23-25, 1977, American Society of Civil Engineers, New York, pp. 332-335.

[8] Arias, A. 1970. A Measure of Earthquake Intensity, in *Seismic Design of Nuclear Power Plants*, R. Hansen, Ed., MIT Press, Massachusetts .

[9] ATC 3-06. 1978. *Tentative Provisions For The Development Of Seismic Regulations For Buildings*, Applied Technology Council, Redwood City, CA.

[10] Atkinson, G. M. 1995. Attenuation and Source Parameters of Earthquakes in the Cascadia Region, *Bull. Seis. Soc. Am.*, 85(5), 1327-1342.

[11] Atwater, B.F. et al. 1995. Summary of Coastal Geologic Evidence for Past Great Earthquakes at the Cascadia Subduction Zone, *Earthquake Spectra*, 11(1), 1-18, 1995.

[12] Bartlett, S.F. and Youd, T.L. 1992. *Empirical Analysis of Horizontal Ground Displacement Generated by Liquefaction-Induced Lateral Spread*, Tech. Rept. NCEER-92-0021, National Center for Earthquake Engineering Research, Buffalo, NY.

[13] Bernreuter, D.L. et al. 1989. *Seismic Hazard Characterization of 69 Nuclear Power Plant Sites East of the Rocky Mountains*, U.S. Nuclear Regulatory Commission, NUREG/CR-5250.

[14] Blume, J.A. 1970. An Engineering Intensity Scale for Earthquakes and other Ground Motions, *Bull. Seis. Soc. Am.*, 60(1), 217-229.

[15] Bolt, B.A. 1973. Duration of Strong Ground Motion, *Proc. 5th World Conf. On Earthquake Engineering*, 1, 1304-1313.

[16] Bolt, B.A. 1993. *Earthquakes*, W.H. Freeman and Co., New York.

[17] Bonilla, M.G. et al. 1984. Statistical Relations Among Earthquake Magnitude, Surface Rupture Length, and Surface Fault Displacement, *Bull. Seis. Soc. Am.*, 74(6), 2379-2411.

[18] Boore, D.M. and Atkinson, G.M. 1987. Stochastic Prediction of Ground Motion and Spectral Response Parameters at Hard-Rock Sites in Eastern North America, *Bull. Seis. Soc. Am.*, 77, 440-487.

[19] Boore, D.M. and Joyner, W.B. 1991. Estimation of Ground Motion at Deep-Soil Sites in Eastern North America, *Bull. Seis. Soc. Am.*, 81(6), 2167-2185.

[20] Boore, D.M., Joyner, W.B. and Fumal, T.E. 1993. Estimation of Response Spectra and Peak Acceleration from Western North American Earthquakes: An Interim Report, U.S.G.S. Open-File Report 93-509, Menlo Park, CA.

[21] Borcherdt, R.D. 1994. New developments in estimating site effects on ground motion, *in ATC-35 Seminar on New Developments in Earthquake Ground Motion Estimation and Implications for Engineering Design Practice*, Applied Technology Council, Redwood City, CA.

[22] Bozorgnia, Y. and Campbell, K.W. 1995. Spectral Characteristics of Vertical Ground Motion in the Northridge and other Earthquakes, *Proc. 4th U.S. Conf. On Lifeline Earthquake Eng.*, pp. 660-667, Am. Soc. Civil Engrs., New York.

[23] Brune, J.N. 1971, 1972. Tectonic Stress and the Spectra of Seismic Shear Waves from Earthquakes, *J. Geophys. Res.*, 75, 4997-5002 (and Correction, 76, 5002).

[24] BSSC. 1994. *NEHRP Recommended Provisions for Seismic Regulations for New Buildings, Part 1: Provisions*, prepared by the Building Seismic Safety Council for the Federal Emergency Management Agency, Building Seismic Safety Council, Washington, D.C.

[25] BSSC. 1994. *NEHRP Recommended Provisions for Seismic Regulations for New Buildings, Part 1: Provision, Part 2: Commentary*, 1994 Edition, Building Seismic Safety Council, Washington, D.C.

[26] Buckle, I G. 1995. Application of Passive Control Systems to the Seismic Retrofit of Historical Buildings in the United States of America. Construction for Earthquake Hazard Mitigation: Seismic Isolation Retrofit of Structures, Proceedings of the 1995 Annual Seminar of the ASCE Metropolitan Section, American Society of Civil Engineers, New York, February 6-7.

[27] Byrne, P.M. et al. 1992. Earthquake Induced Displacement of Soil-Structure Systems, *Proc. 10th World Conf. On Earthquake Eng.*, p. 1407-1412, Earthquake Engineering Research Institute, Oakland, CA.

[28] Campbell, K.W. 1985. Strong Ground Motion Attenuation Relations: A Ten-Year Perspective, *Earthquake Spectra*, 1(4), 759-804.

[29] Campbell, K.W. and Bozorgnia, Y. 1994. Near-Source Attenuation of Peak Horizontal Acceleration from Worldwide Accelerograms Recorded from 1957 to 1993, Proc. Fifth U.S. National Conference on Earthquake Engineering, Earthquake Engineering Research Institute, Oakland, CA.

[30] Carlson, J.D. and Spencer, Jr., B.F. 1996. Magneto-Rheological Fluid Dampers for Semi-Active Seismic Control, Proceedings of the 3rd International Conference on Motion and Vibration Control, September 1-6, Chiba, Japan, 3, 35-40.

[31] Chopra, A.K. 1981. *Dynamics of Structures, A Primer*, Earthquake Engineering Research Institute, Oakland CA.

[32] Clough, R.W. and Penzien, J. 1975. *Dynamics of Structures*, McGraw-Hill, New York.

[33] Coffman, J.L., von Hake, C.A., and Stover, C.W. 1980. *Earthquake History of the United States*, U.S. Dept. of Commerce, NOAA, Pub. 41-1, Washington, D.C.

[34] Constantinou, M C. and Symans, M D. 1993. Seismic Response of Structures with Supplemental Damping. Structural Design of Tall Buildings, 2(2), 77-92.

[35] Cornell, C.A. 1968. Engineering Seismic Risk Analysis, *Bull. Seis. Soc. Am.*, 58(5), 1583-1606.

[36] Cornell, C.A. and Merz, H.A. 1973. Seismic Risk Analysis Based on a Quadratic Magnitude Frequency Law, *Bull. Seis. Soc. Am.*, 63(6) 1992-2006.

[37] Crouse, C. B. 1991. Ground-Motion Attenuation Equations For Earthquakes On The Cascadia Subduction Zone, *Earthquake Spectra*, 7(2) 201-236.

[38] Darragh, R.B. Huang, M.J., and Shakal, A.F. 1994. Earthquake Engineering Aspects of Strong Motion Data from Recent California Earthquakes, Proc. Fifth U.S. National Conf. Earthquake Engineering, v. III, 99-108, Earthquake Engineering Research Institute, Oakland, CA.

[39] Dewey, J.W. et al. 1995. Spatial Variations of Intensity in the Northridge Earthquake, in Woods, M.C. and Seiple. W.R., Eds., *The Northridge California Earthquake of 17 January 1994*, Calif. Dept. Conservation, Div. Mines and Geology, Special Publ. 116, p. 39-46.

[40] Donovan, N.C. and Bornstein, A.E. 1978. Uncertainties in Seismic Risk Procedures, *J. Geotech. Div.*, 104(GT7), 869-887.

[41] Dyke, S.J., Spencer, Jr., B.F., Sain, M.K., and Carlson, J.D. In press. Modeling and Control of Magnetorheological Dampers for Seismic Response Reduction, *Smart Mater. Struc.*

[42] Dyke, S.J., Spencer, Jr., B.F., Sain, M.K., and Carlson, J.D. 1996. Experimental Verification of Semi-Active Structural Control Strategies Using Acceleration Feedback, Proceedings of the 3rd International Conference on Motion and Vibration Control, September 1-6, Chiba, Japan, 3, 291-296.

[43] Electric Power Research Institute. 1986. *Seismic Hazard Methodology for the Central and Eastern United States*, EPRI NP-4726, Menlo Park, CA.

[44] Esteva, L. 1976. *Seismicity*, in Lomnitz, C. and Rosenblueth, E., Eds., *Seismic Risk and Engineering Decisions*, Elsevier, New York.

[45] Evernden, J. F. 1991. Computer programs and data bases useful for prediction of ground motion resulting from earthquakes in California and the conterminous United States, U.S. Geological Survey Open-file report 91-338, Menlo Park, CA.

[46] Greenwood, R.B. 1995. Characterizing blind thrust fault sources — an overview, in Woods, M.C. and Seiple. W.R., Eds., *The Northridge California Earthquake of 17 January 1994*, Calif. Dept. Conservation, Div. Mines and Geology, Special Publ. 116, p. 279-287.

[47] Gumbel, E.J. 1958. *Statistics of Extremes*, Columbia University Press, New York.

[48] Gutenberg, B. and Richter, C.F. 1954. *Seismicity of the Earth and Associated Phenomena*, Princeton University Press, Princeton, NJ.

[49] Gutenberg, B. and Richter, C. F. 1956. Magnitude and Energy of Earthquakes, *Annali de Geofisica*, 9(1), 1-15.

[50] Habermann, R. E. 1987. Man-Made Changes of Seismicity Rates, *Bull. Seis. Soc. Am.*, 77(1), 141-159.

[51] Hamada, M., O'Rourke, T D., Ed. 1992. *Case Studies of Liquefaction and Lifeline Performance During Past Earthquakes, Volume 1: Japanese Case Studies.* National Center for Earthquake Engineering Research, State University of New York, Buffalo, NY.

[52] Hanks, T.C. and Johnston, A.C. 1992. Common Features of the Excitation and Propagation of Strong Ground Motion for North American Earthquakes, *Bull. Seis. Soc. Am.*, 82(1), 1-23.

[53] Hanks, T.C. and Kanamori, H. 1979. A Moment Magnitude Scale, *J. Geophys. Res.*, 84, 2348-2350.

[54] Hanks, T.C. and McGuire, R.K. 1981. The Character of High Frequency Strong Ground Motion, *Bull. Seis. Soc. Am.*, 71, 2071-2095.

[55] Hanson, R.D., Aiken, I.D., Nims, D.K., Richter, P.J., and Bachman, R.E. 1993. State-of-the-Art and State-of-the-Practice in Seismic Energy Dissipation, Proceedings of ATC-17-1 Seminar on Seismic Isolation, Passive Energy Dissipation, and Active Control, San Francisco, CA, March 11-12, Volume 2; Passive Energy Dissipation, Active Control, and Hybrid Control Systems, Applied Technology Council, Redwood City, CA, 449-471.

[56] Harlan, M.R. and Lindbergh, C. 1988. An Earthquake Vulnerability Analysis of the Charleston, South Carolina, Area, Rept. No. CE-88-1, Dept. of Civil Eng., The Citadel, Charleston, SC.

[57] Hausmann, M.R. 1990. *Engineering Principles of Ground Modification*, McGraw-Hill, New York.

[58] Hopper, M.G. 1985. Estimation of Earthquake Effects Associated with Large Earthquakes in the New Madrid Seismic Zone, U.S.G.S. Open File Report 85-457, Washington, D.C.

[59] Housner, G. 1984. Historical View of Earthquake Engineering, *Proc. Post-Conf. Volume, Eighth World Conf. On Earthquake Engineering*, Earthquake Engineering Research Institute, Oakland, CA., as quoted by S. Otani [96].

[60] Housner, G.W. 1963. The Dynamic Behaviour of Water Tanks, *Bull. Seis. Soc. Am.*, 53(2), 381-387.

[61] Housner, G.W. and Masri, S.F., Eds. 1990. Proceedings of the U.S. National Workshop on Structural Control Research, 25-26 October, University of Southern California, USC Publication No. M9013.

[62] Housner, G.W., Masri, S.F., and Soong, T.T. 1992. Recent Developments in Active Structural Control Research in the U.S.A., Invited Presentation at the First European Conference on Smart Structures & Materials, University of Strathclyde, Glasgow, UK, 12-14 May, B. Culshaw, P.T. Gardiner, and A. McDonach, Eds., Institute of Physics Publishing, Bristol, U.K., pp 201-206.

[63] Hudson, D.E. 1979. *Reading and Interpreting Strong Motion Accelerograms*, Earthquake Engineering Research Institute, Oakland, CA.

[64] IAEE. 1992. Earthquake *Resistant Regulations: A World List-1992.* Rev. ed., International Association for Earthquake Engineering, Tokyo.

[65] Jasperse, B.H. and Ryan, C.R. 1992. Stabilization and Fixation Using Soil Mixing: Grouting, Soil Improvement, and Geosynthetics, *ASCE Geotechnical Special Publication No. 30*, p. 1273-1284.

[66] Jennings, C.W. 1994. Fault Activity Map of California and Adjacent Areas, Dept. of Conservation, Div. Mines and Geology, Sacramento, CA.

[67] Joyner, W.B. and Boore, D.M. 1988. Measurements, Characterization and Prediction of Strong Ground Motion, in *Earthquake Engineering and Soil Dynamics II - Recent Advances in Ground-Motion Evaluation*, J.L. v. Thun, Ed., Geotechnical Spec. Publ. No. 20., American Soc. Civil Engrs., New York.

[68] Kameda, H. and Takagi, H. 1981. Seismic Hazard Estimation Based on Non-Poisson Earthquake Occurrences, *Mem. Fac. Eng.*, Kyoto University, v. XLIII, Part 3, July, Kyoto.

[69] Kanai, K. 1983. *Engineering Seismology*, University of Tokyo Press, Tokyo.

[70] Kawashima, K. and Aizawa, K. 1989. Bracketed and Normalized Duration of Earthquake Ground Acceleration, *Earthquake Eng. Struct. Dynam.*, 18, 1041-1051.

[71] Kelly, J. and Michell, C. 1990. Earthquake Simulator Testing of a Combined Sliding Bearing and Rubber Bearing Isolation System, Report No. UCB/EERC-87/04 December, University of California at Berkeley.

[72] Kelly, J.M. and Way, D. 1991. Economic Feasibility and Seismic Rehabilitation of Existing Buildings Via Base Isolation. Seismic Retrofit of Historic Buildings Conference Workbook, Proceedings of the Second Technical Conference on the Seismic Retrofit of Historic Buildings, San Francisco, November 17-19. Look, D.L., Ed., Western Chapter of the Association of Preservation Technology, San Francisco.

[73] Lawson, A.C. and Reid, H.F. 1908-10. *The California Earthquake Of April 18, 1906. Report Of The State Earthquake Investigation Commission, California.* State Earthquake Investigation Commission, Carnegie Institution of Washington, Washington, D.C.

[74] Lomnitz, C. 1974. *Global Tectonics and Earthquake Risk*, Elsevier, New York.

[75] Lou, J.Y.K., Lutes, L.D., and Li, J.J. 1994. Active Tuned Liquid Damper for Structural Control, Proceedings of the First World Conference on Structural Control: International Association for Structural Control, Los Angeles, 3-5 August, Housner, G.W., et al., Eds., International Association for Structural Control, Los Angeles, 2, TP1-70–TP1-79.

[76] Luco, J.E., Mita, A. 1992. Active Control of The Seismic Response of Tall Non-Uniform Buildings, Proceedings of the Tenth World Conference on Earthquake Engineering, 19-24 July, Madrid; A A Balkema, Rotterdam, 4, 2143-2148.

[77] McGuire, R. K. 1978. FRISK: *Computer Program for Seismic Risk Analysis Using Faults as Earthquake Sources.* U.S. Geological Survey, Reports — United States Geological Survey Open File 78-1007.

[78] McGuire, R.K. and Barnhard, T.P. 1979. The Usefulness of Ground Motion Duration in Predicting the Severity of Seismic Shaking, *Proc. 2nd U.S. Natl. Conf. on Earthquake Engineering*, Earthquake Engineering Research Institute, Oakland, CA.

[79] McGuire, R.K., Ed. 1993. *Practice of Earthquake Hazard Assessment*. International Association of Seismology and Physics of the Earth's Interior.

[80] Meeting on Up-dating of MSK-64. 1981. Report on the Ad-hoc Panel Meeting of Experts on Up-dating of the MSK-64 Seismic Intensity Scale, Jene, 10-14 March 1980, *Gerlands Beitr. Geophys.*, Leipzeig 90, 3, 261-268.

[81] Midorikawa, S. 1991. Attenuation of Peak Ground Acceleration and Velocity From Large Subduction Earthquakes, *Proc. Fourth Intl. Conf. On Seismic Zonation*, Stanford University, August 25-29, 1991, Earthquake Engineering Research Institute, Oakland, CA, 2, 179-186.

[82] Mitchell, J.K. 1981. Soil Improvement: State-of-the-Art, *Proc. 10th Intl. Conf. Soil Mech. Found. Eng.*, 4, 509-565, Stockholm.

[83] Mohraz, B. 1976. A Study of Earthquake Response Spectra for Different Geological Conditions, *Bull. Seis. Soc. Am.*, 66, 915-935.

[84] Murphy J.R. and O'Brien, L.J. 1977. The Correlation of Peak Ground Acceleration Amplitude with Seismic Intensity and Other Physical Parameters, *Bull. Seis. Soc. Am.*, 67(3), 877-915.

[85] Nacer, N. and Hanson, R.D. 1994. Inelastic Behavior of Supplemental Steel Damping Devices. Proceedings of the Second International Conference on Earthquake Resistant Construction and Design, Berlin, 15-17 June, Savidis, S.A., Ed., A A Balkema, Rotterdam, 2, 805-812.

[86] National Academy Press. 1988. *Probabilistic Seismic Hazard Analysis,* National Academy of Sciences, Washington, D.C.

[87] NEIC. 1996. Database of Significant Earthquakes Contained in *Seismicity Catalogs,* National Earthquake Information Center, Golden, CO.

[88] Newmark, N.M. 1965. Effects of Earthquakes on Dams and Embankments, *Geotechnique,* 15(2), 129-160.

[89] Newmark, N.M. 1973. *A Study of Vertical and Horizontal Earthquake Spectra,* Dir. Of Licensing, U.S. Atomic Energy Commission, Washington, D.C.

[90] Newmark, N.M. and Hall, W.J. 1982. *Earthquake Spectra and Design,* Earthquake Engineering Research Institute, Oakland, CA.

[91] Nishenko, S.P. and Buland, R. 1987. A Generic Recurrence Interval Distribution For Earthquake Forecasting, *Bull. Seis. Soc. Am.*, 77, 1382-1399.

[92] NRC. 1985. *Liquefaction of Soils During Earthquakes,* National Research Council, National Academy Press, Washington, D.C.

[93] O'Rourke, T D. and Hamada, M., Ed. 1992. Case Studies of Liquefaction and Lifeline Performance During Past Earthquakes: Volume 2, United States Case Studies. National Center for Earthquake Engineering Research, State University of New York, Buffalo, NY.

[94] O'Rourke, T.D., Pease, J.W., and Stewart, H. E. 1992. Lifeline Performance and Ground Deformation During the Earthquake, in O'Rourke, T., Ed. Geological Survey (U.S.) *Loma Prieta, California, Earthquake Of October 17, 1989: Marina District.* U.S. Government Printing Office, Washington, D.C.

[95] Ohsaki, Y. 1966. Niigata Earthquakes, 1964 Building Damage and Condition, Soils and Foundations, Japanese Soc. Of Soil Mechanics and Foundation Engineering, 6(2), 14-37. March.

[96] Otani, S. 1995. A Brief History of Japanese Seismic Design Requirements, *Concrete International.*

[97] Paz, M., Ed. 1994. *International Handbook of Earthquake Engineering: Codes, Programs, and Examples,* Chapman & Hall, New York.

[98] Peng, M.H., Elghadamsi, F., and Mohraz, B. 1989. A Simplified Procedure for Constructing Probabilistic Response Spectra, *Earthquake Spectra,* 5(2), Earthquake Engineering Research Institute, Oakland.

[99] Perry, C.L., Fierro, E.A., Sedarat, H., and Scholl, R.E. 1993. Seismic Upgrade in San Francisco Using Energy Dissipation Devices, *Earthquake Spectra,* 9(3), 559-580.

[100] Prevost, J.H. 1981. *DYNA-FLOW: A Nonlinear Transient Finite Element Analysis Program,* Rept. No. 81-SM-1, Dept. Civil Eng., Princeton University, Princeton, NJ.

[101] Reid, H.F. 1910. The Mechanics of the Earthquake, the California Earthquake of April 18, 1906, Report of the State Investigation Committee, v. 2, Carnegie Institution of Washington, Washington, D.C.

[102] Reiter, L. 1990. *Earthquake Hazard Analysis, Issues and Insights,* Columbia University Press, NY.

[103] Richter, C. F. 1935. An Instrumental Earthquake Scale, *Bull. Seis. Soc. Am.* 25, 1- 32.

[104] Richter, C.F. 1958. *Elementary Seismology,* W.H. Freeman and Co., San Francisco, CA.

[105] Sadigh, K., Egan, J., and Youngs, R. 1986. Specification of Ground Motion for Seismic Design of Long Period Structures, *Earthquake Notes,* 57, 13.

[106] Schnabel, P.B., Lysmer, J., and Seed, H.B. 1972. SHAKE — *A Computer Program for Earthquake Response Analysis of Horizontally Layered Sites,* Earthquake Engineering Research Center, Rept. No. EERC-72-12, University of California at Berkeley, CA.

[107] Scholl, R.E. 1994. Comparison of Conventional and Damped Seismic Retrofits of a Two-Story Steel Frame Building, Proceedings of the Fifth U.S. National Conference on Earthquake Engineering, July 10-14, Chicago, IL, Earthquake Engineering Research Institute, Oakland, CA, I, pages 725-733.

[108] Scholz, C.H. 1990. *The Mechanics of Earthquakes and Faulting,* Cambridge University Press, MA.

[109] Schwartz, D.P. 1988. Geologic Characterization of Seismic Sources: Moving into the 1990s, in *Earthquake Engineering and Soil Dynamics II — Recent Advances in Ground-Motion Evaluation,* J.L. v. Thun, Ed., Geotechnical Spec. Publ. No. 20, *Am. Soc. Civil Eng.,* New York.

[110] Schwartz, D.P. and Coppersmith, K.J. 1984. Fault Behavior and Characteristic Earthquakes: Examples from the Wasatch and San Andreas Faults, *J. Geophys. Res.,* 89, 5681-5698.

[111] SEAOC. 1980. *Recommended Lateral Force Requirements and Commentary,* Seismology Committee, Structural Engineers of California, San Francisco, CA.

[112] Seed, H.B. and Wilson, S.D. 1967. The Turnagain Heights Landslide, Anchorage, Alaska, *J. Soil Mech. Found. Div., Am. Soc. Civil Eng.,* 93, SM4, 325-353.

[113] Seed, H.B. and Idriss, I.M. 1982. Ground Motions and Soil Liquefaction during Earthquakes, Earthquake Engineering Research Institute, Oakland, CA.

[114] Slemmons, D.B. 1977. State-of-the-Art for Assessing Earthquake Hazards in the United States, Report 6: Faults and Earthquake Magnitude, U.S. Army Corps of Engineers, Waterways Experiment Station, Misc. Paper s-73-1, 129 pp.

[115] Somerville, P. 1989. Strong Ground Motion Attenuation in the Puget Sound-Portland Region, *Proceedings Of Conference XLVIII: 3rd Annual Workshop On Earthquake Hazards in the Puget Sound, Portland Area;* March 28-30, 1989, Portland, Oregon; Hays-Walter, W., Ed. U.S. Geological Survey, Reston, VA.

[116] Soong, T.T., Masri, S.F., and Housner, G.W. 1991. An Overview of Active Structural Control Under Seismic Loads, *Earthquake Eng. Res. Inst. Spectra,* 7(3), 483-506.

[117] Soong, T.T and Costantinou, M.C., Eds. 1994. Passive and Active Structural Vibration Control in Civil Engineering, CISM International Centre for Mechanical Sciences, Vol. 345, Springer-Verlag, New York.

[118] Spencer, Jr., B.F., Dyke, S.J., Sain M.K., and Carlson, J.D. In press. Phenomenological Model of a Magnetorheological Damper, *J. Eng. Mech., ASCE.*

[119] Spencer, Jr., B.F., Sain, M.K., Won, C.-H., Kaspari, Jr., D.C., and Sain, P.M. 1994. Reliability-Based Measures of Structural Control Robustness, *Structural Safety,* 15, 111-129.

[120] Stein, R.S. and Yeats, R.S. 1989. Hidden Earthquakes, *Sci. Am.,* June.

[121] Stepp, J.C. 1972. Analysis of Completeness of the Earthquake Sample in the Puget Sound Area and Its Effect on Statistical Estimates of Earthquake Hazard, *Proc. First Conf. Microzonation,* Seattle, WA.

[122] Structural Engineers Association of California. 1988. *Recommended Lateral Force Requirements and Tentative Commentary,* Structural Engineers Association of California, San Francisco, CA.

[123] Toro, G.R. and McGuire, R.K. 1987. An Investigation into Earthquake Ground Motion Characteristics in Eastern North America, *Bull. Seis. Soc. Am.,* 77, 468-489.

[124] Trifunac, M.D. and Brady, A.G. 1975. A Study on the Duration of Strong Earthquake Ground Motion, *Bull. Seis. Soc. Am.,* 65, 581-626.

[125] Trifunac, M.D. and Novikova, E.I. 1995. State of the Art Review on Strong Motion Duration, *Prof. 10th European Conf. On Earthquake Engineering,* pp. 131-140.

[126] Uniform Building Code. 1994. Volume 2, Structural Engineering Design Provisions, Intl. Conf. Building Officials, Whittier.

[127] U.S. Army. 1992. *Seismic Design for Buildings* (Army: TM 5-809-10; Navy: NAVFAC P-355; USAF: AFM-88-3, Chapter 13). Washington D.C.: Departments of the Army, Navy, and Air Force, 1992. 407 pages. Available from the National Technical Information Service (NTIS), Military Publications Division, Washington.

[128] Usami, T. 1981. *Nihon Higai Jishin Soran* (List of Damaging Japanese Earthquakes), University of Tokyo Press (in Japanese).

[129] Wald, D.J., Burdick, L.J., and Somerville, P.G. 1988. Simulation of Acceleration Time Histories Close to Large Earthquakes, in *Earthquake Engineering and Soil Dynamics II — Recent Advances in Ground-Motion Evaluation*, J.L. v. Thun, Ed., Geotechnical Spec. Publ. No. 20, *Am. Soc. Civil Eng.*, New York.

[130] Wells, D.L. and Coppersmith, K.J. 1994. Empirical Relationships Among Magnitude, Rupture Length, Rupture Width, Rupture Area and Surface Displacement, *Bull. Seis. Soc. Am.*, 84(4), 974-1002.

[131] Wheeler, R.L. et al. 1994. Elements of Infrastructure and Seismic Hazard in the Central United States, U.S.G.S. Prof. Paper 1538-M, Washington, D.C.

[132] Whittaker, A., Bertero, V., Alonso, J., and Thompson, C. 1989. Earthquake Simulator Testing of Steel Plate Added Damping and Stiffness Elements, Earthquake Engineering Research Center, University of California, Berkeley, SEL TA654.6.R37 no.89/02. Report: UCB-EERC-89-02., 201 pages.

[133] Woo, G., Wood, R., and Muir. 1984. *British Seismicity and Seismic Hazard*, in *Proc. Eighth World Conf. Earthquake Eng.*, 1, 39-44, Earthquake Engineering Research Institute, Oakland, CA.

[134] Wood, H.O. and Neumann, Fr. 1931. Modified Mercalli Intensity Scale of 1931, *Bull. Seis. Soc. Am.*, 21, 277-283.

[135] Xia, C. and Hanson, R.D. 1992. Influence of Adas Element Parameters on Building Seismic Response. *J. Struc. Eng.*, 118(7), 1903-1918.

[136] Yamazaki, F. 1993. Comparative Study of Attenuation Characteristics of Ground Motion in Europe, North America and Japan, *Bull. Earthquake Resistant Structure Res. Center*, University of Tokyo, 26, 39-56.

[137] Yegulalp, T.M. and Kuo, J.T. 1974. Statistical Prediction of the Occurrence of Maximum Magnitude Earthquakes, *Bull. Seis. Soc. Am.*, 64(2), 393-414.

[138] Youngs, R. R. and Coppersmith, K J. 1989. Attenuation Relationships for Evaluation of Seismic Hazards From Large Subduction Zone Earthquakes, *Proc. Conference XLVIII: 3rd Annual Workshop On Earthquake Hazards in the Puget Sound, Portland Area;* March 28-30, 1989, Portland, OR, Hays-Walter, W., Ed., U.S. Geological Survey, Reston, VA.

[139] Youngs, R.R. and Coppersmith, K.J. 1987. Implication of Fault Slip Rates and Earthquake Recurrence Models to Probabilistic Seismic Hazard Estimates, *Bull. Seis. Soc. Am.*, 75, 939-964.

Further Reading

A number of attenuation relations have been developed for other regions, such as China, Japan, New Zealand, the Trans-Alpide areas, etc. including the following.

[1] Ambrayses, N. N. 1995. Prediction of Earthquake Peak Ground Acceleration In Europe. *Earthquake Engineering and Structural Dynamics*, 24(4), 467-490.

[2] Caillot, V. and Bard, P.Y. 1993. Magnitude, Distance and Site Dependent Spectra From Italian Accelerometric Data, *European Earthquake Engineering*, 6(1), 37-48.

[3] Capuano, P., Gasparini, P., Peronaci, M., and Scarpa, R. 1992. Strong Ground Motion and Source Parameters for Earthquakes in the Apennines, Italy, *Earthquake Spectra*, 8(4), 529-554.

[4] Dan, K., Ishii, T., and Ebihara, M. 1993. Estimation of Strong Ground Motions in Meizoseismal Region of the 1976 Tangshan, China, Earthquake. *Bull. Seis. Soc. Am.*, 83, 6, 1756-1777.

[5] Dowrick, D J. and Sritharan, S. 1993. Attenuation of Peak Ground Accelerations in Some Recent New Zealand Earthquakes, *Bull. New Zealand Natl. Soc. Earthquake Eng.* 26(1), 3-13.

[6] Dowrick, D.J. 1992. Attenuation of Modified Mercalli Intensity in New Zealand Earthquakes, *Earthquake Engineering and Structural Dynamics*, 21(3), 181-196.

[7] *Earthquake Motion and Ground Conditions: In Commemoration of the 20th Anniversary of the Research Subcommittee on Earthquake Ground Motion, the Architectural Institute of Japan.* 1993. Architectural Institute of Japan, Tokyo.

[8] Fukushima, Y. and Tanaka, T. 1991. New Attenuation Relation for Peak Horizontal Acceleration of Strong Earthquake Ground Motion in Japan, *Shimizu Tech. Res. Bull.*, 10, 1-11.

[9] Grandori, G. 1991. Macroseismic Intensity Versus Epicentral Distance: The Case of Central Italy, *Tectonophysics*, 193, 1-3, 165-171.

[10] Hatzidimitriou, P., Papazachos, C., Kiratzi, A., and Theodulidis, N. 1993. Estimation of Attenuation Structure and Local Earthquake Magnitude Based on Acceleration Records in Greece, *Tectonophysics*, 217(3/4), 243-253.

[11] Matuschka, T. and Davis, B. K. 1991. Derivation of an Attenuation Model in Terms of Spectral Acceleration for New Zealand. *Proceedings [Of The] Pacific Conference on Earthquake Engineering*, Auckland, New Zealand, 20-23 November, 1991, New Zealand National Society For Earthquake Engineering, Wellington, 2, 123-134.

[12] Molas, G. L. and Yamazaki, F. 1995. Attenuation of Earthquake Ground Motion in Japan Including Deep Focus Events, *Bull. Seis. Soc. Am.*, 85, 5, 1343-1358.

[13] Monachesi, G. 1994. Seismic Hazard Assessment Using Intensity Point Data, *Soil Dynamics and Earthquake Engineering*, 13, 3, 219-226.

[14] Niazi, M. and Bozorgnia, Y. 1992. 1990 Manjil, Iran, Earthquake: Geology and Seismology Overview, Pga Attenuation, and Observed Damage, *Bull. Seis. Soc. Am.*, 82(2), 774-799.

[15] *Proceedings of the International Workshop on Strong Motion Data.* 1994. Japan Port and Harbour Research Institute, Yokosuka, Japan.

[16] Ruan, A. and Sun, C. 1992. A Study on Attenuation Law of Seismic Ground Motion in the Loess Region of Northwestern China, *Earthquake Research In China*, 6, 4, 431-442.

[17] Tao, X. and Zheng, G. 1991. Intensity Attenuation Relationship For Seismic Zonation of China, *Proceedings of the Fourth International Conference On Seismic Zonation*, Stanford University, August 25-29, 1991; Earthquake Engineering Research Institute, Oakland, CA.